WV IMAGES

Satellite Image Interpretation and Applications
EUMeTrain Online Course , 10 – 30 June 2011

Christo Georgiev
NIMH, Bulgaria

INTRODICTION

The radiometer SEVIRI of Meteosat Second Generation (MSG) provides data from 2 channels in the water vapour absorption band (6.2 and 7.3 µm).

Among these two WV channels, the radiation in Channel 6.2 µm is more easily absorbed by water vapour and has a larger information content.

Channel 6.2 µm is the primary WV channel, broadly used in image format for the purposes of weather analysis and forecasting based on its synoptic scale interpretation , see e.g.

Weldon & Holmes (1991); Bader et al., 1995;

Santurette & Georgiev, 2005.

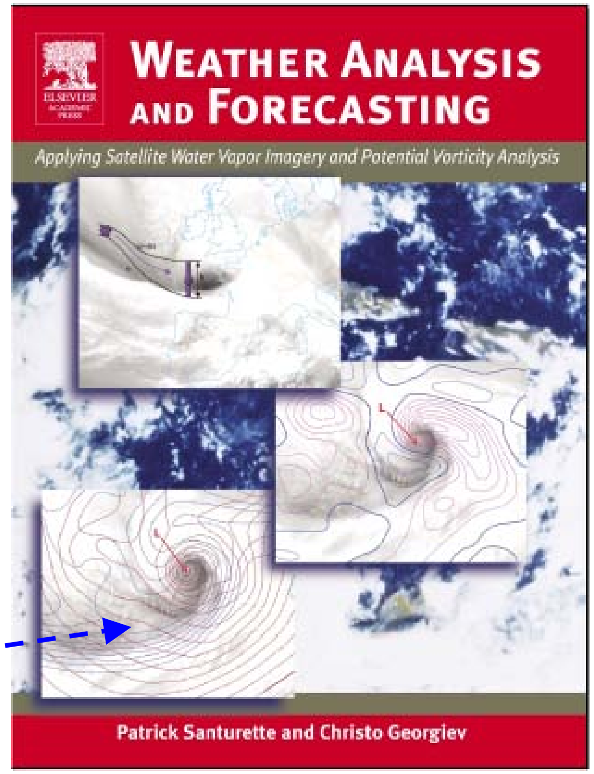

The other MSG WV channel 7.3 µm can also be used in operational forecasting environment for detecting mid-level moisture features associated with low-level thermodynamic conditions.

Radiance

The satellite measures intensity of radiation that is referred to as 'radiance', and may be converted to brightness temperature, or to image grey shade. The radiance in window IR and WV channels is emitted by objects such as cloud top elements and the earth surface.

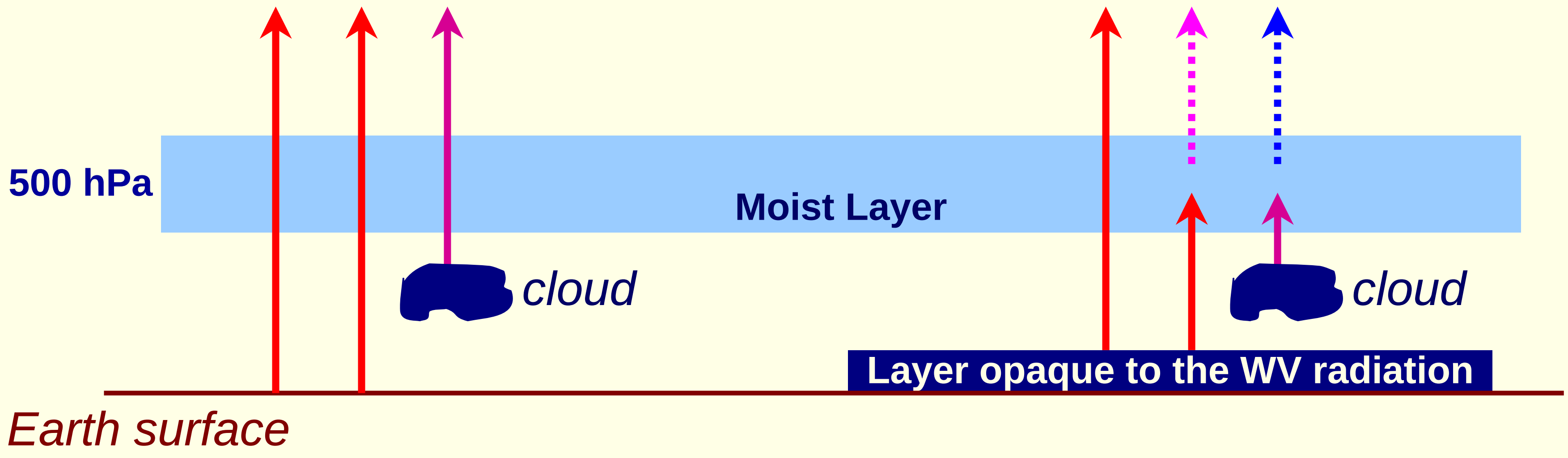

- The radiation in IR window channels (10.8 µm) will reach the satellite after no absorption.

  The derived brightness temperature equals the physical temperature of the object, which radiates.

- For the WV channels (6.2 µm) , some portion of the upcoming radiation is absorbed by water vapour and then re-emitted by the atmosphere.

  The absorption and re-emission depends on the vapour pressure in various ways for different channels.

Two <u>radiation effects</u> are of special importance for interpretation and application of data from the WV absorption channels (see Georgiev et al. 2007):

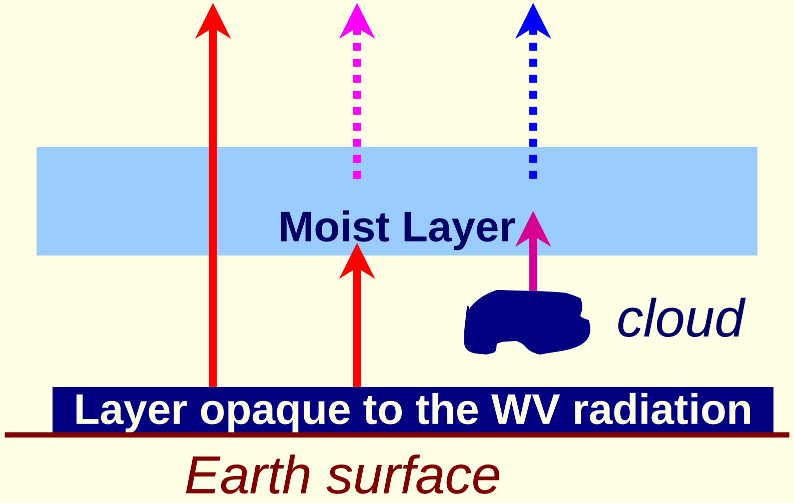

- ✓ **The <u>effect of portioning</u> between the contributions of the radiation originating from bellow, which penetrates through the moist layer and the radiation emitted by the moist layer itself.**

  The "portioning effect" influences the radiation of 6.2 μm and 7.3 μm channels in different ways and allows these channels to be sensitive to tropospheric moisture at different altitudes.

- ✓ **The "<u>sensitivity range</u>", which provides an indication of the channels' ability to detect differences in humidity of atmospheric layers at various altitudes.**

(for details see end of the presentation)

WV IMAGES in CHANNELS 6.2 and 7.3 µm

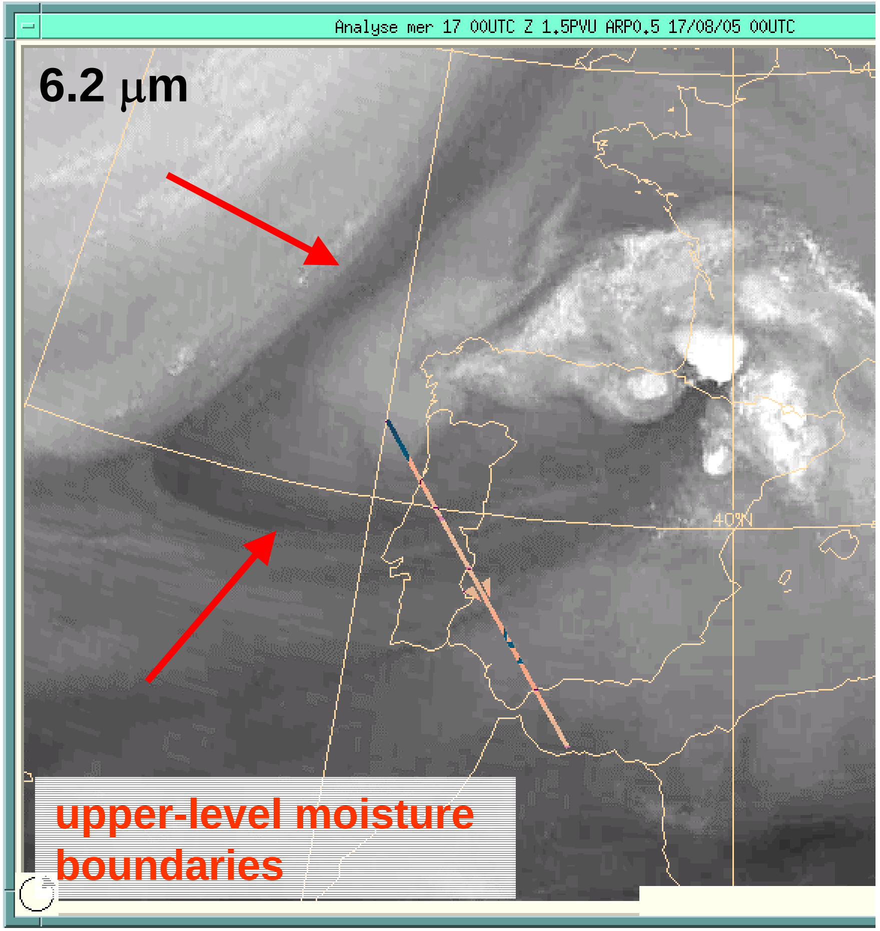

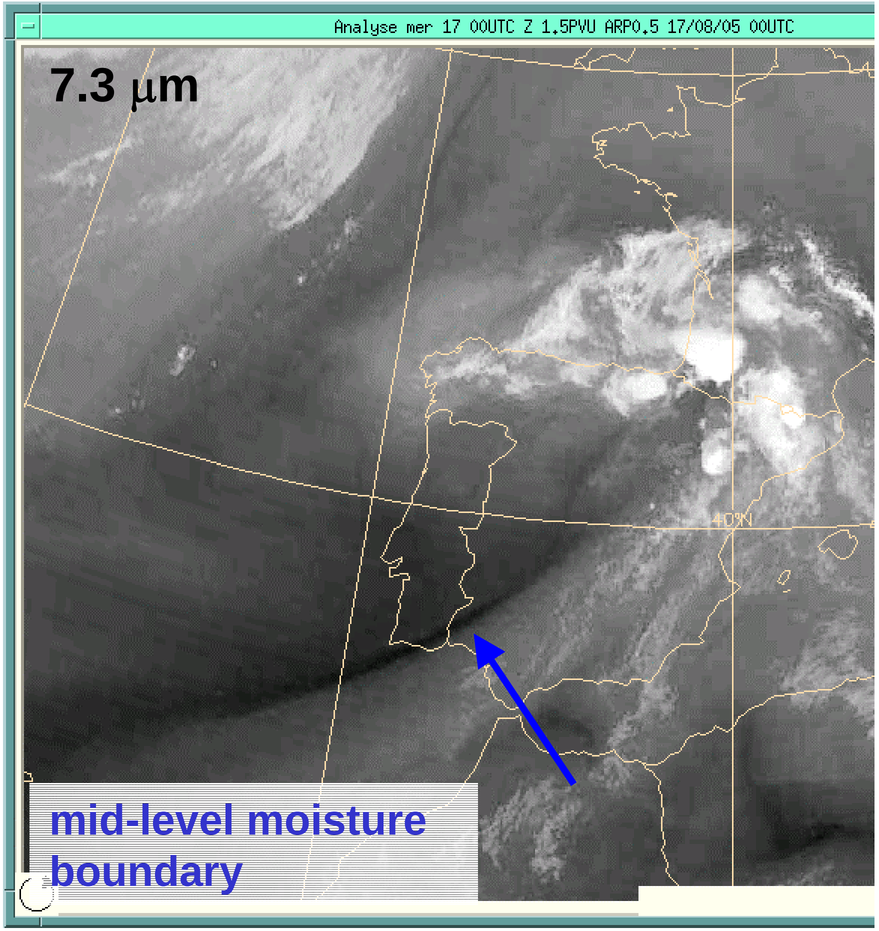

The imagery features in <u>the two MSG WV channels may differ significantly</u> in situations of <u>strong troposphere dynamics</u>. The radiance in WV 6.2 channel depends on the temperature and humidity only above 600 hPa and only upper-level structures are visible by the 6.2 µm, the lower humidity being displayed in darker grey shades.
The 7.3 µm radiance is sensitive to moisture patterns in middle troposphere and some low-level features can be visible by this channel in certain conditions.

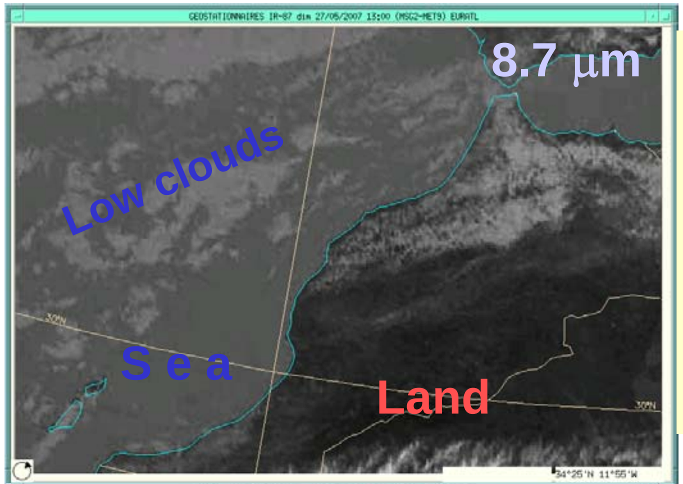

8.7 μm IR channel:

• Radiation reaching the satellite is slightly absorbed by atmospheric water vapour.

• Various objects of the earth surface and atmosphere may be distinguished due to differences in their temperature.

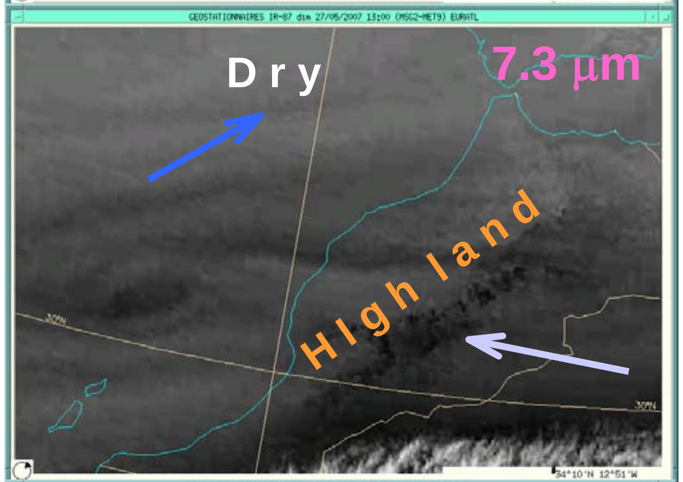

7.3 μm WV channel:

• Radiation is sensitive to detect mid- to low-level atmospheric moisture and mid/high-level clouds.

• Low-level clouds may be not visible in case of moist air above these clouds.

• High mountain surface may be seen as a dark feature if little moisture is present above.

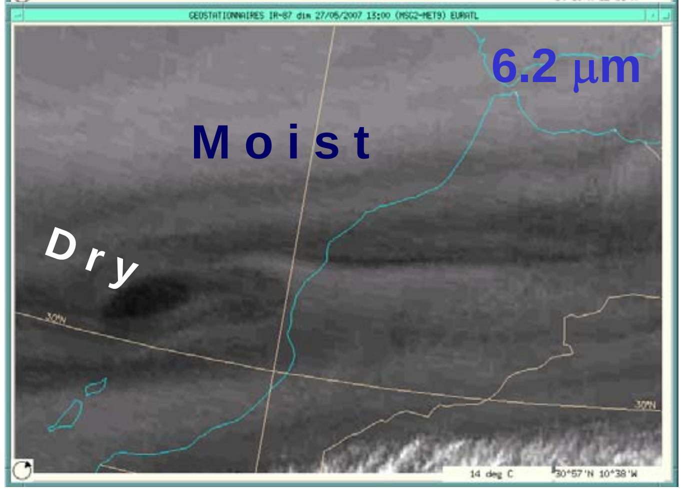

6.2 μm WV channel:

• Radiation is sensitive to upper- and mid-level atmospheric moisture. Due to strong absorption, low-level features (earth surface, low clouds) are not visible.

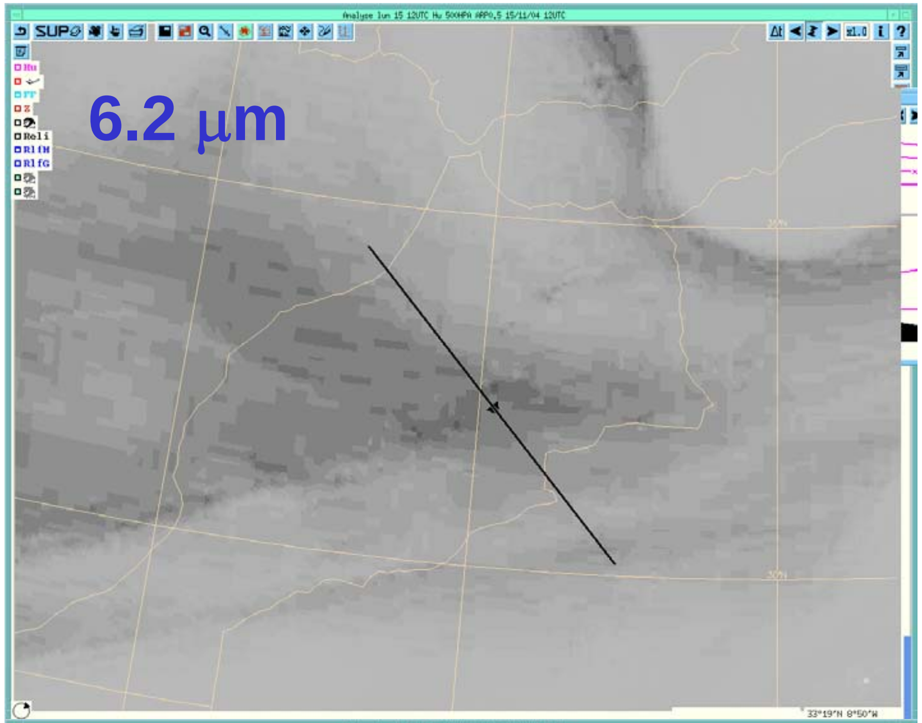

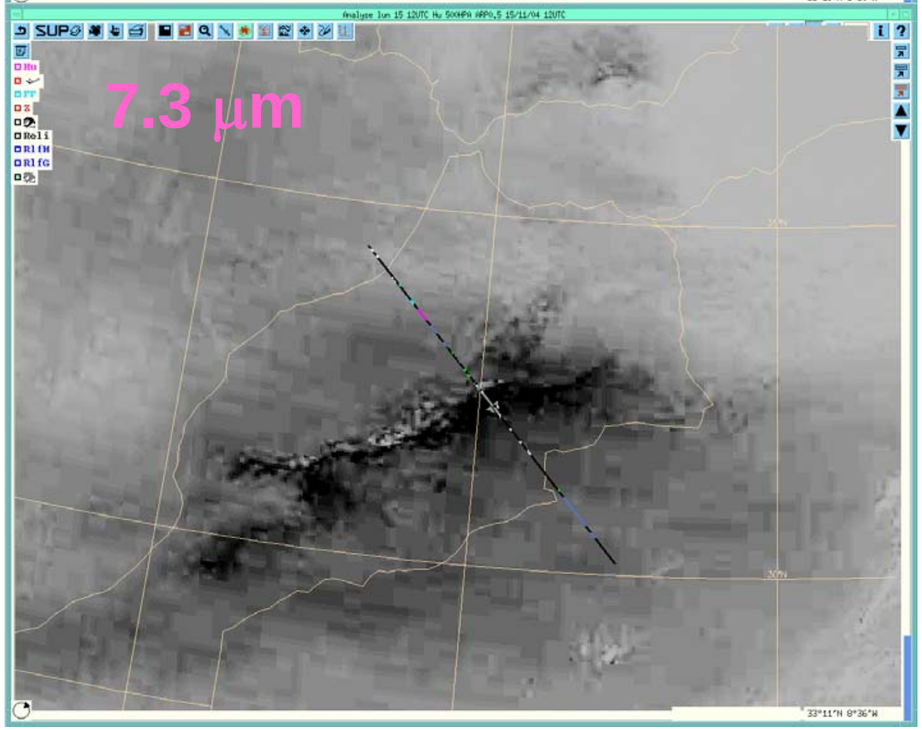

Upper-level moisture

Looking at the image grey shades in the 6.2 µm and 7.3 µm MSG channels, indicate the position of the following vertical moisture distribution:

- Dry air stripe at upper troposphere

  and

- Moist mid-level air below.

WV imagery 6.2 μm
Synoptic applications

- The water vapour is a conservative tracer of upper-level large scale atmospheric motion (which, in its great part, is approximately adiabatic and hydrostatic).
- Therefore WV images provide general information on the flow patterns at mid-upper troposphere (600 – 300 hPa).
- The basis for synoptic scale applications of WV imagery is that moist and dry regions as well as the boundaries between them often relate to significant upper-level flow features such as troughs and ridges, deformation zones, jet streams, vorticity, blocking regime.
- A relevant dynamic approach is needed for an efficient operational use of WV images in order to link the satellite information to the dynamics of upper-troposphere.

6.2 μm WV IMAGERY DIAGNOSIS

UPPER-LEVEL

Potential Vorticity Analysis
by using WV imagery

Potential Vorticity Concept

- **The Potential Vorticity (PV) is a product of the absolute vorticity and the static stability (**Hoskins, B., 1997**).**

  Units: **10^{-6} m^2 s^{-1} K kg^{-1}** or **'PV-unit' (PVU)**

- **The PV is an effective parameter for studying the appearance and evolution of dynamical structures at synoptic scale due to its important properties (see Santurette & Georgiev, 2005) :**

  - ✓ **Conservation for adiabatic frictionless motions**
  - ✓ **Specific climate distribution in the atmosphere**
    - **In the middle and upper troposphere PV is ranging from 0.5 to 1.0 PVU**
    - **In the stratosphere PV > 3.0 PVU due to the strong increase of the static stability.**

TROPOPAUSE DYNAMIC ANOMALY

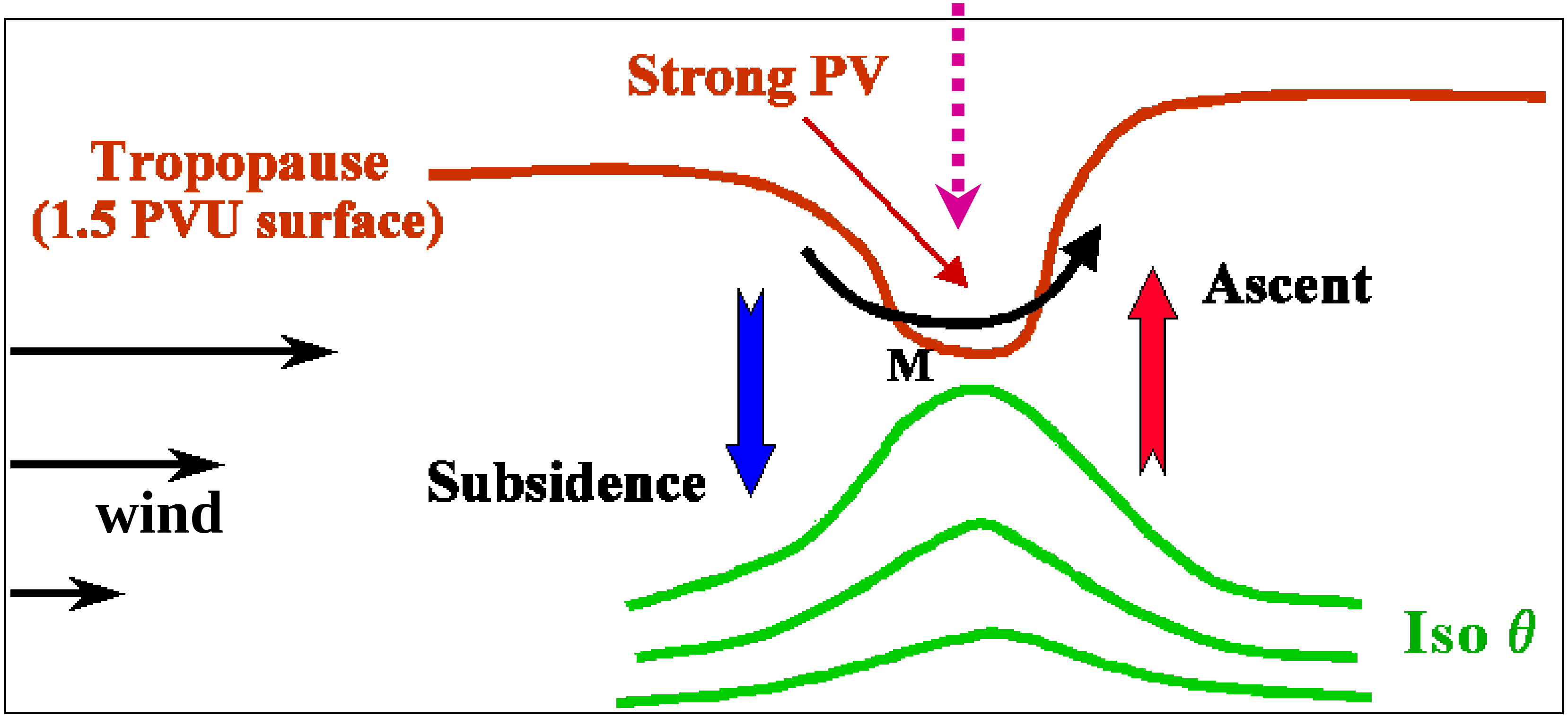

In terms of the PV concept, the tropopause in mid-latitudes may be represented by the <u>surface of constant PV = 1.5 PVU</u> ($10^{-6}\ m^2\ s^{-1}\ K\ kg^{-1}$**), and considered as the "dynamical tropopause" (see Santurette & Georgiev, 2005).**

An upper tropospheric anomaly of high PV, advected down to middle troposphere corresponds to an area of the folding of the dynamical tropopause associated with a stratospheric intrusion.

Such a low tropopause area is referred to as a PV anomaly or a "tropopause dynamic anomaly".

In the upper-air analysis, the most significant dynamic feature is the PV anomaly (or tropopause dynamic anomaly)

CROSS-SECTION

05/08/2005 1200 UTC

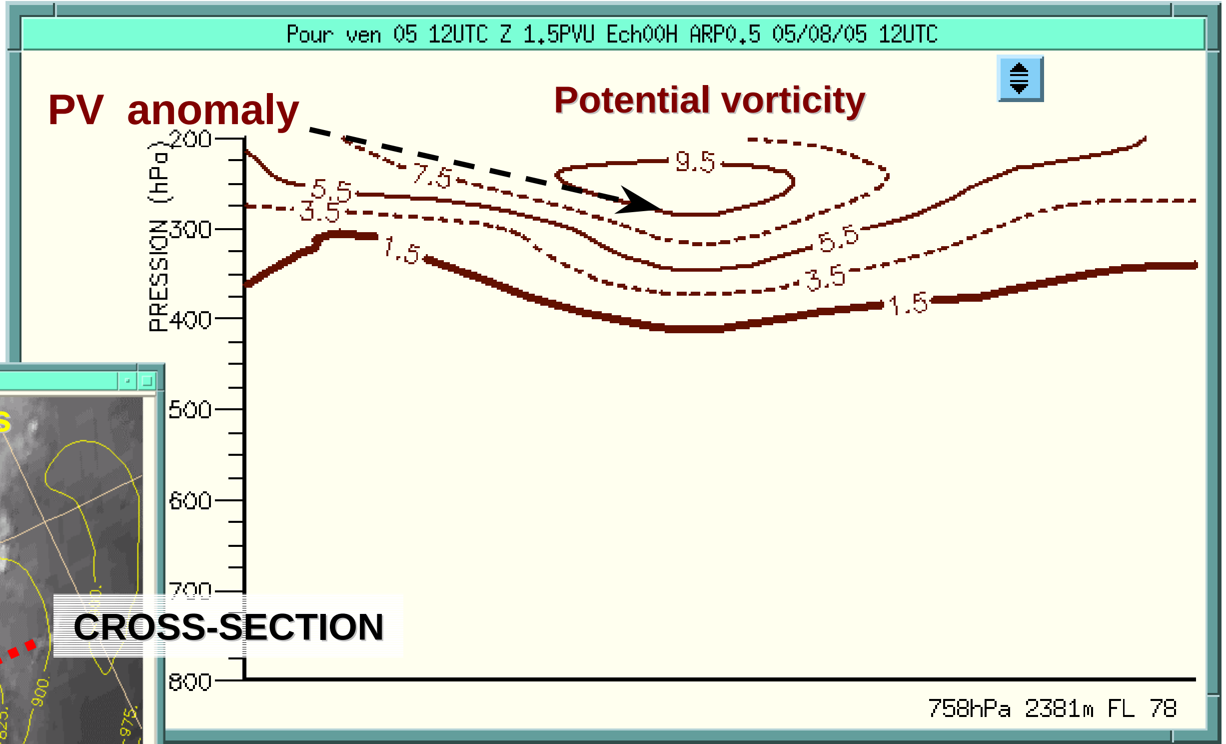

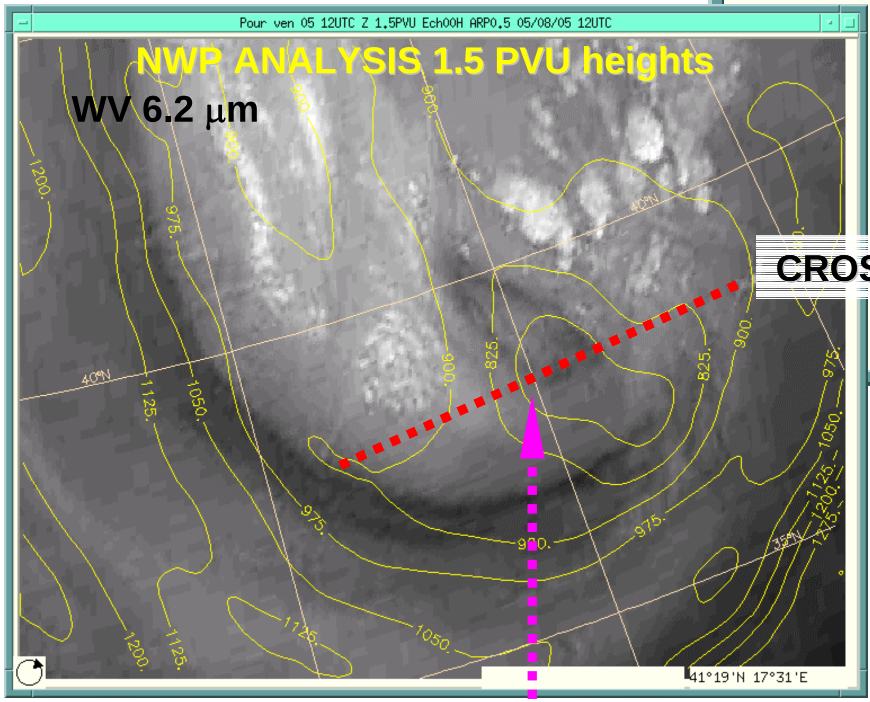

PV anomaly (or tropopause dynamic anomaly) is seen in a 6.2 µm image as a dark dry zone or vorticity feature

How the PV anomaly influences the troposphere thermodynamics in the real atmosphere, analyzed by a NWP model?

In the upper-air analysis, the most significant dynamic feature is the **PV anomaly (or tropopause dynamic anomaly)**

CROSS-SECTION

05/08/2005 1200 UTC

NWP ANALYSIS 1.5 PVU heights

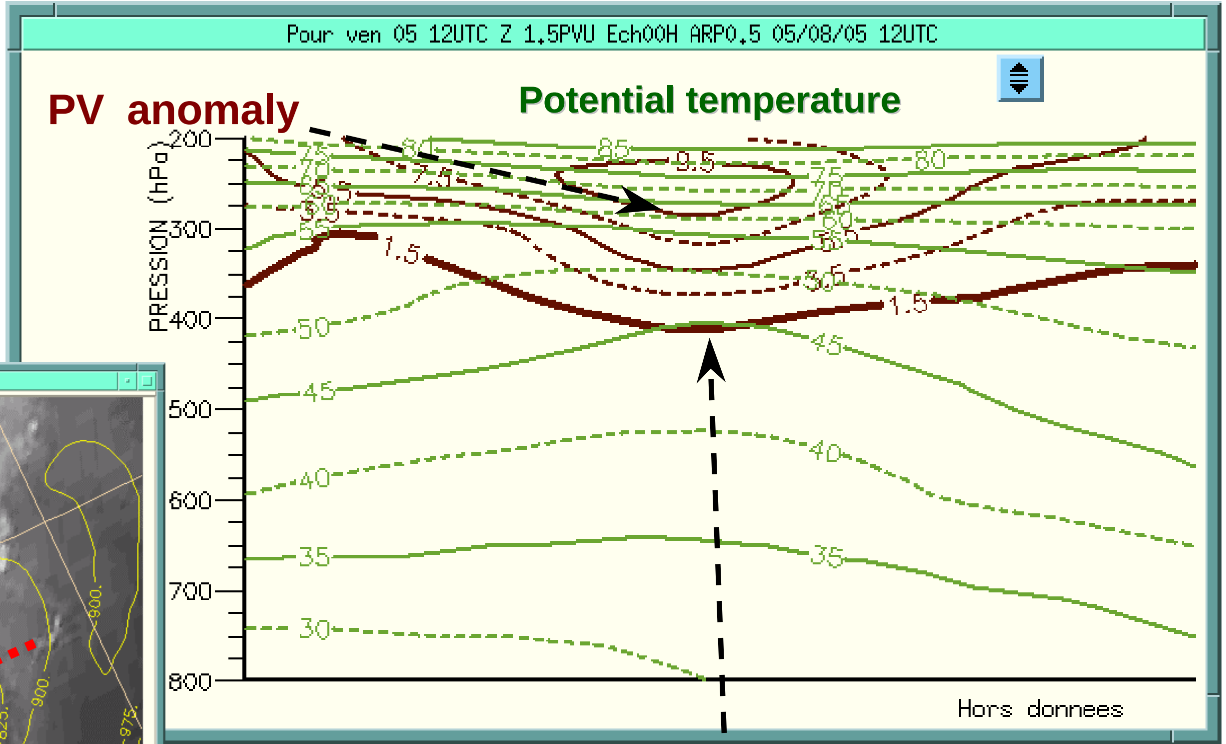

potential temperature surfaces rising to compensate the increase of static stability above

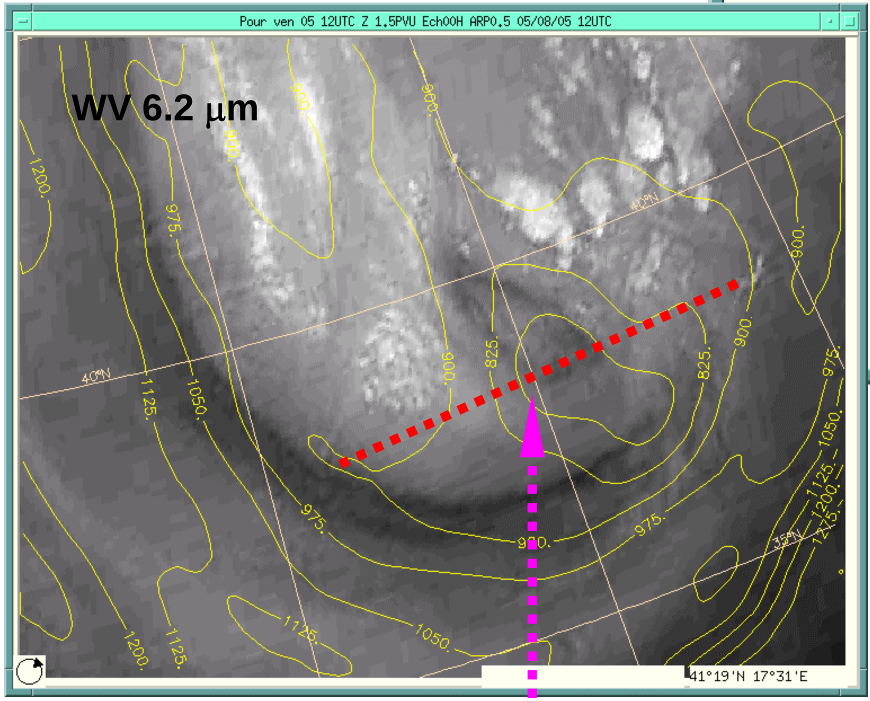

PV anomaly (or tropopause dynamic anomaly) seen in a 6.2 µm image as a dark dry zone or vorticity feature

In the upper-air analysis, the most significant dynamic feature is the **PV anomaly (or tropopause dynamic anomaly)**

CROSS-SECTION

05/08/2005 1200 UTC

NWP ANALYSIS 1.5 PVU heights

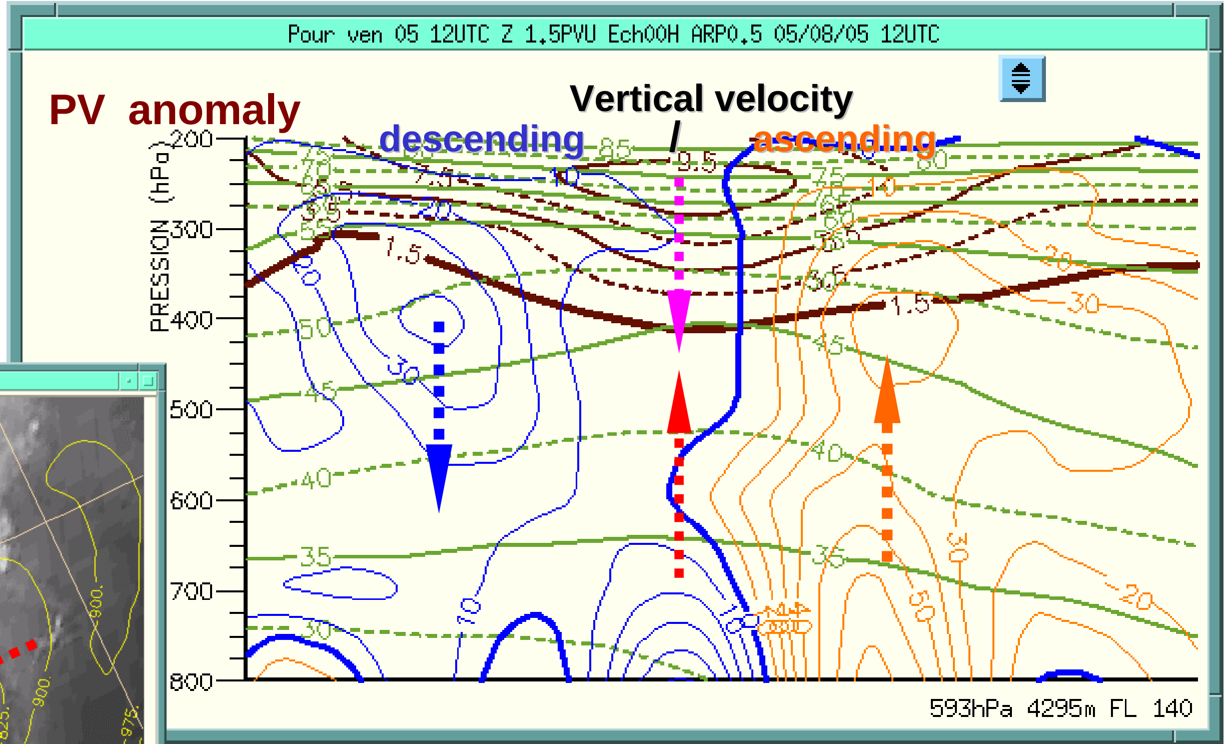

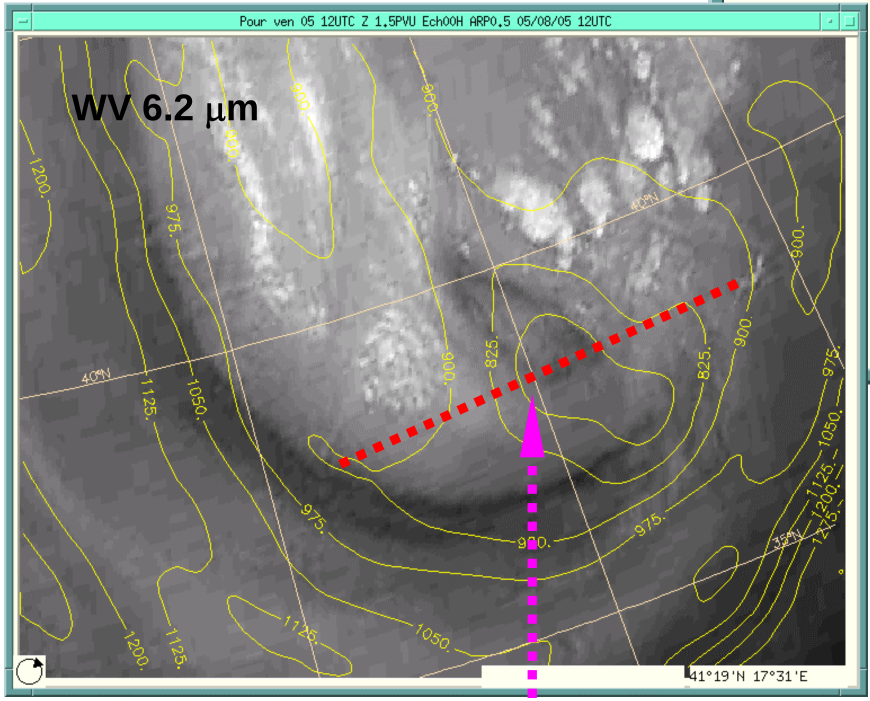

PV anomaly (or tropopause dynamic anomaly) seen in a 6.2 µm image as a dark dry zone or vorticity feature

In a baroclinic flow increasing with height, the intrusion of PV anomaly in the troposphere produces vertical motion: the deformation of the potential temperature surfaces induces

ascending motion ahead of the anomaly

&

descending motion behind the anomaly

Tropopause dynamic anomaly

Dry stratospheric intrusion

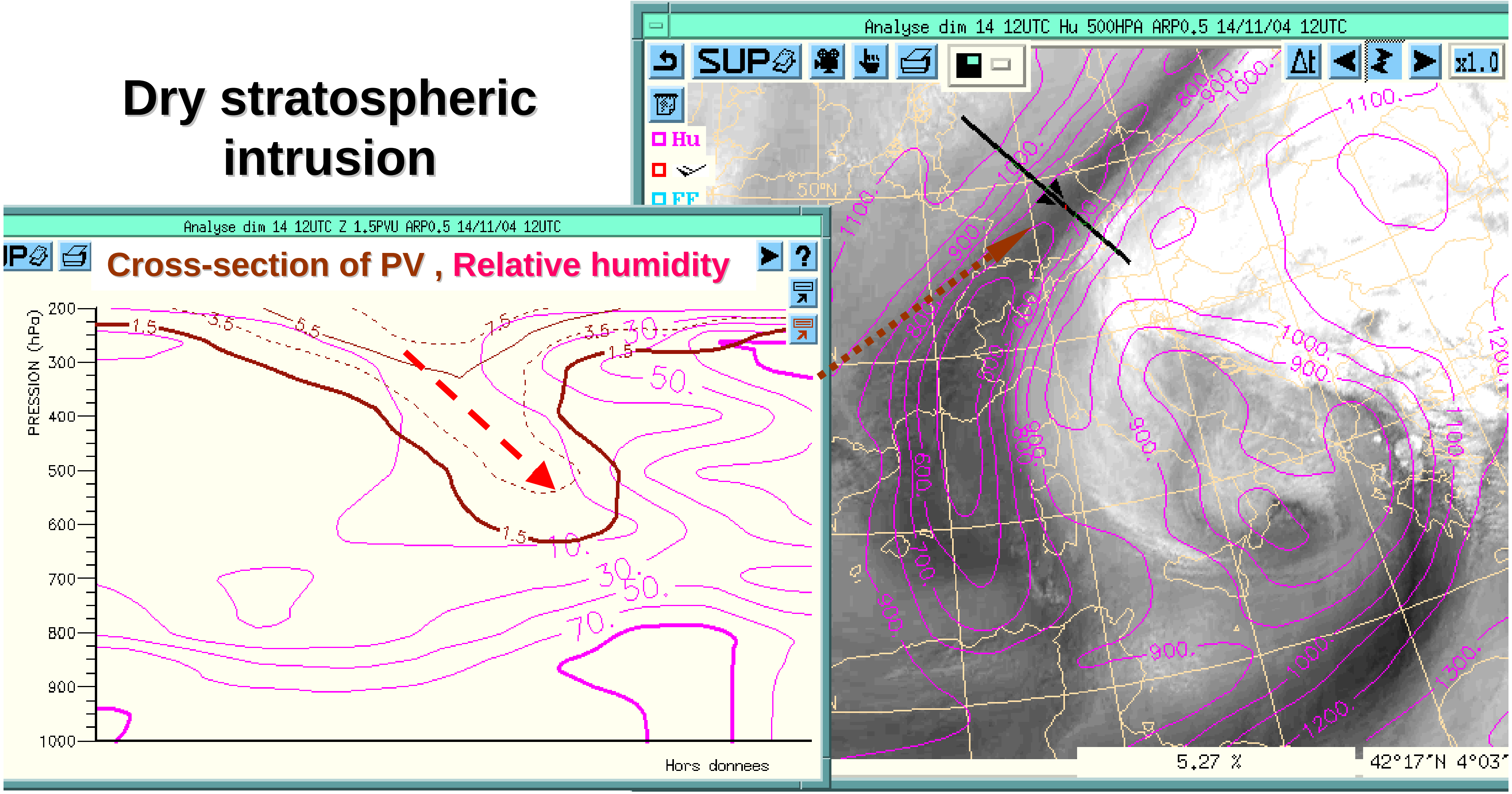

A PV anomaly is associated with very dry stratospheric air down to middle troposphere along with the zone of tropopause folding. The NWP model sees the dynamical tropopause at 600 hPa confimed by the WV image.

PV concept and upper air soundings

6.2 μm image, 1.5 PVU heights

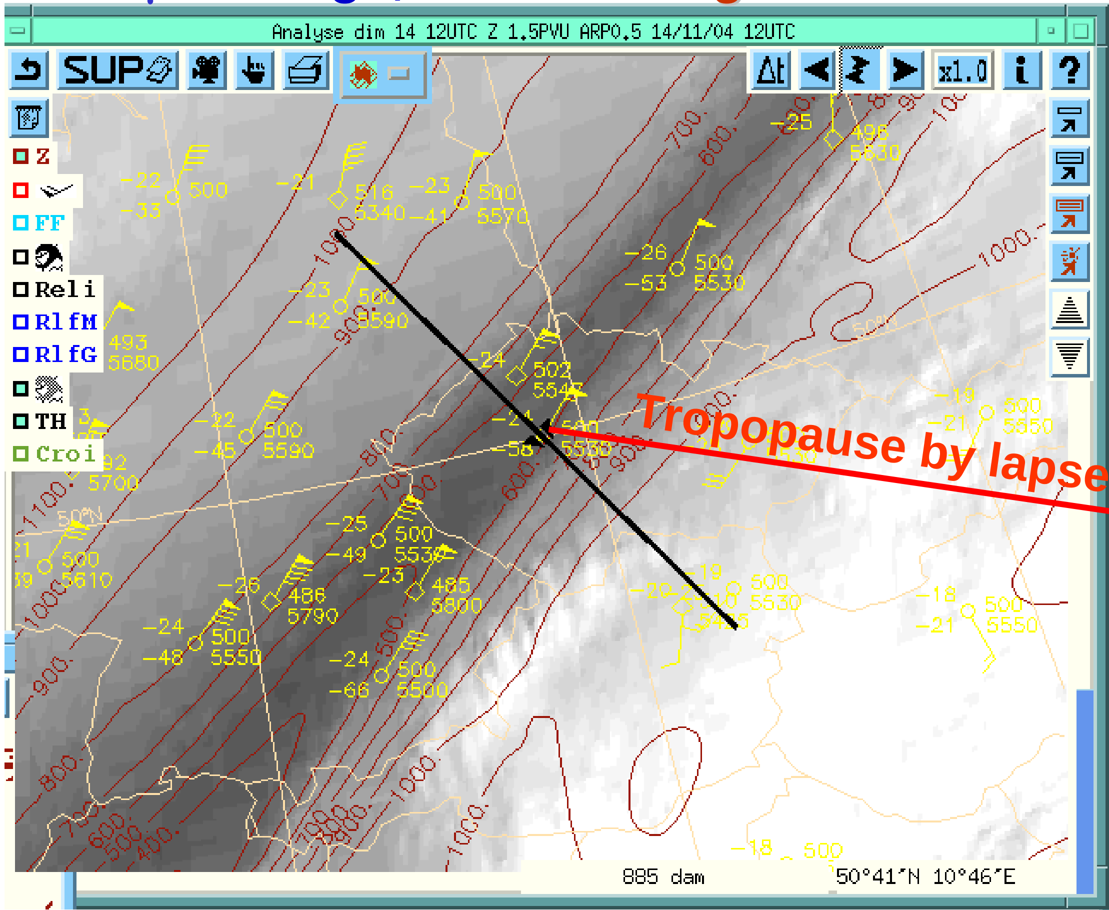

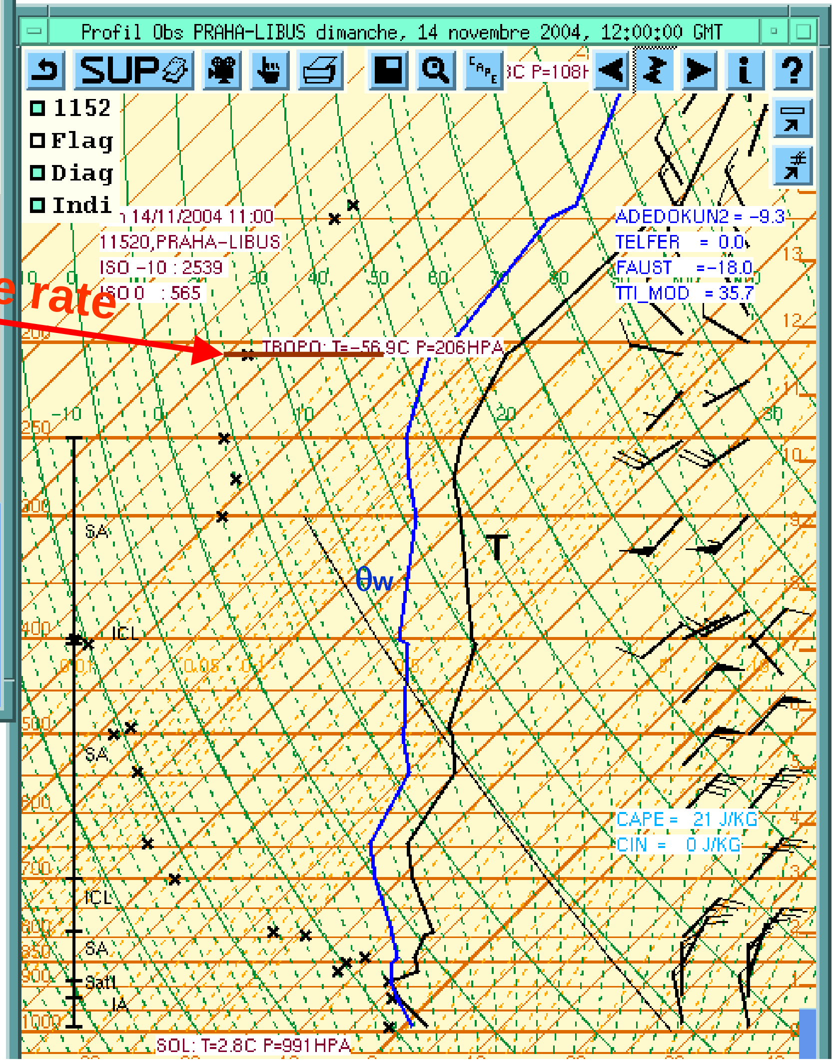

The tropopause level, derived by using temperature lapse rate is not correct with references to the wind field and WV image (as an observational tool) in terms of PV concept.

PV concept and upper air soundings

6.2 µm image, 1.5 PVU heights

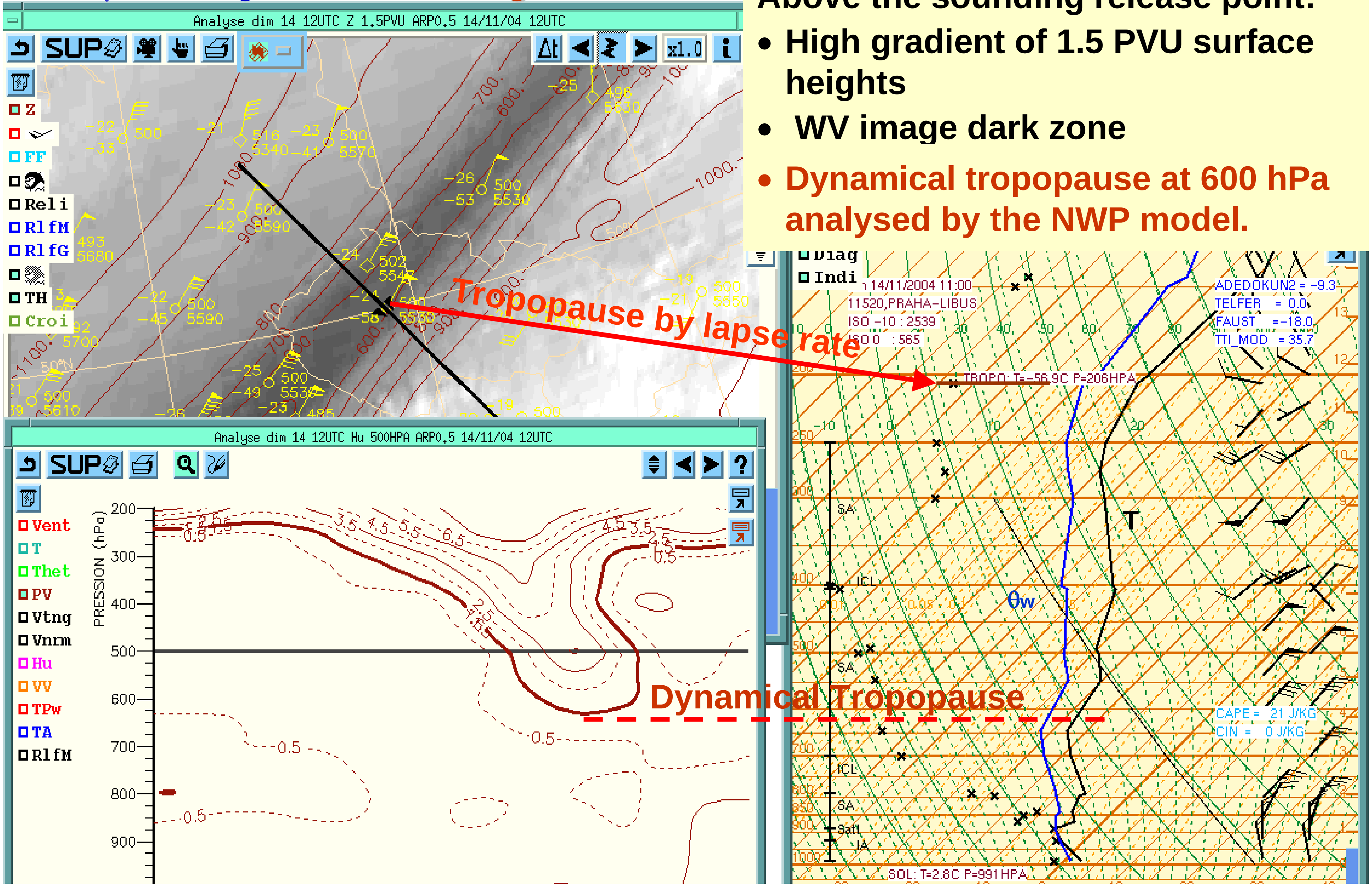

Above the sounding release point:

- **High gradient of 1.5 PVU surface heights**
- **WV image dark zone**
- **Dynamical tropopause at 600 hPa analysed by the NWP model.**

WV imagery and mid/upper level dynamical fields

1.5 PVU surface heights / wind at 300 hPa (only > 100 kt)

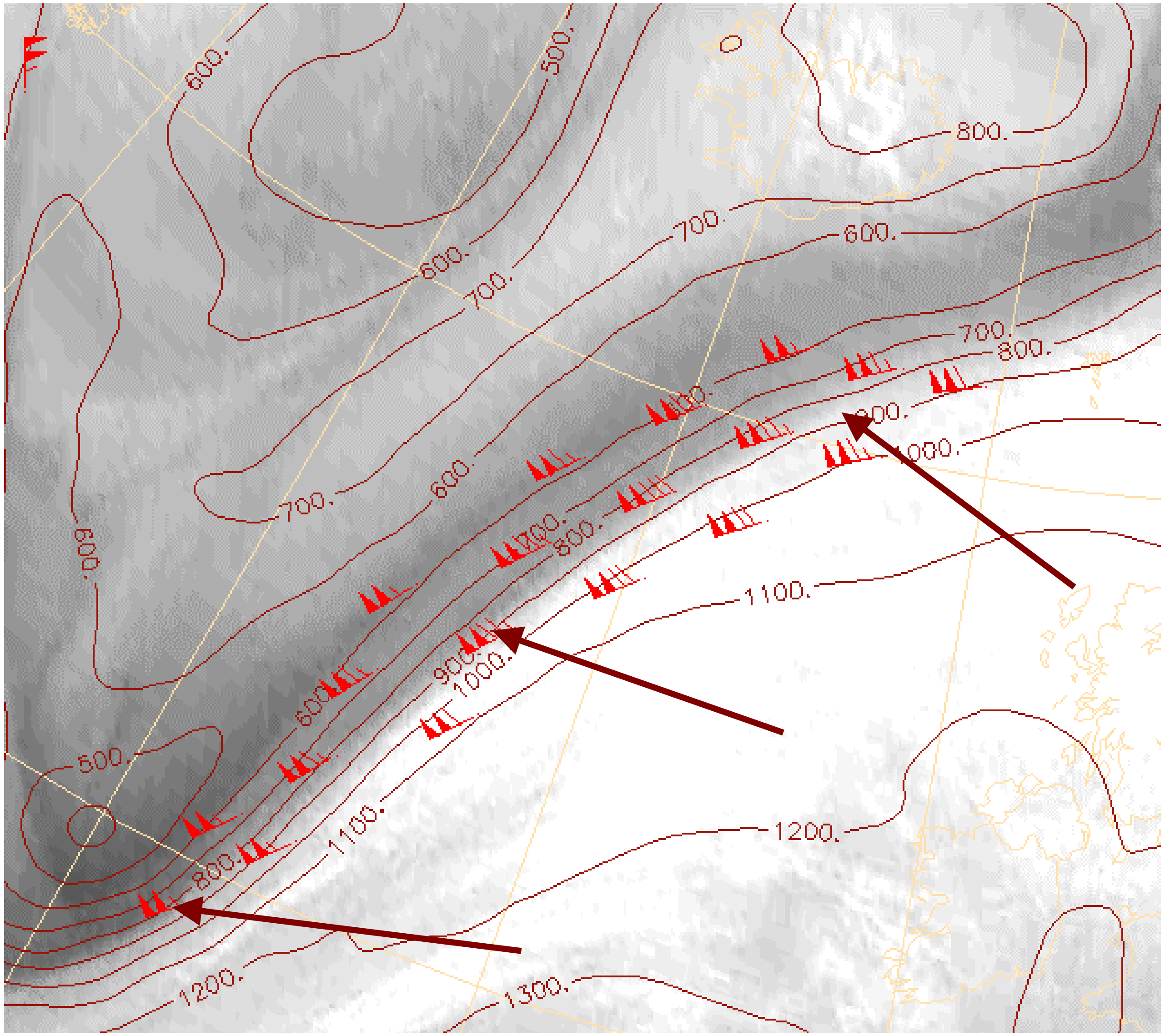

An area of strong gradient of the dynamical tropopause heights produces sharp boundary between different moisture regime on the WV image: Stratospheric (dry) and Tropospheric (moist) air. This boundary is also aligned with the zone of the highest upper-level wind speed.

WV imagery and mid/upper level dynamical fields

Contours of wind speed > 100 kt / wind > 80 kt at 300 hPa

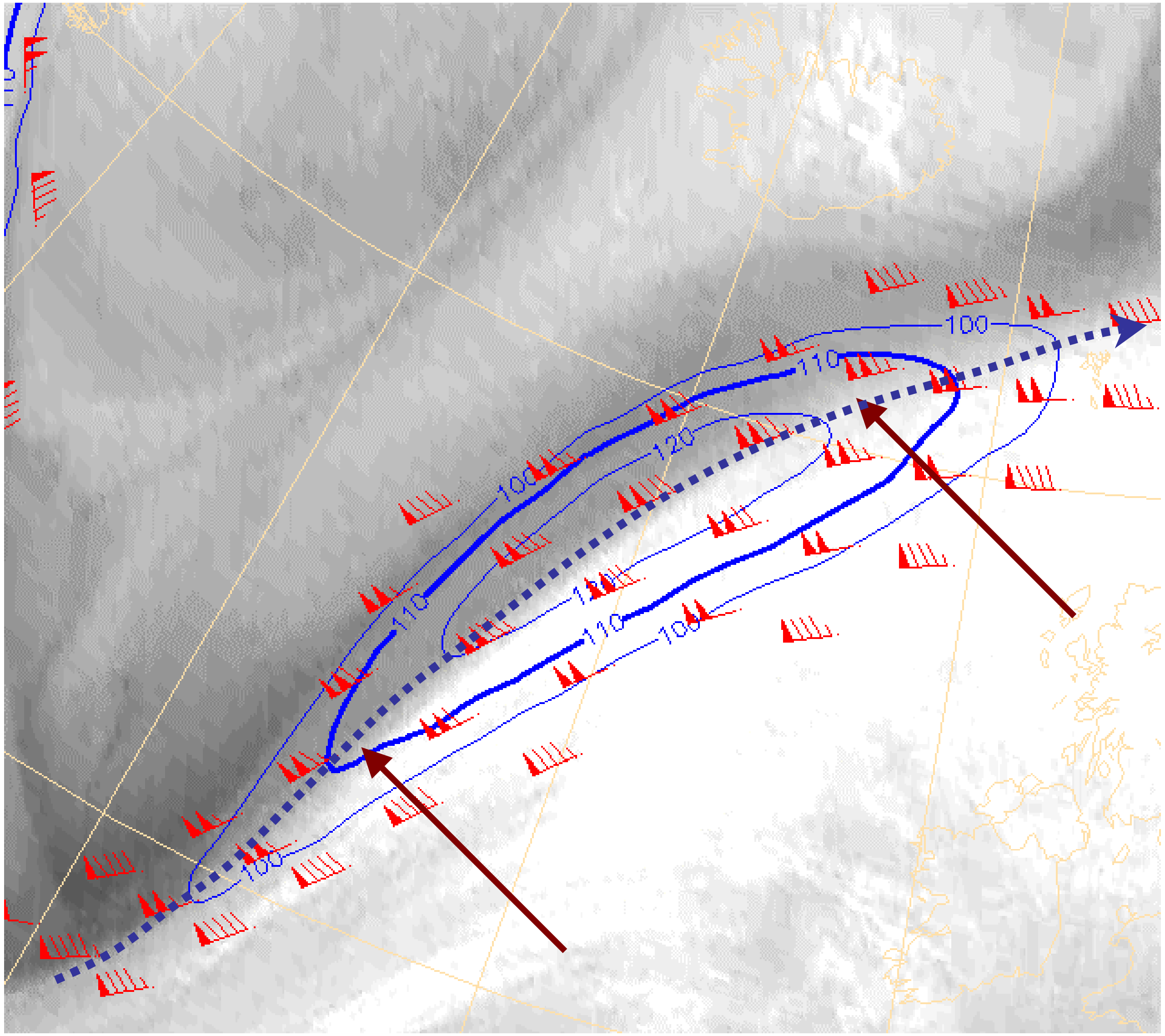

Generally, the moisture boundaries on the WV images oriented from southwest to northeast are nearly coincident with well defined jet stream axes.

The jet streak is likely along the most contrast part of the moisture boundary in the WV image.

UPPER-LEVEL JET AND PV ANOMALY

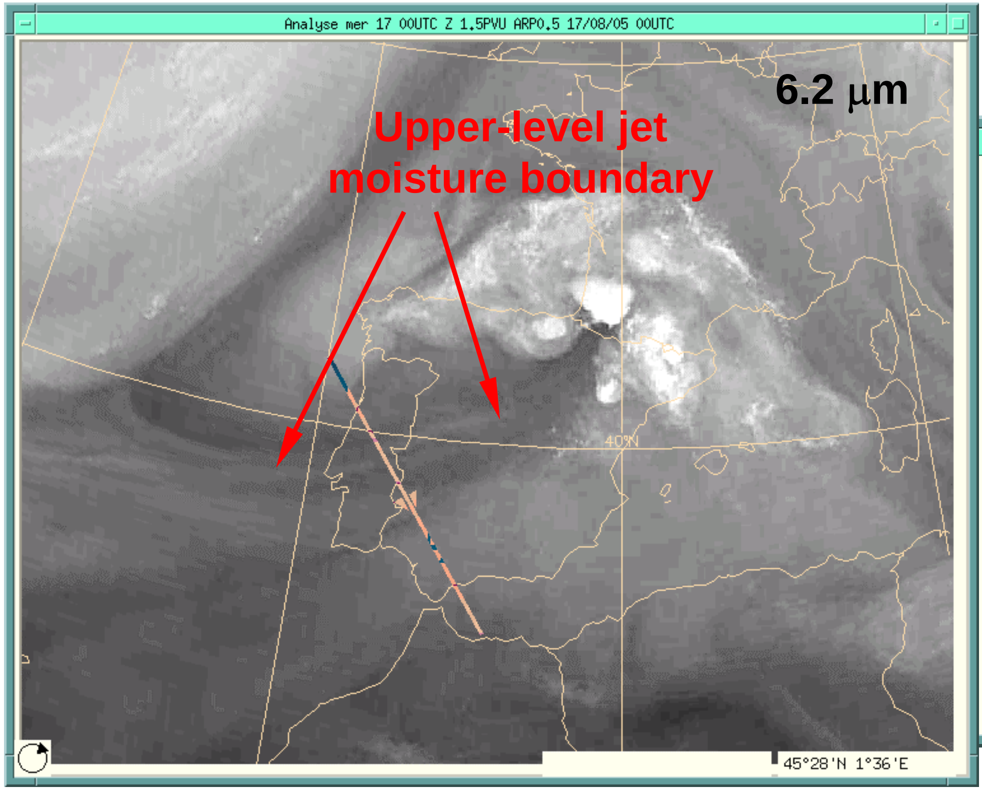

Cross-section of wind and
potential vorticity (PV)

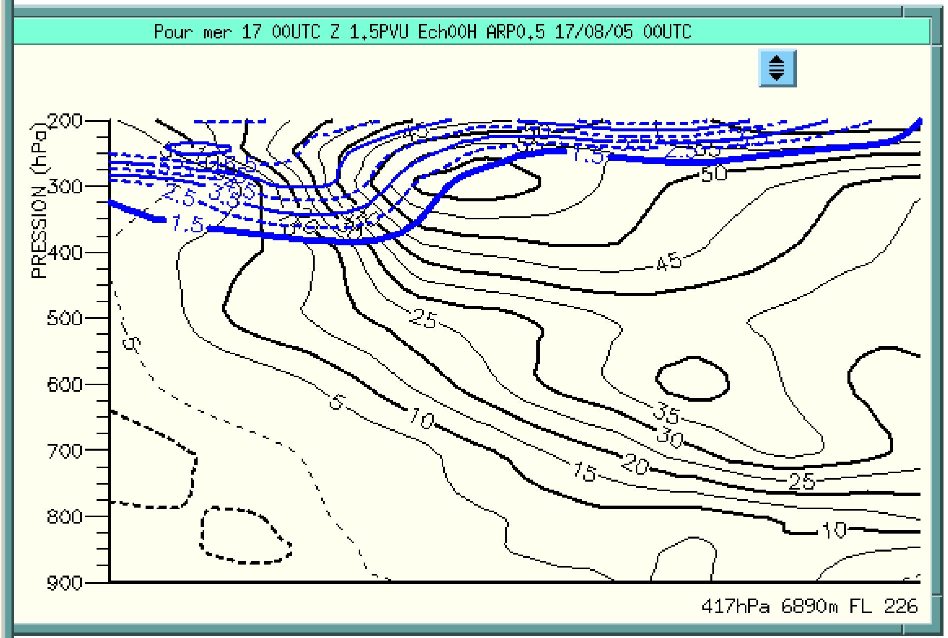

The dynamical structure of the jet stream zone in the view of the PV concept may be seen in the vertical cross-section across the moisture boundary in the 6.2 μm image.

UPPER-LEVEL JET AND PV ANOMALY

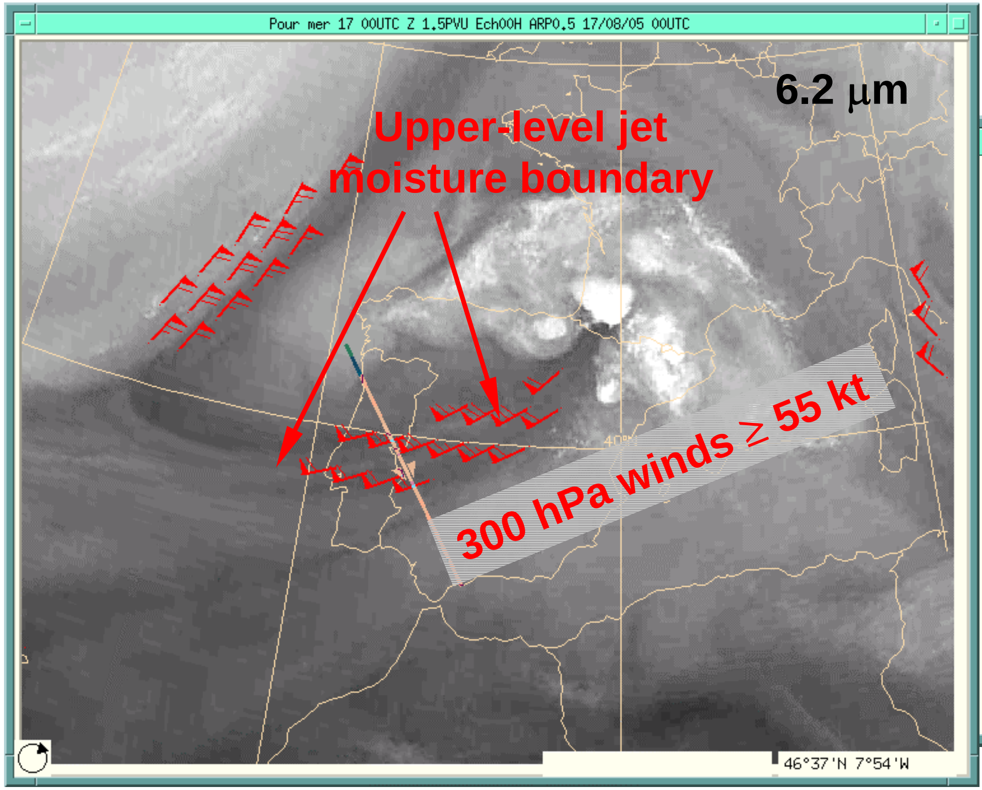

Cross-section of wind and potential vorticity (PV)

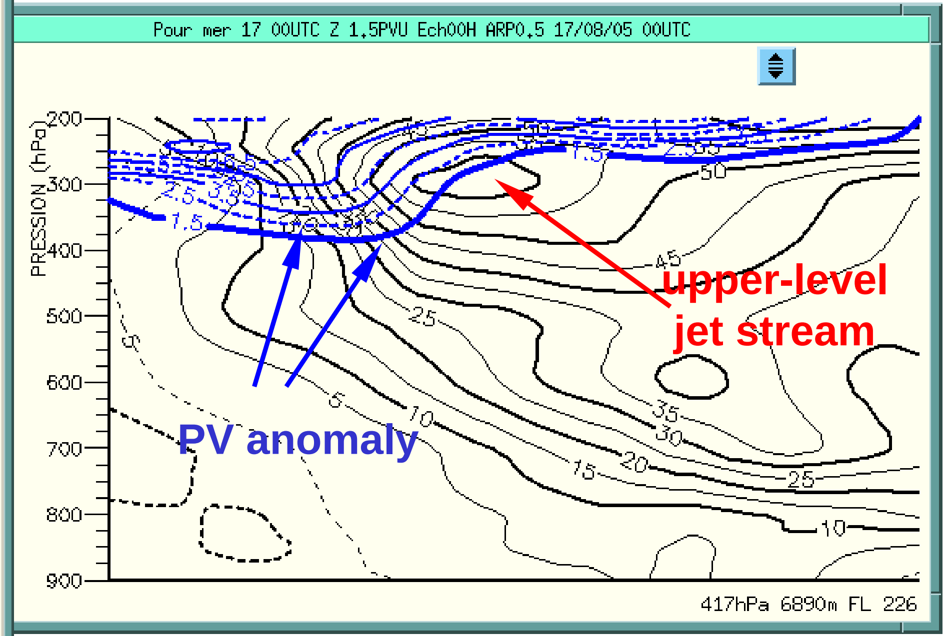

The dynamical structure of the jet stream zone in the view of the PV concept: vertical cross-section across the moisture boundary in the 6.2 µm image.

The position of the maximum wind-speed contour coincides with the zone of folding of the tropopause (1.5 PVU constant surface) associated with an upper-troposphere PV anomaly.

6.2 μm WV IMAGERY DIAGNOSIS

UPPER-LEVEL FORCING OF CYCLOGENESIS

A case over the Eastern Meditarranean
18 – 20 March 2009

Polar cyclogenesis over Eastern Mediterranean

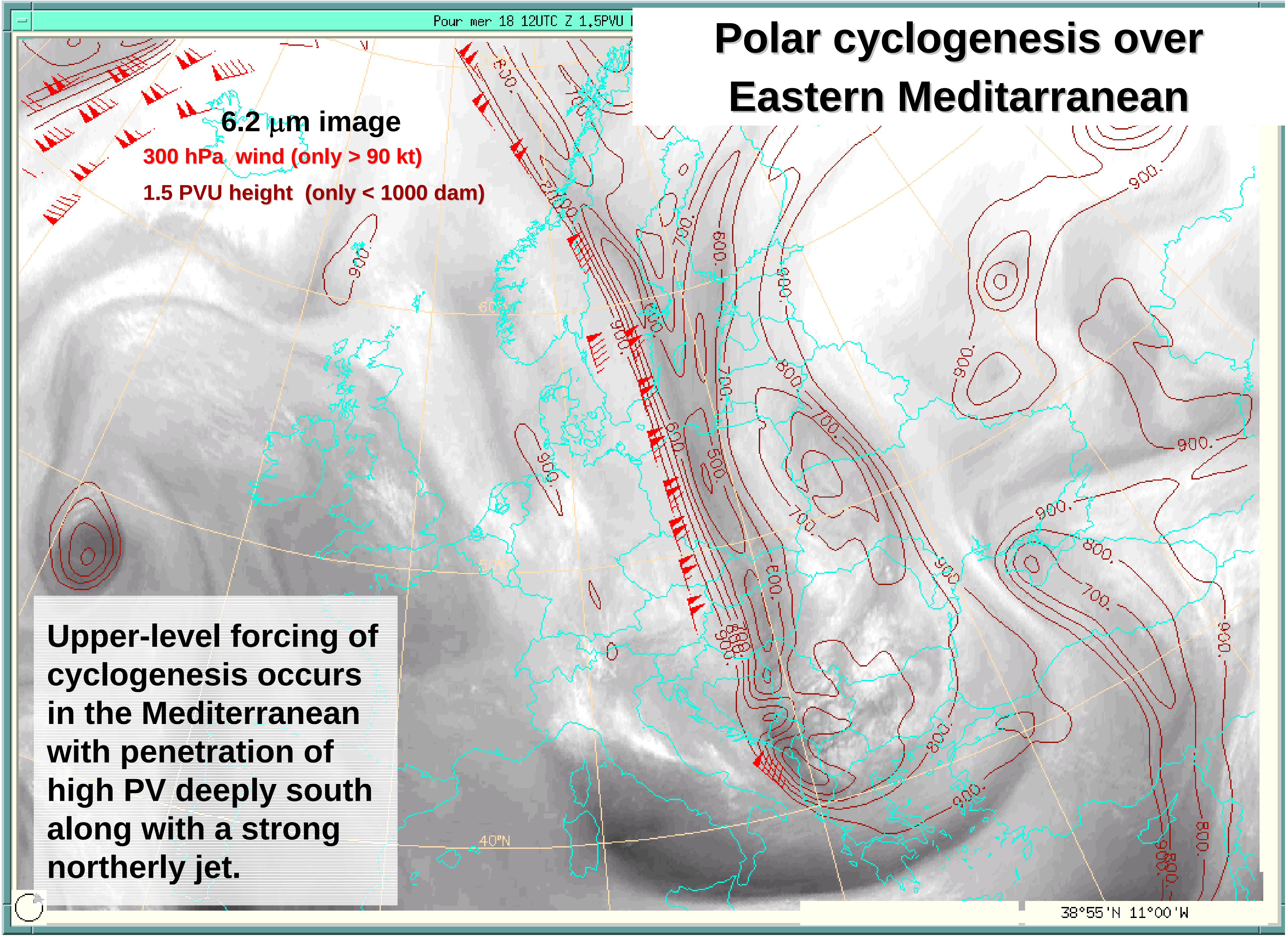

Upper-level forcing of cyclogenesis occurs in the Mediterranean with penetration of high PV deeply south along with a strong northerly jet.

Polar cyclogenesis over Eastern Mediterranean

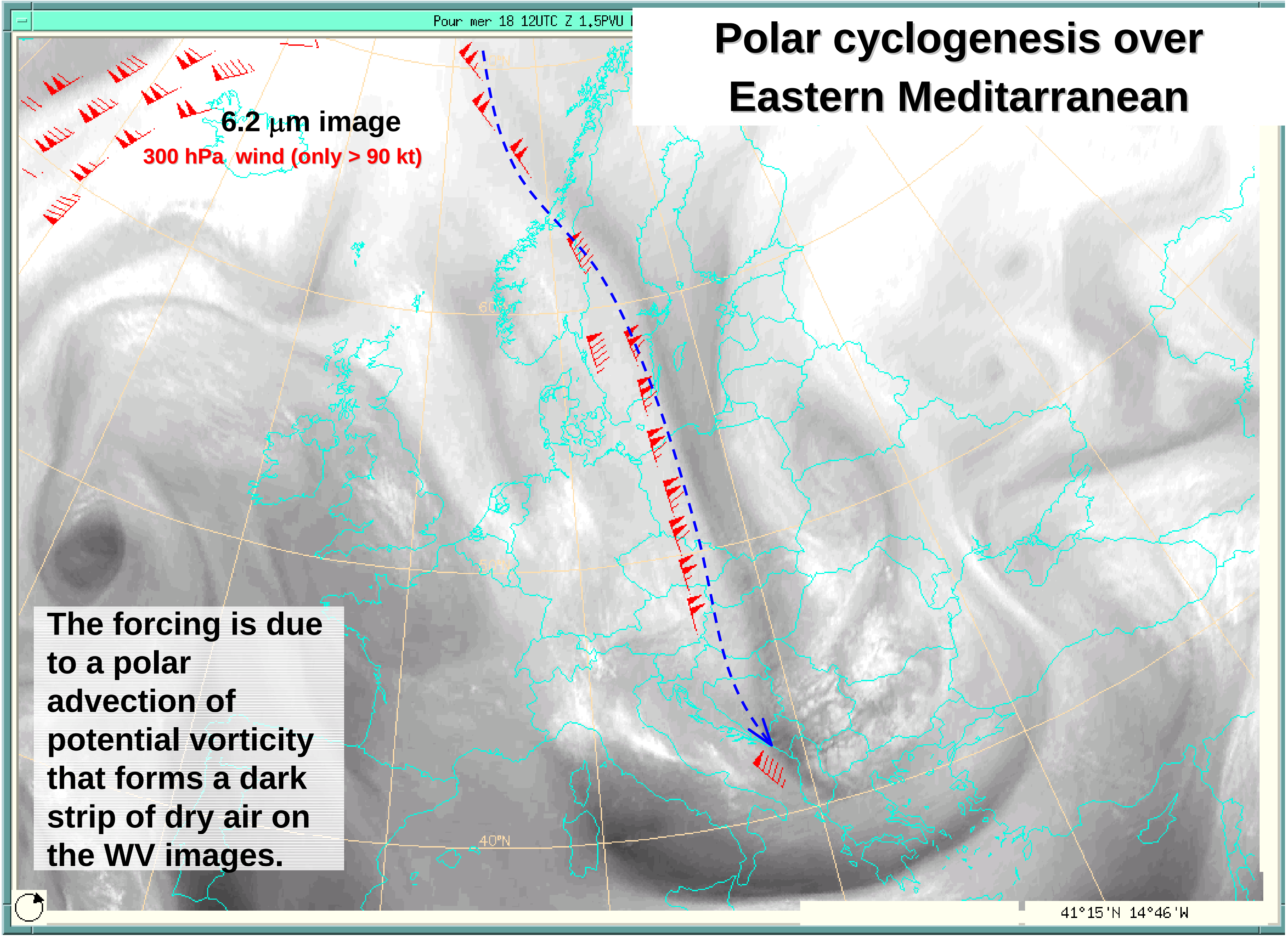

The forcing is due to a polar advection of potential vorticity that forms a dark strip of dry air on the WV images.

Polar cyclogenesis over Eastern Meditarranean

6.2 µm, 1.5 PVU height (> 1000 dam), 300 hPa wind (> 90 kt), 850 hPa θ_w (> 6 °C) 12 UTC

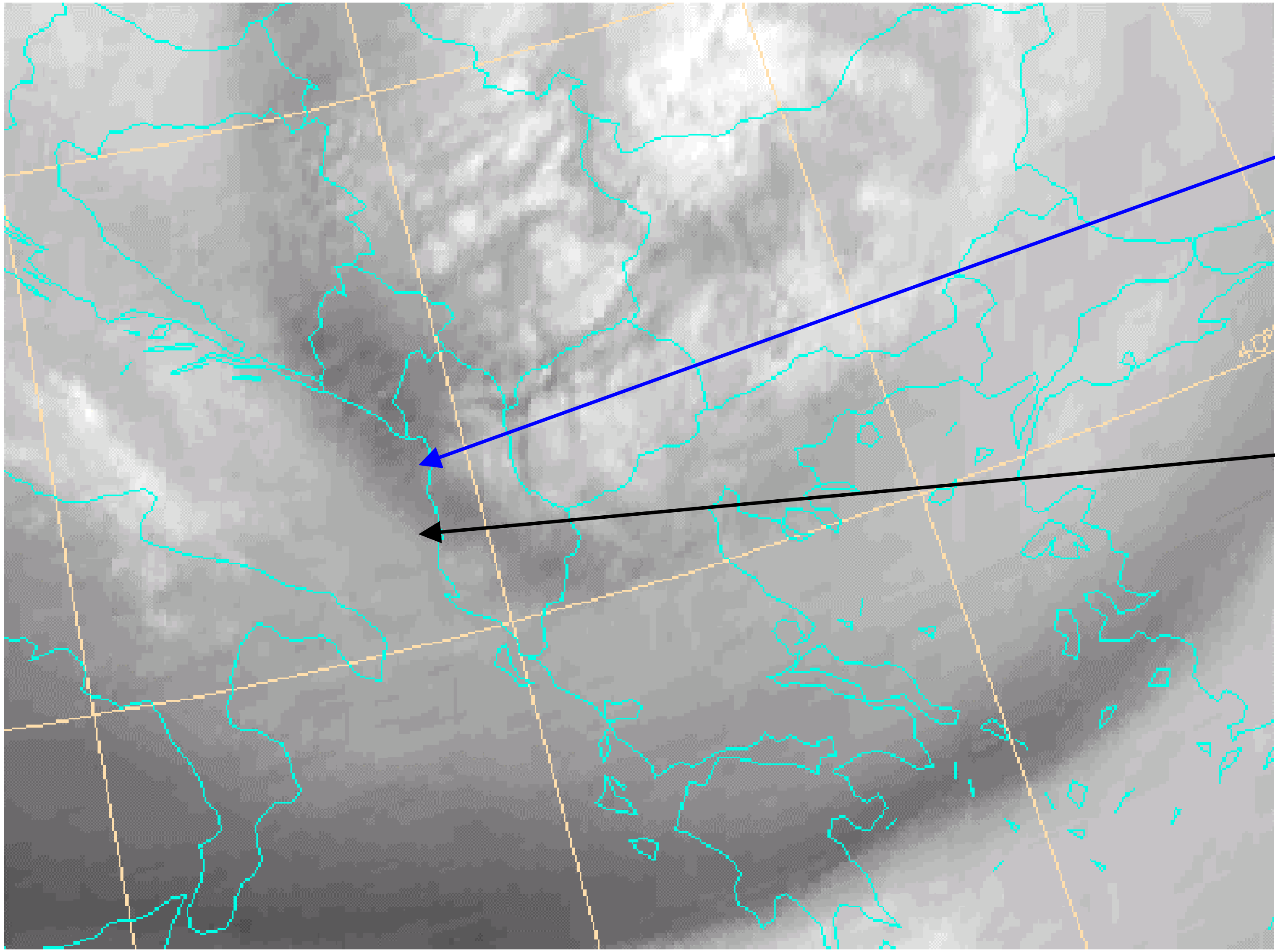

Ingredients:

Tropopause anomaly:
- WV image dark zone

Polar jet stream
- WV image moisture boundary

Polar cyclogenesis over Eastern Meditarranean

6.2 µm, 1.5 PVU height < 900 dam), and 1.5 PVU wind (> 90 kt), 850 hPa θ_w (> 6 °C) 12 UTC

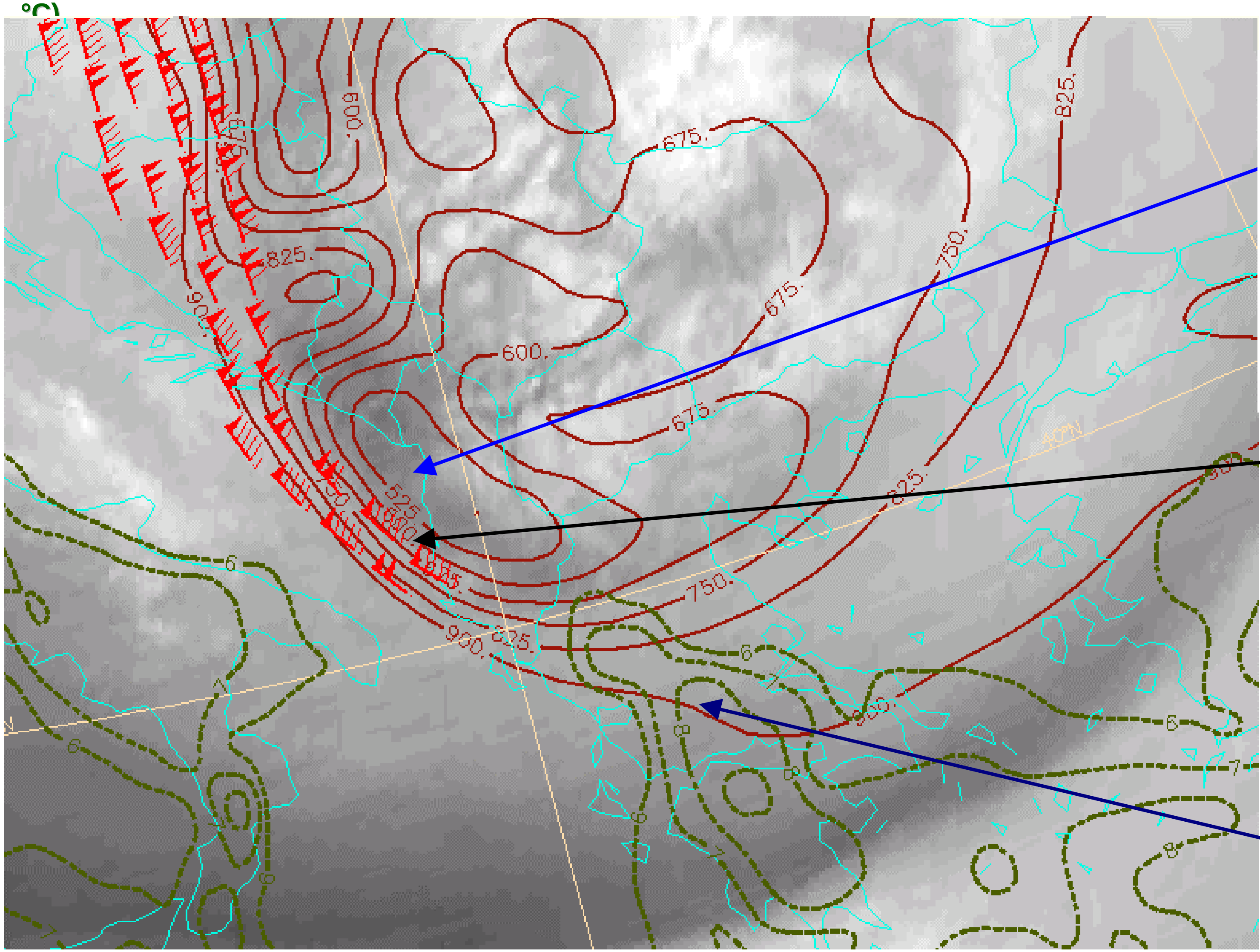

Ingredients:

Tropopause anomaly:
- WV image dark zone
- low (500hPa) dynamical tropopause

Polar jet stream
- WV image moisture boundary
- gradient zone of the dynamical tropopause height

Low-level warm anomaly

Polar cyclogenesis over Eastern Meditarranean

6.2 µm, 500 hPa Abs. vorticity (only > 30.10-5/s), 500 hPa heights

at 12 UTC

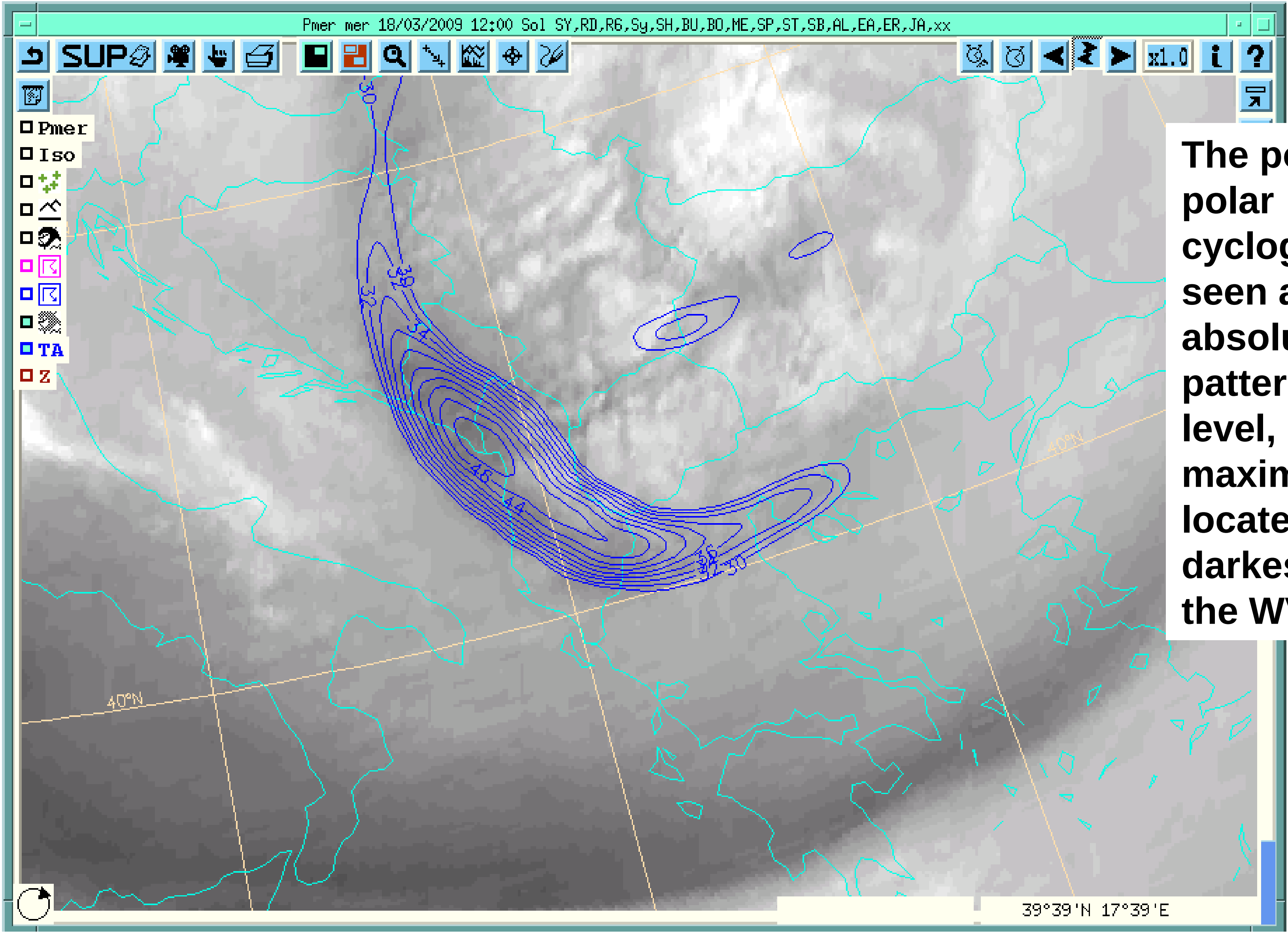

The potential for polar cyclogenesis is seen as a strong absolute vorticity pattern at mid-level, its maximum being located at the darkest part of the WV image.

Polar cyclogenesis over Eastern Meditarranean

6.2 µm, 500 hPa Abs. vorticity (only > 30.10-5/s), 500 hPa heights

at 12 UTC

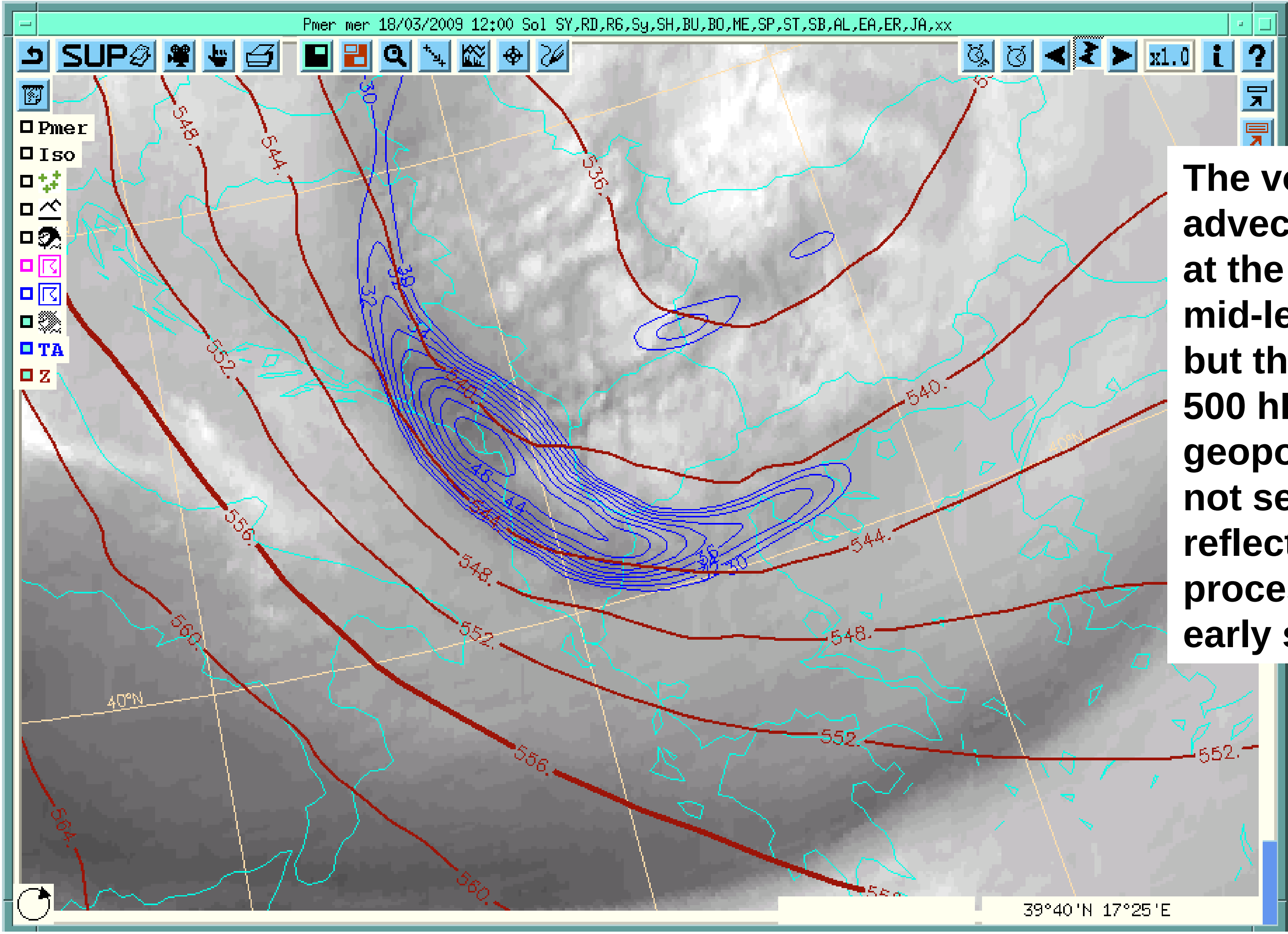

The vorticity advection occurs at the base of the mid-level trough, but the field of 500 hPa geopotential is not sensitive to reflect the process at an early stage.

Polar cyclogenesis over Eastern Meditarranean

6.2 µm, 500 hPa Abs. vorticity (only > 30.10^{-5}/s), MSLP obs. (each 2 hPa)

at 15 UTC

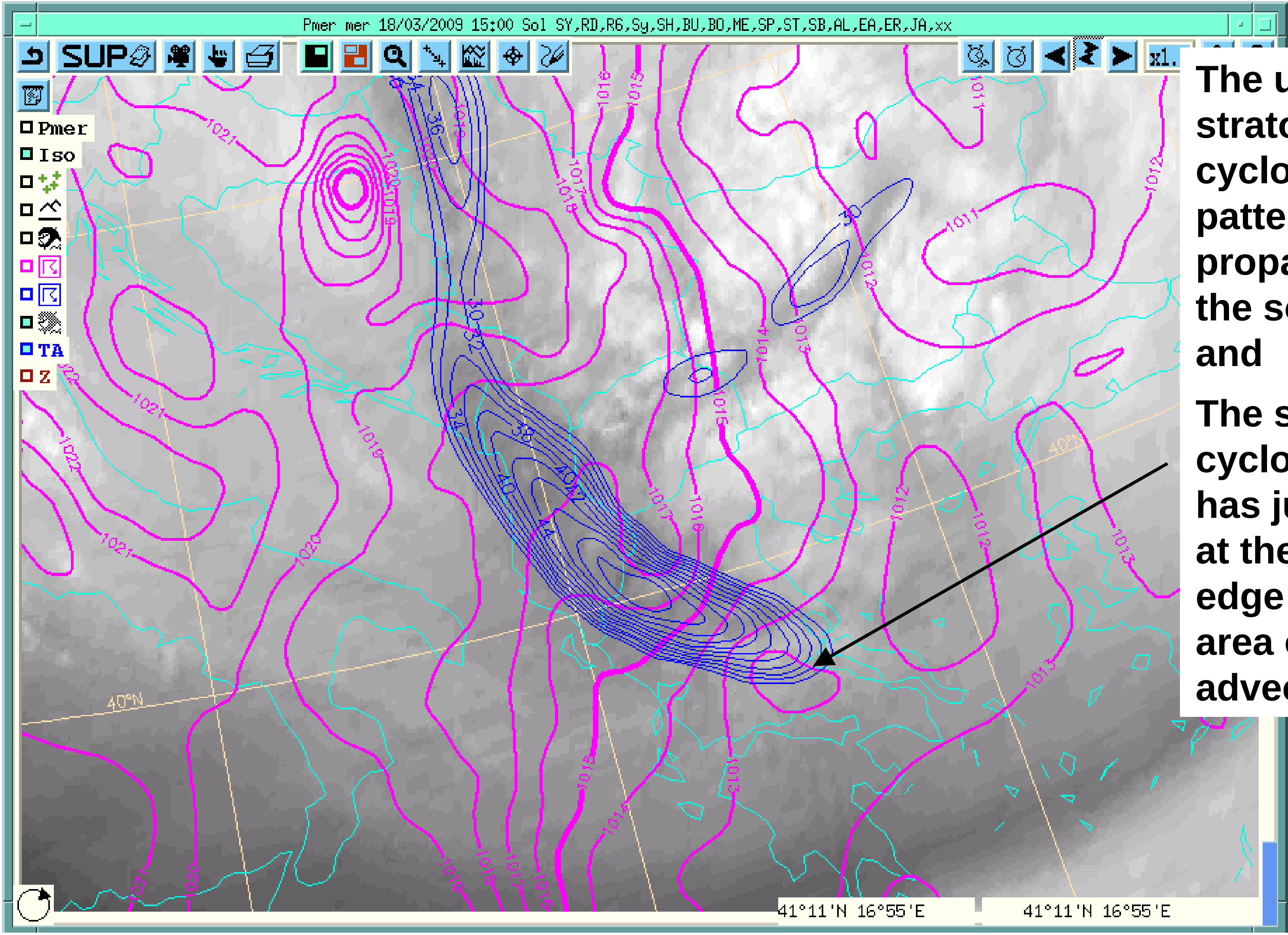

The upper-level stratospheric cyclonic vorticity pattern propagated to the south-east and

The surface cyclogenesis has just started at the leading edge of the area of vorticity advection

Polar cyclogenesis over Eastern Meditarranean

6.2 µm, 1.5 PVU heights (< 900 dam), 1.5 PVU wind (>90 kt),), 850 hPa θ_w (> 6 °C)

at 15 UTC

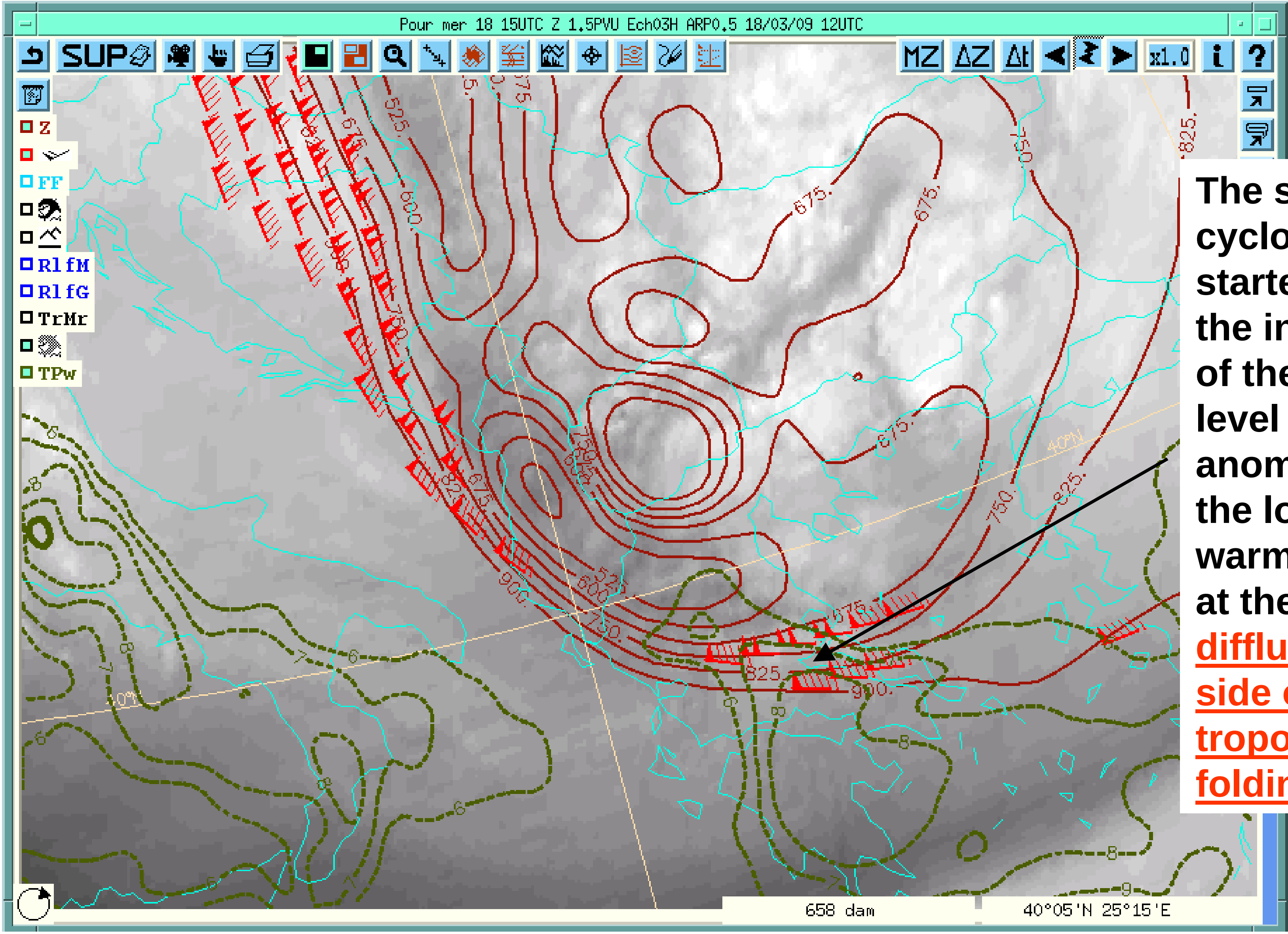

The surface cyclogenesis started after the interaction of the upper-level PV anomaly with the low-level warm anomaly at the leading diffluent-flow side of the tropopause folding .

Polar cyclogenesis over Eastern Meditarranean

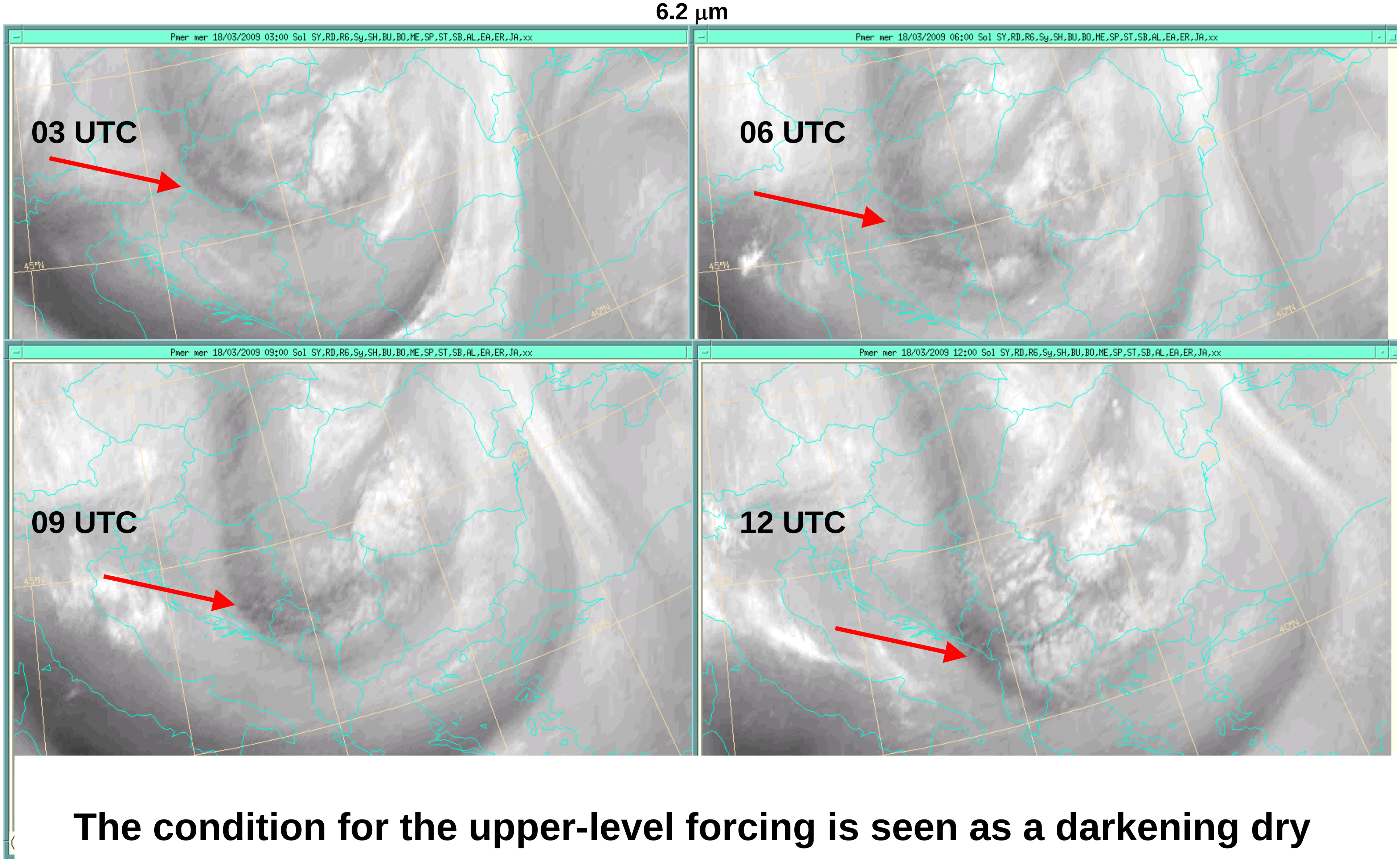

The condition for the upper-level forcing is seen as a darkening dry zone in the sequence of 6.2 μm WV image.

WV imagery patterns of cyclone dynamics

18/03 12 UTC

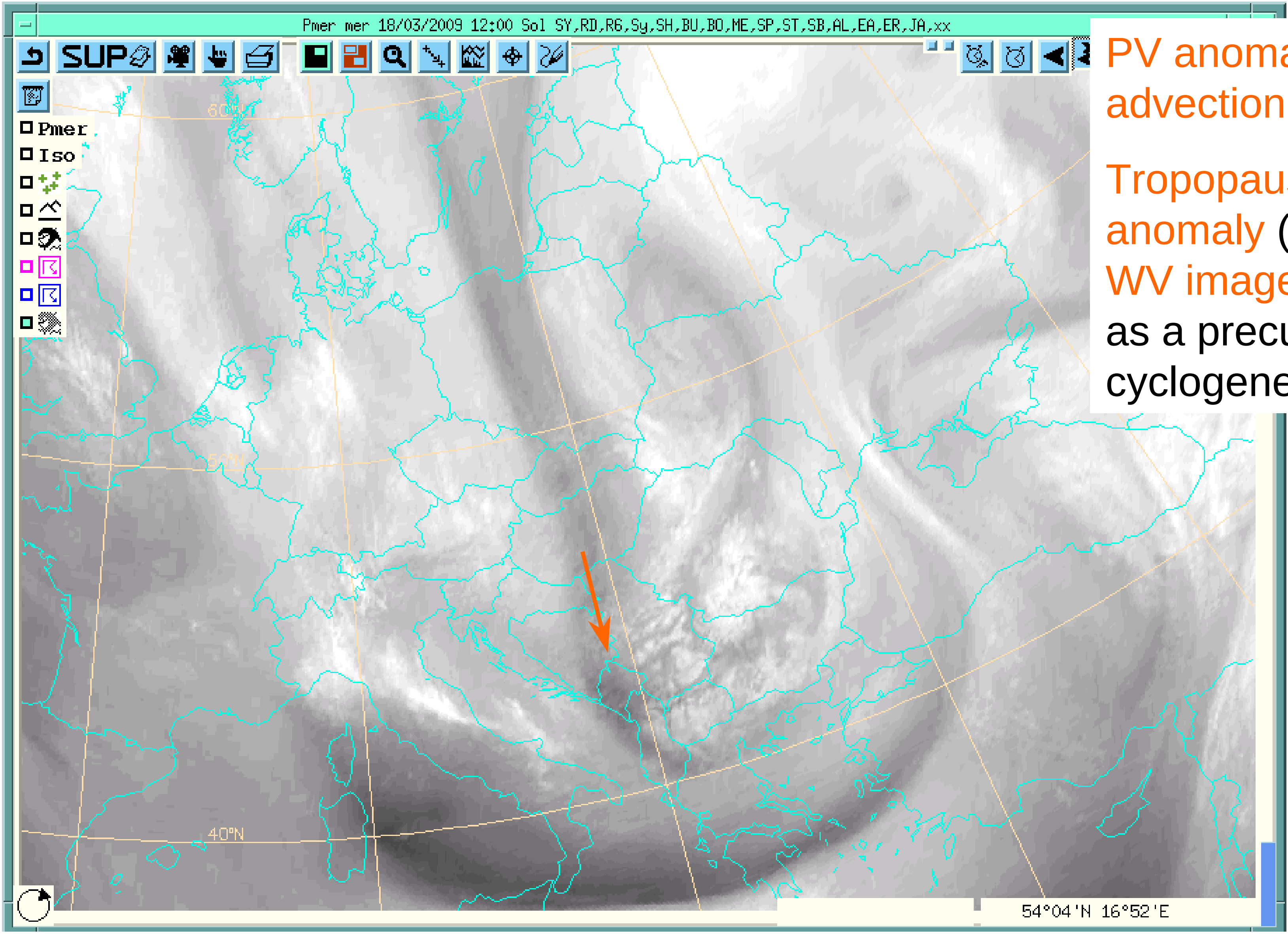

PV anomaly advection

Tropopause dynamic anomaly (darkening WV image dry zone) as a precursor of cyclogenesis

WV imagery patterns of cyclone dynamics

6.2 µm

18/03 21 UTC

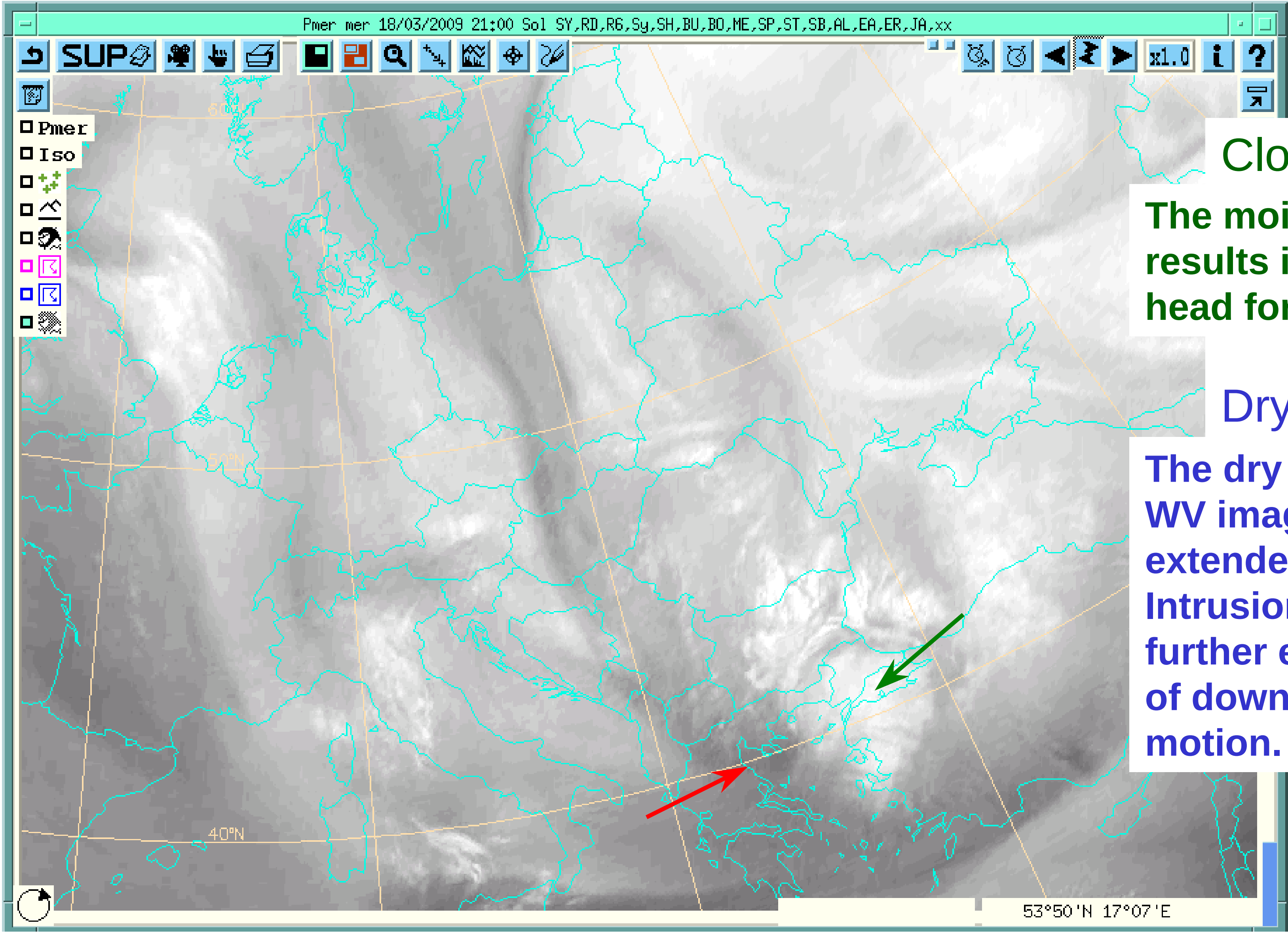

Cloud head

The moist ascent results in a cloud head formation.

Dry intrusion

The dry zone in the WV imagery has extended to a Dry Intrusion related to further expanding of downward motion.

WV imagery patterns of cyclone dynamics

6.2 μm, MSLP obs. (each 2 hPa)

19/03 00 UTC

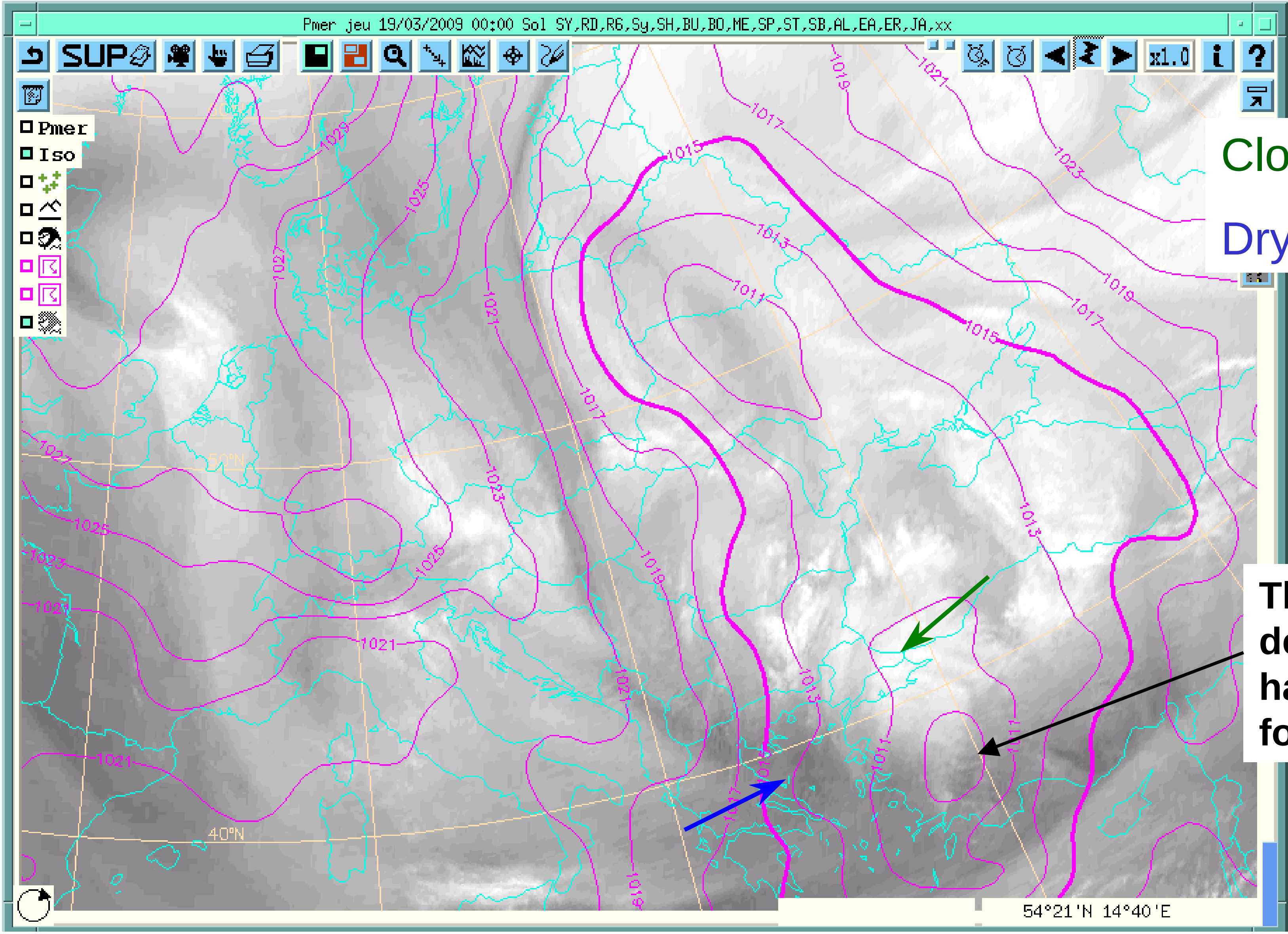

Cloud head

Dry intrusion

The surface depression has already formed.

WV imagery patterns of cyclone dynamics

6.2 µm, MSLP obs. (each 2 hPa)

19/03 03 UTC

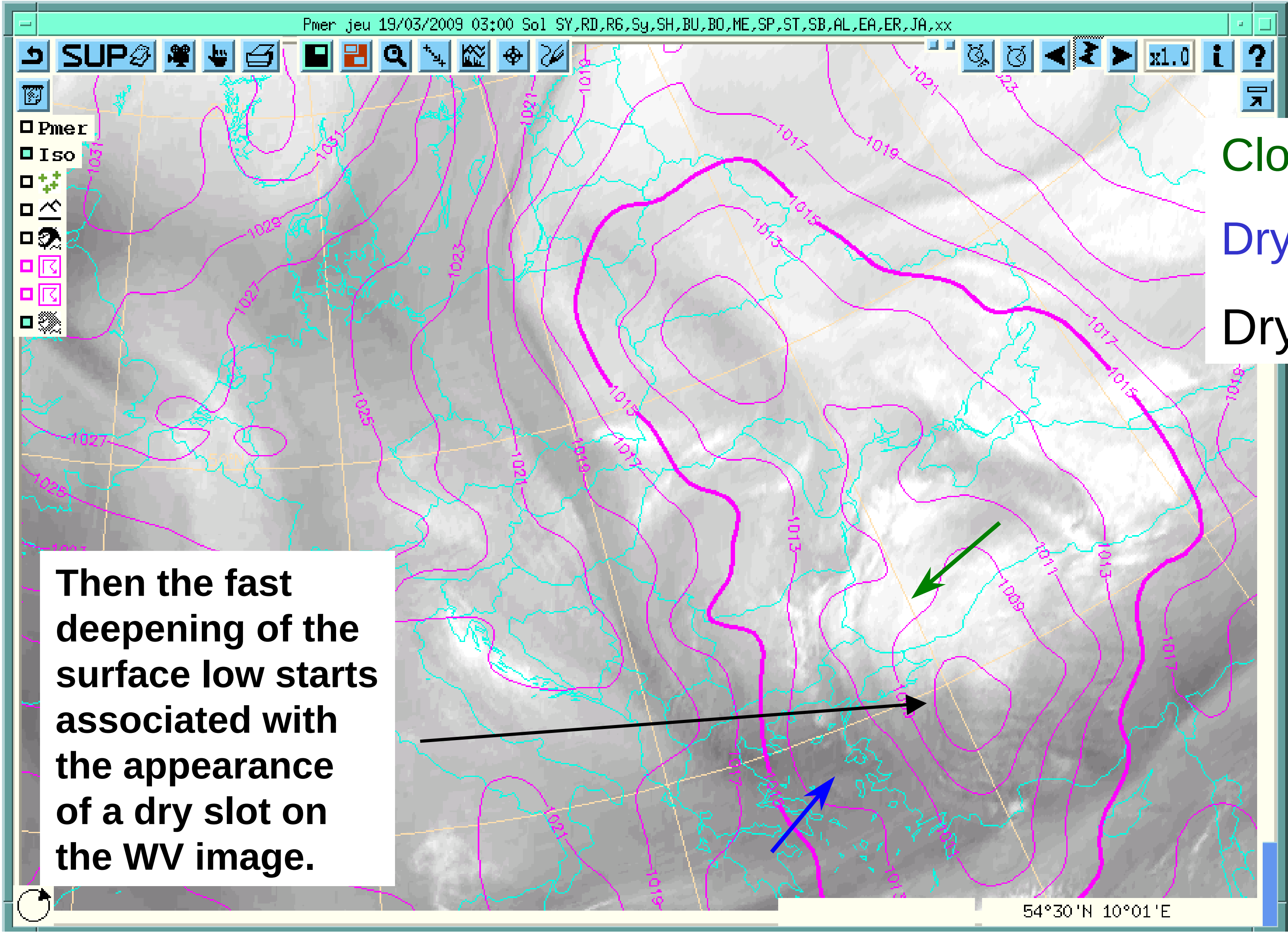

Cloud head

Dry intrusion

Dry slot

Then the fast deepening of the surface low starts associated with the appearance of a dry slot on the WV image.

WV imagery patterns of cyclone dynamics

6.2 μm

19/03 09 UTC

Looking at the image grey shades in the 6.2 μm, indicate the position of the dry slot related to the surface cyclogenesis.

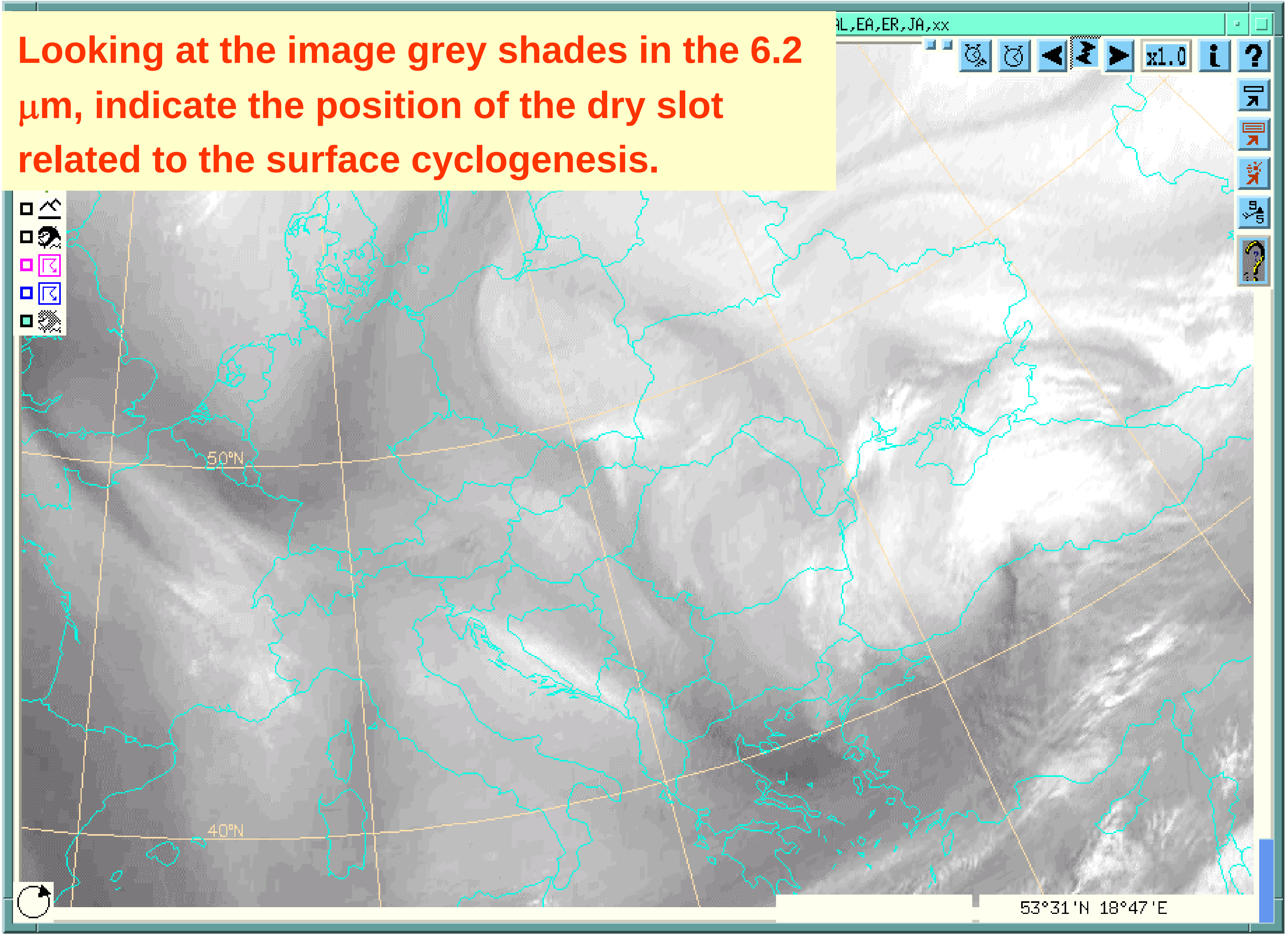

WV imagery patterns of cyclone dynamics

6.2 µm, MSLP obs. (each 2 hPa)

19/03 09 UTC

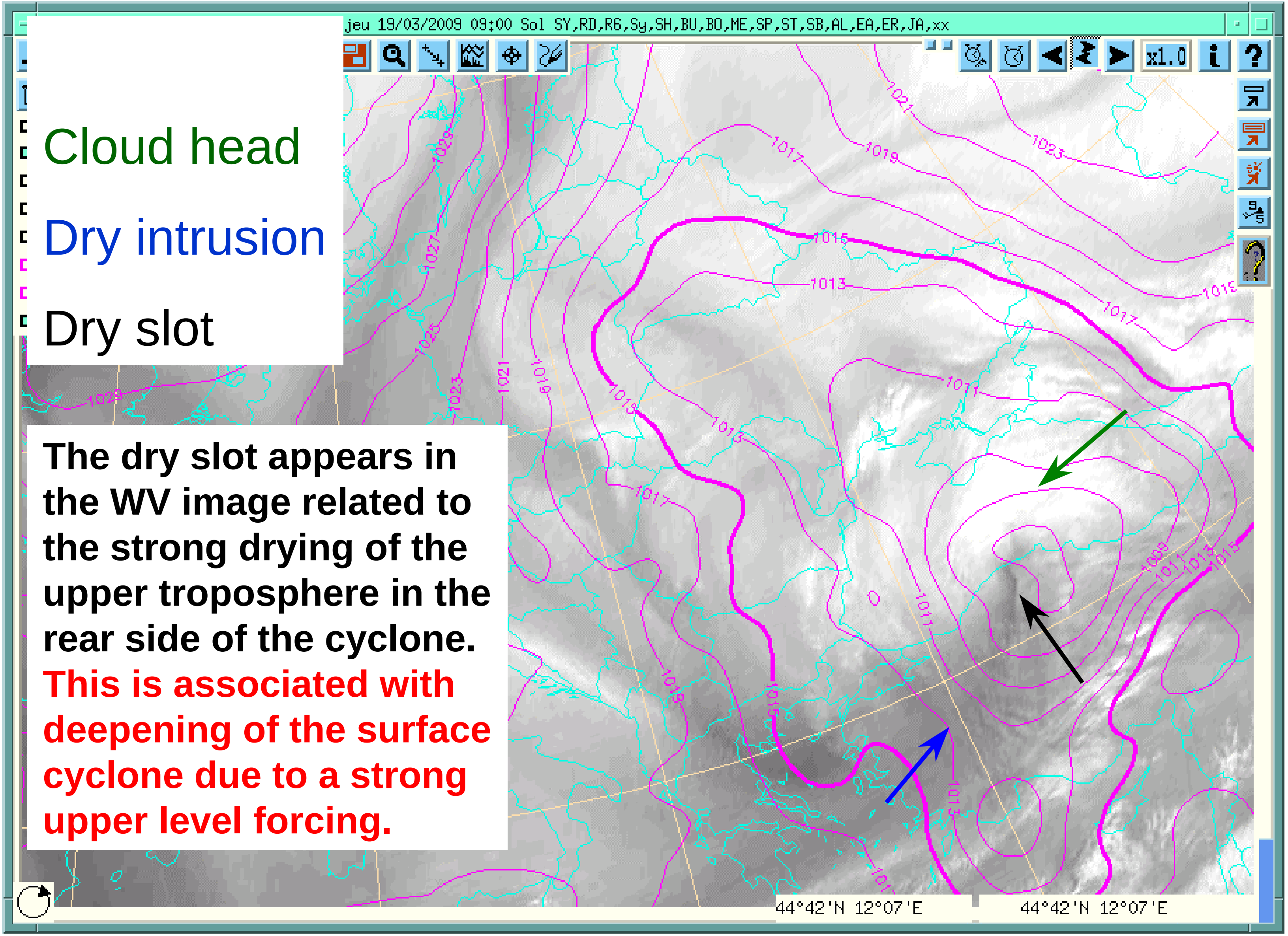

The dry slot appears in the WV image related to the strong drying of the upper troposphere in the rear side of the cyclone. This is associated with deepening of the surface cyclone due to a strong upper level forcing.

Polar cyclogenesis over Eastern Mediterranean

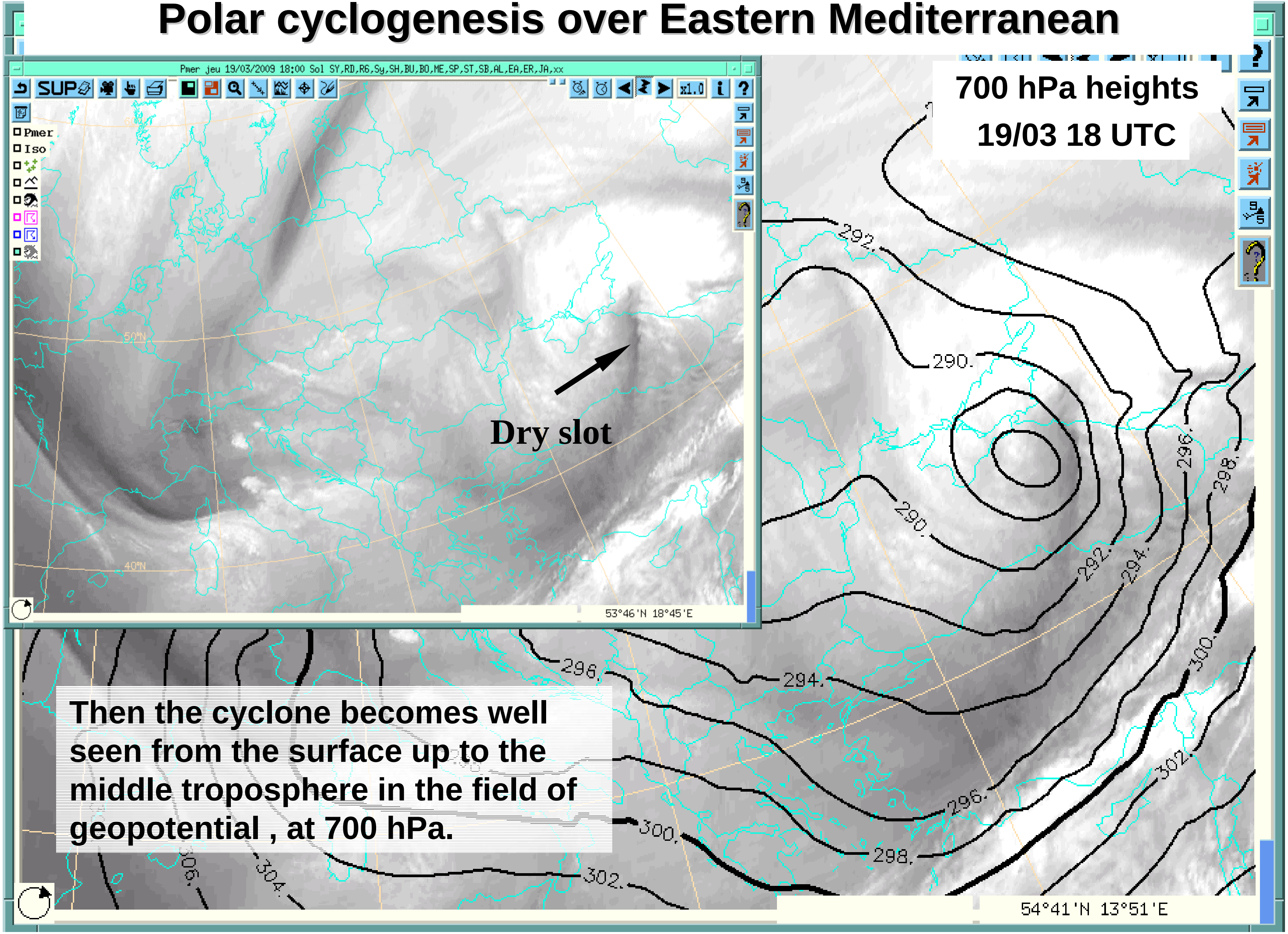

Then the cyclone becomes well seen from the surface up to the middle troposphere in the field of geopotential , at 700 hPa.

Polar cyclogenesis over Eastern Mediterranean

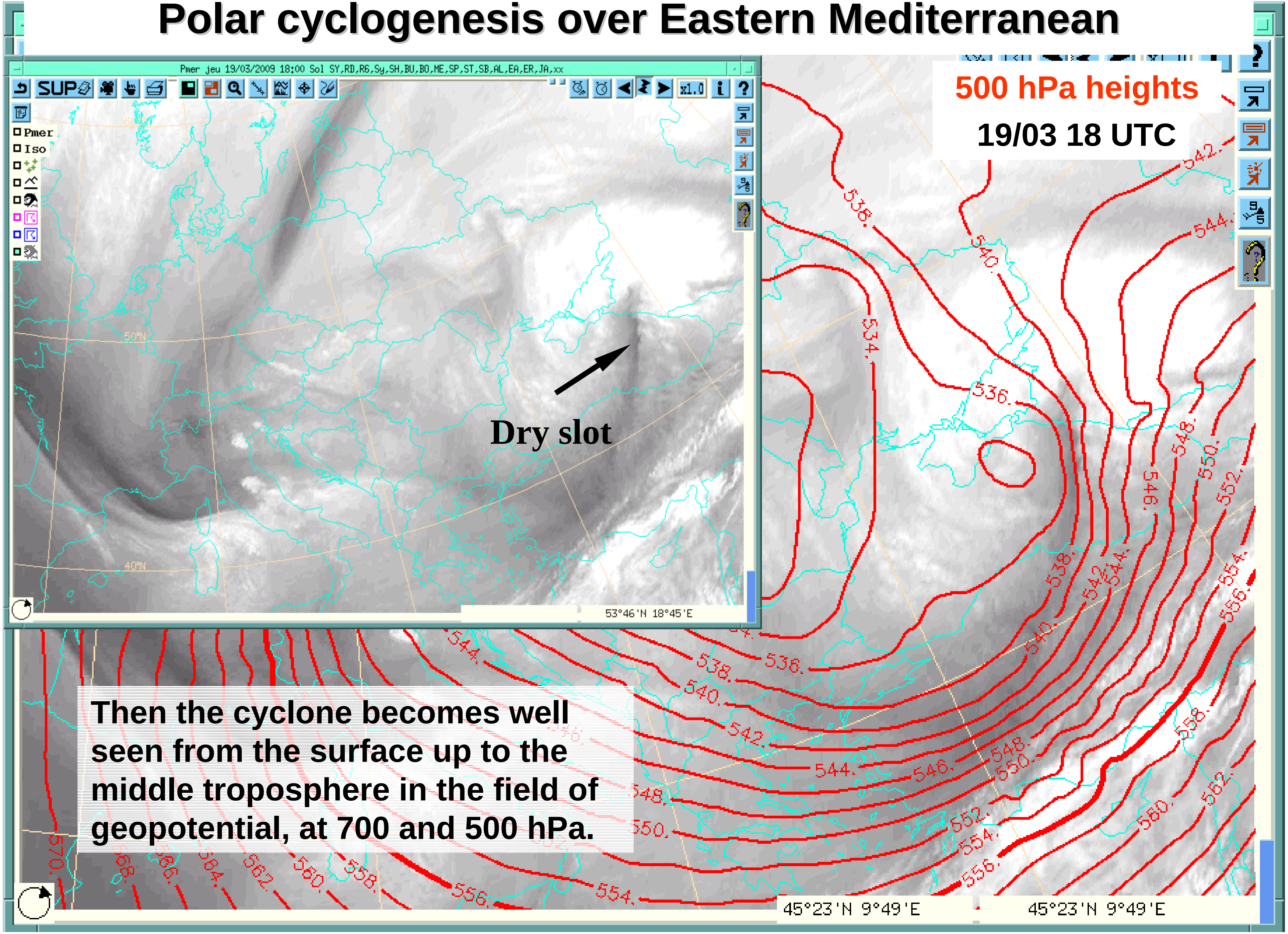

WV imagery patterns of cyclone dynamics

19/03 21 UTC

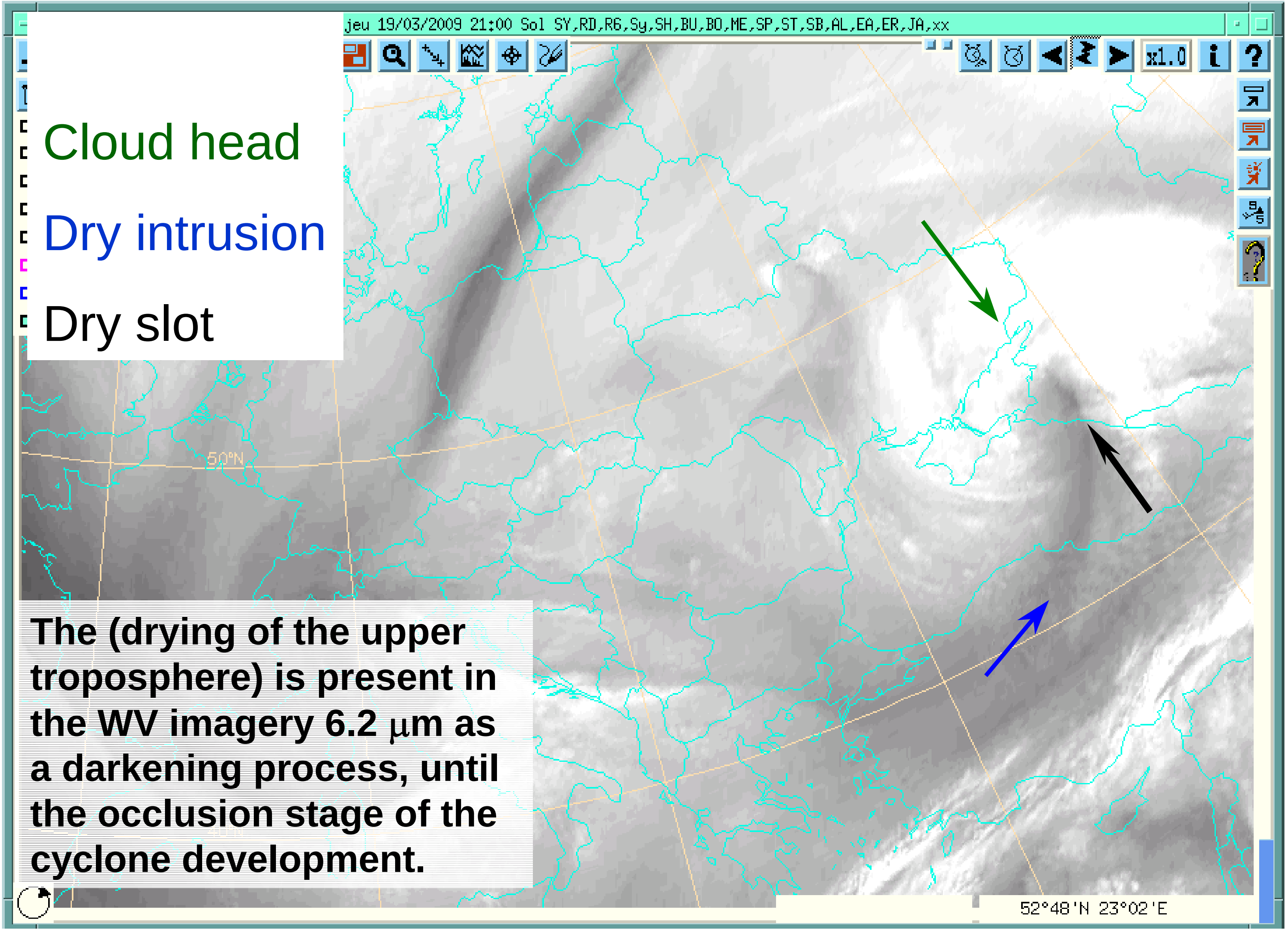

The (drying of the upper troposphere) is present in the WV imagery 6.2 µm as a darkening process, until the occlusion stage of the cyclone development.

WV imagery patterns of cyclone dynamics

19/03 00 UTC

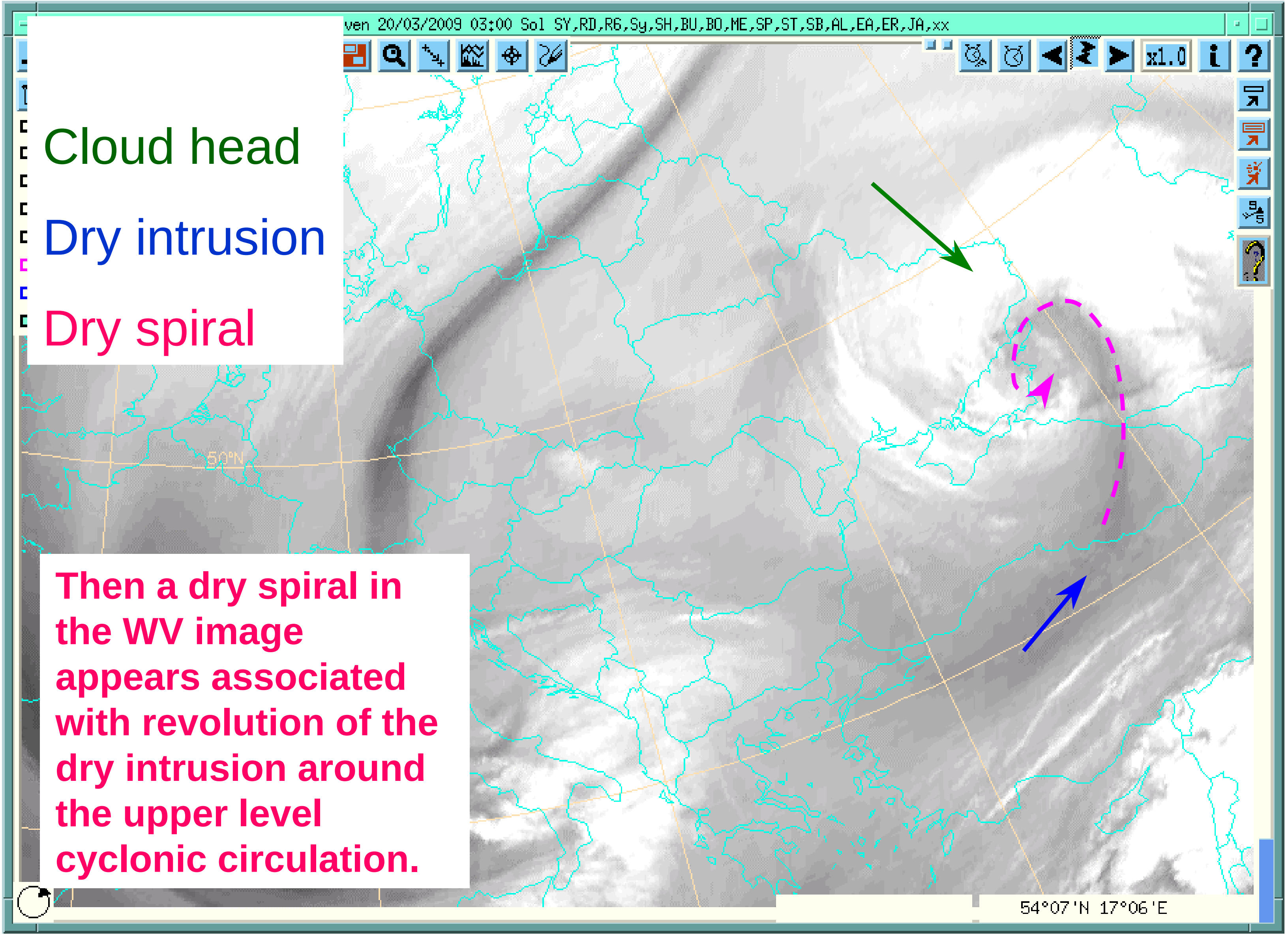

Cloud head

Dry intrusion

Dry spiral

Then a dry spiral in the WV image appears associated with revolution of the dry intrusion around the upper level cyclonic circulation.

WV imagery patterns of cyclone dynamics

6.2 µm, MSLP obs. (each 2 hPa)

19/03 03 UTC

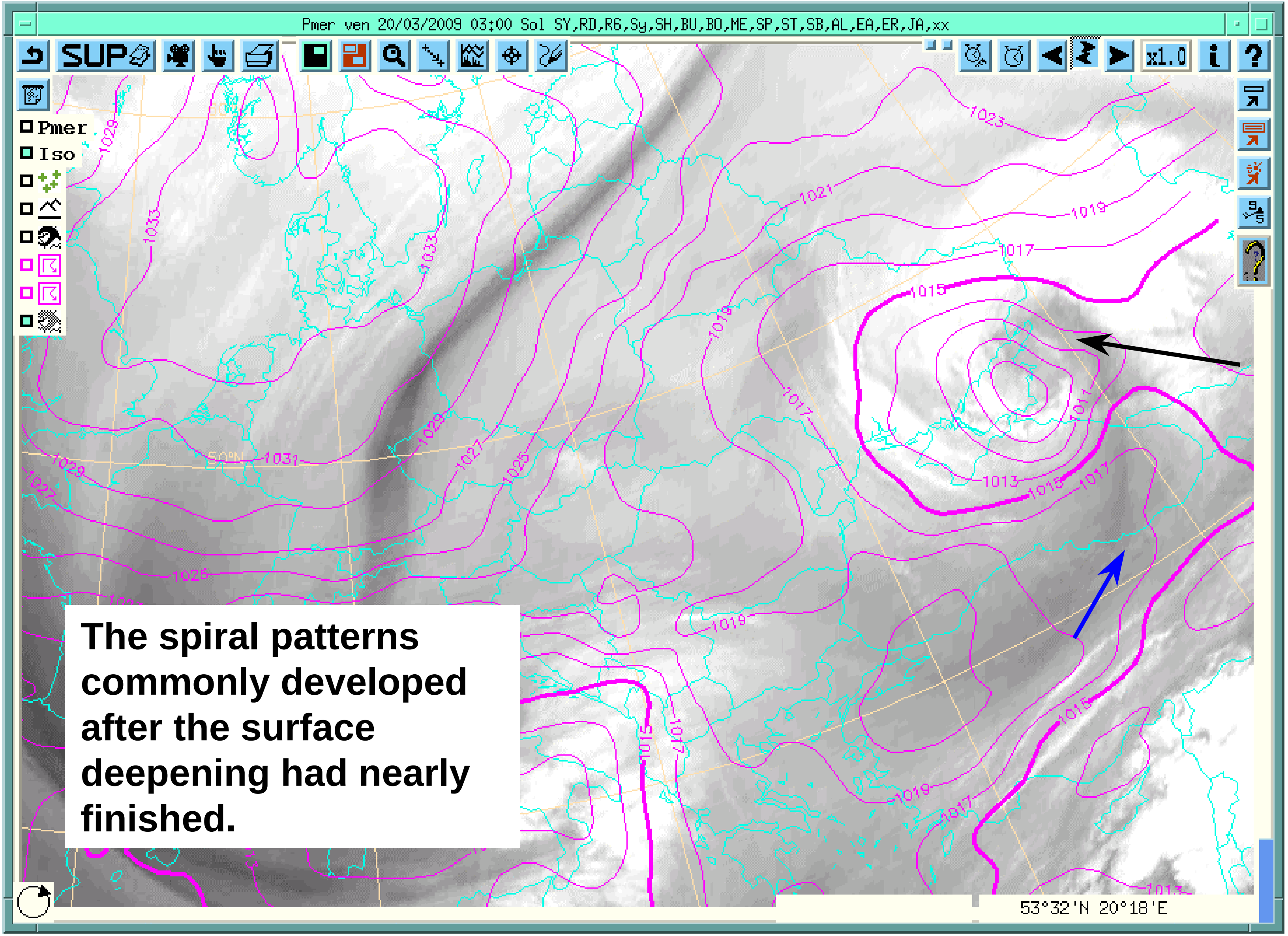

The spiral patterns commonly developed after the surface deepening had nearly finished.

Dry spiral

Dry intrusion

PV concept, jet stream analysis and cyclone development

Detection of NWP errors in dynamical model performance

NWP ERRORS
WV imagery jet stream analysis

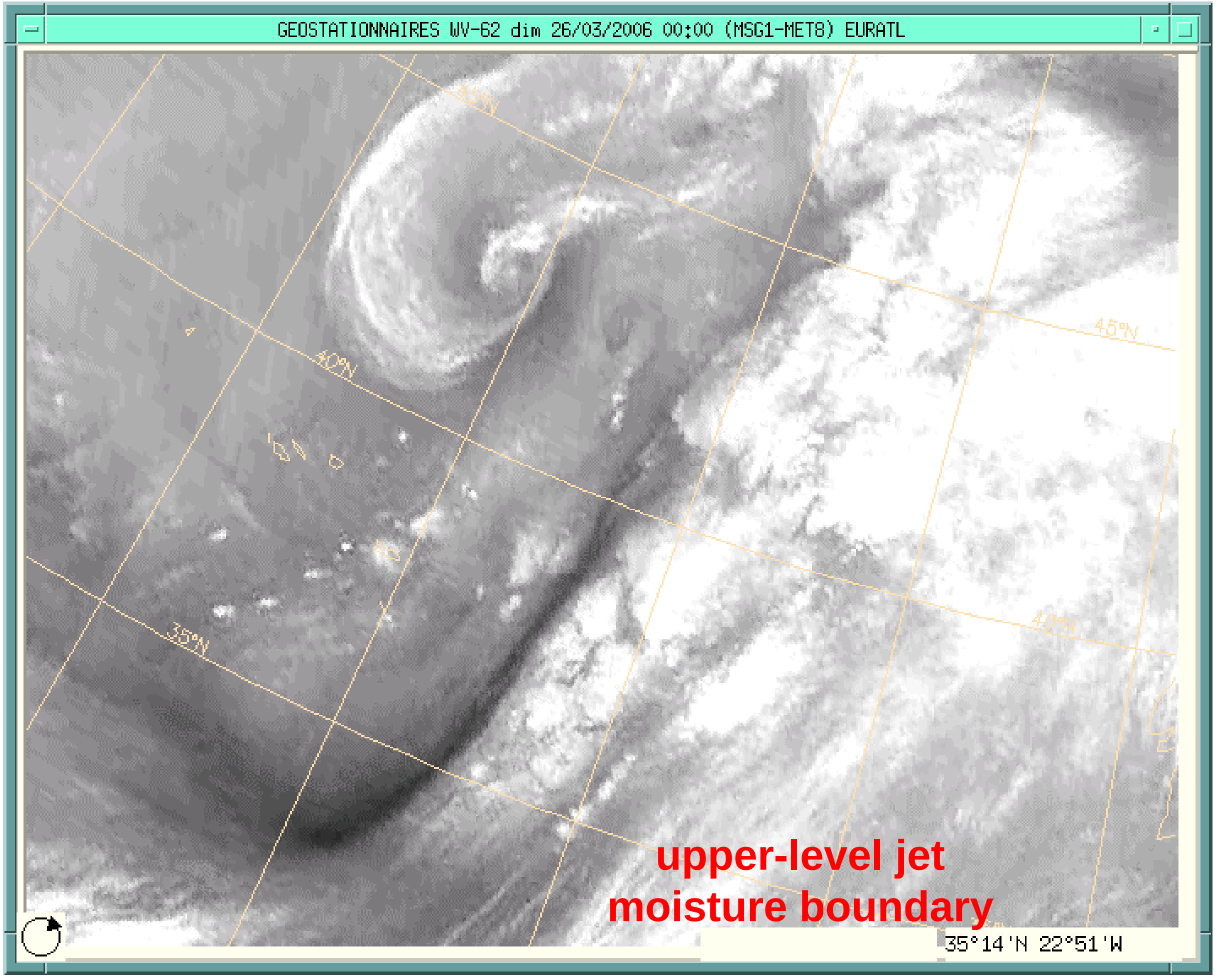

Applying WV imagery in 6.2 μm channel and PV analysis provides with a basis of methods for check on the validity of NWP output and improving early forecasts (Santurette & Georgiev, 2005).

The dynamically active regions are marked by tropopause dynamic anomalies (or, equally, positive PV anomalies) and strengthening jets.

Looking at the 6.2 μm image, indicate the position of the upper-level jet .

NWP ERRORS
WV imagery analysis

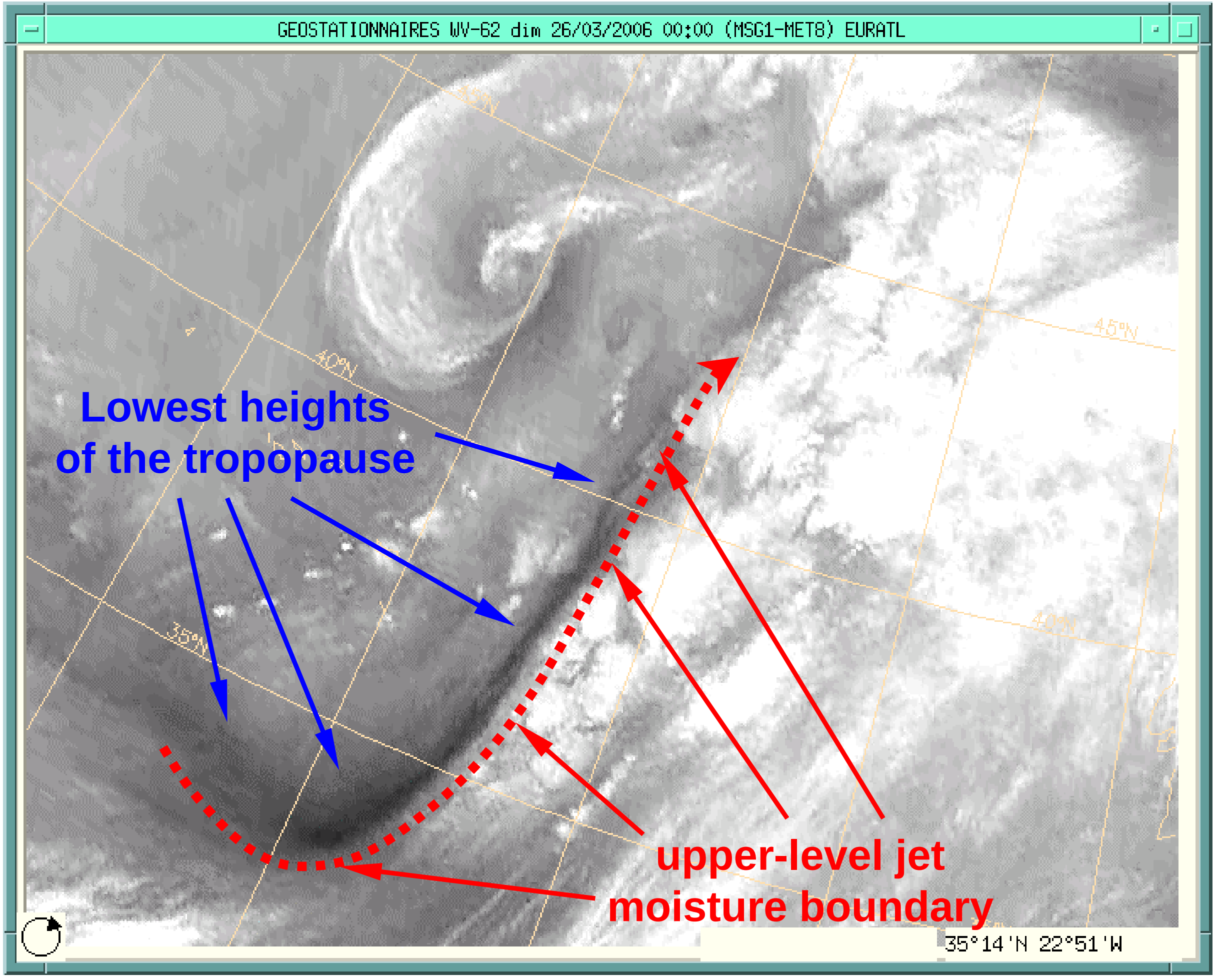

Applying WV imagery in 6.2 μm channel and PV analysis provides with a basis of methods for check on the validity of NWP output and improving early forecasts (Santurette & Georgiev, 2005).

Dynamically active regions are marked by a tropopause dynamic anomaly (or, equally, positive PV anomaly) and strengthening of the jet

The jet stream corresponds to a strong dark/light gradient on the 6.2 μm image with a dark zone of dry air related to a tropopause dynamic anomaly on the polar side of the jet .

NWP ERRORS
WV imagery PV analysis

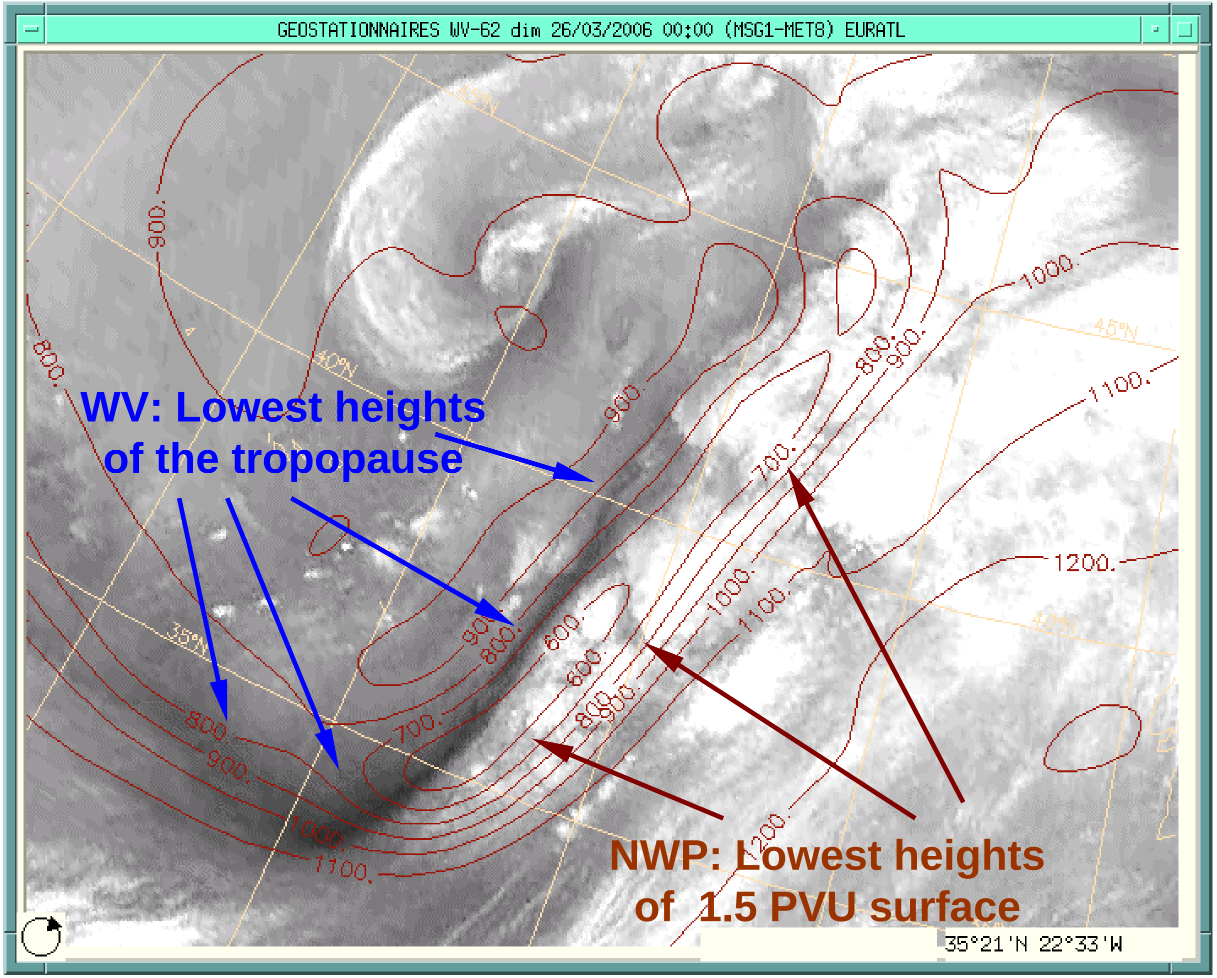

In the real atmosphere, shown by the satellite observations, the region of the lowest heights of the dynamical tropopause is located just rear to the darkest strip on the 6.2 μm image .

In this case, the ARPEGE model analysis has the minimum heights of the 1.5 PVU surface further east of the dry zone of the stratospheric intrusion related to the dark area on the WV image.

This mismatch is a sign for an error in the dynamical performance of the NWP model.

NWP ERRORS
WV imagery jet stream analysis

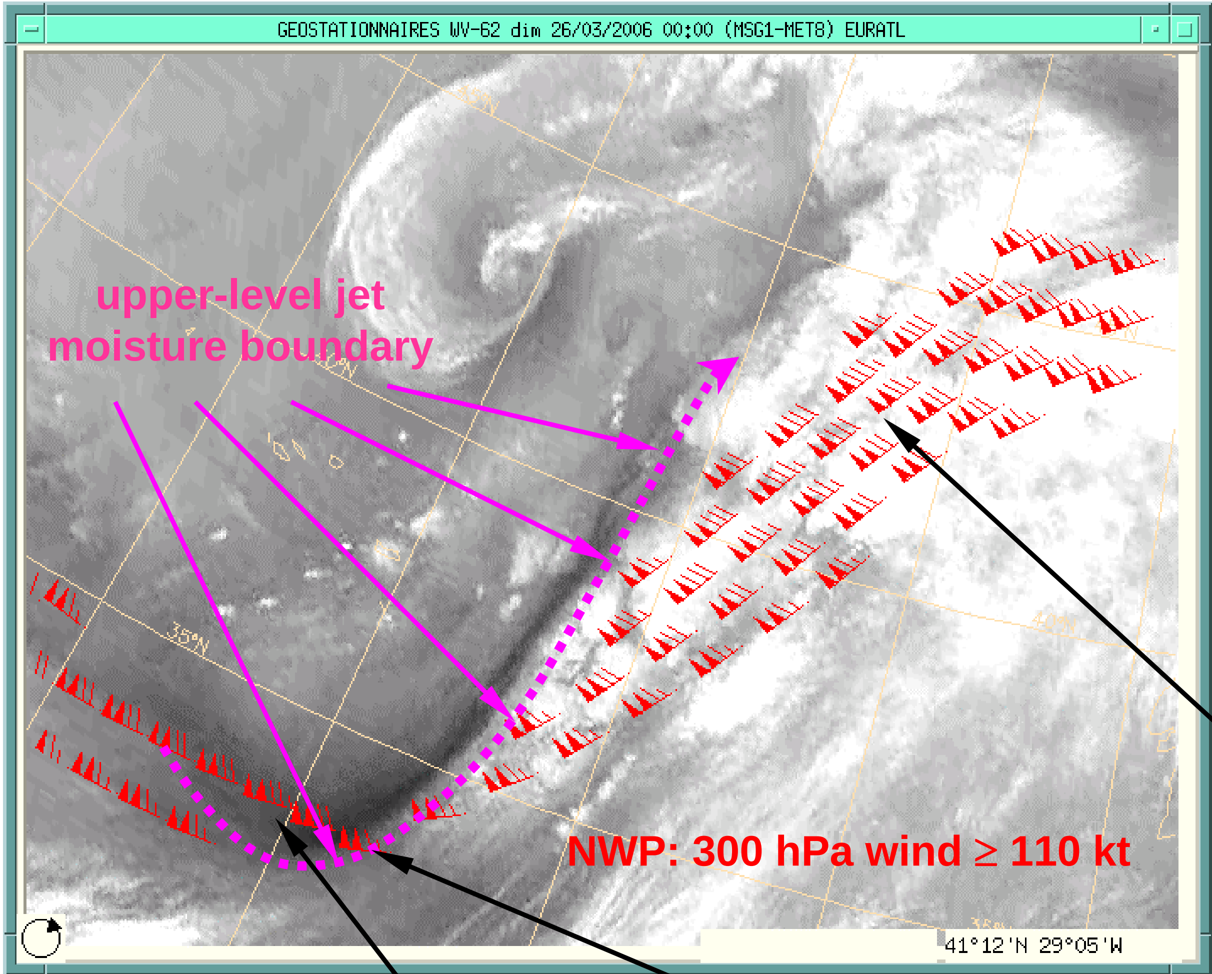

The error is clearly seen in the WV imagery jet stream analysis.

In the real atmosphere, the jet corresponds to a strong dark/light gradient on the 6.2 µm image with a dark zone on the polar side.

In this case, the ARPEGE model analysis has the jet further north-east of the WV boundary in the leading part of the trough.

In the base of the trough, the wrong model performance sees the jet across the WV image dark stripe and then across the jet moisture boundary.

NWP ERRORS
WV imagery jet stream analysis

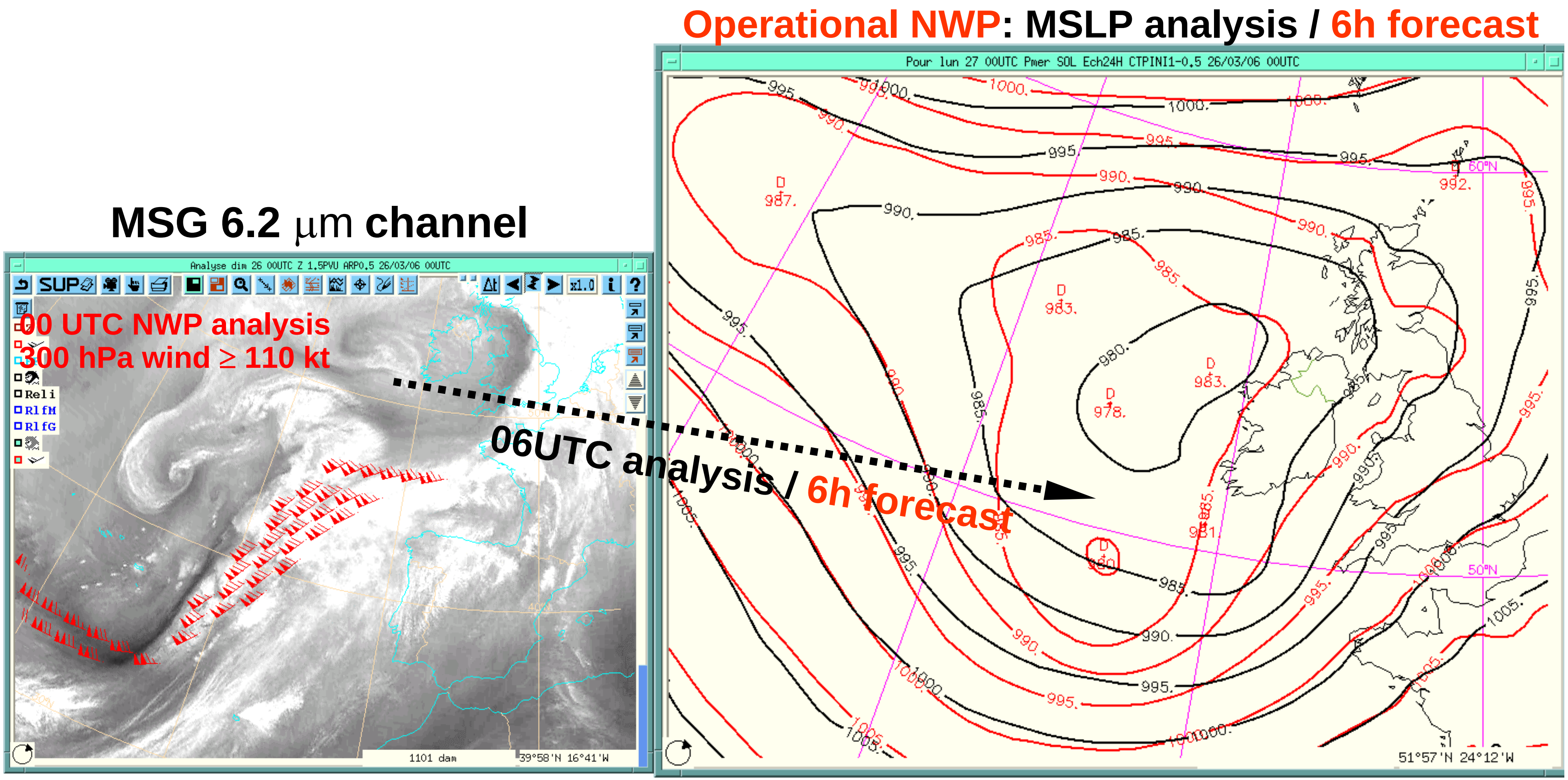

As a result,

the operational NWP model did not predict correctly the cyclone development downstream the area of wrong jet stream numerical analysis.

6.2 μm WV IMAGERY DIAGNOSIS

MID-UPPER LEVEL ENVIRONMENT OF DEEP MOIST CONVECTION

A large portion of severe convective weather occurs in synoptic disturbances where upper-level synoptic-scale forcing mechanisms act in addition to a conditional instability of the atmosphere. There is an association between large-scale systems and moist deep convection (Doswell, 1987).

The forecasters can diagnose the upper-troposphere forcing for vertical motion by looking at the WV imagery patterns related to PV anomalies, jet streams, diffluent (divergent) flow.

6.2 μm WV IMAGERY DIAGNOSIS

Deep moist convection in blocking regime

Animation 1

DEEP MOIST CONVECTION IN BLOCKING REGIME ***06 August 2007***

MSG IR 10.8, colored brightness temperature < - 40 °C

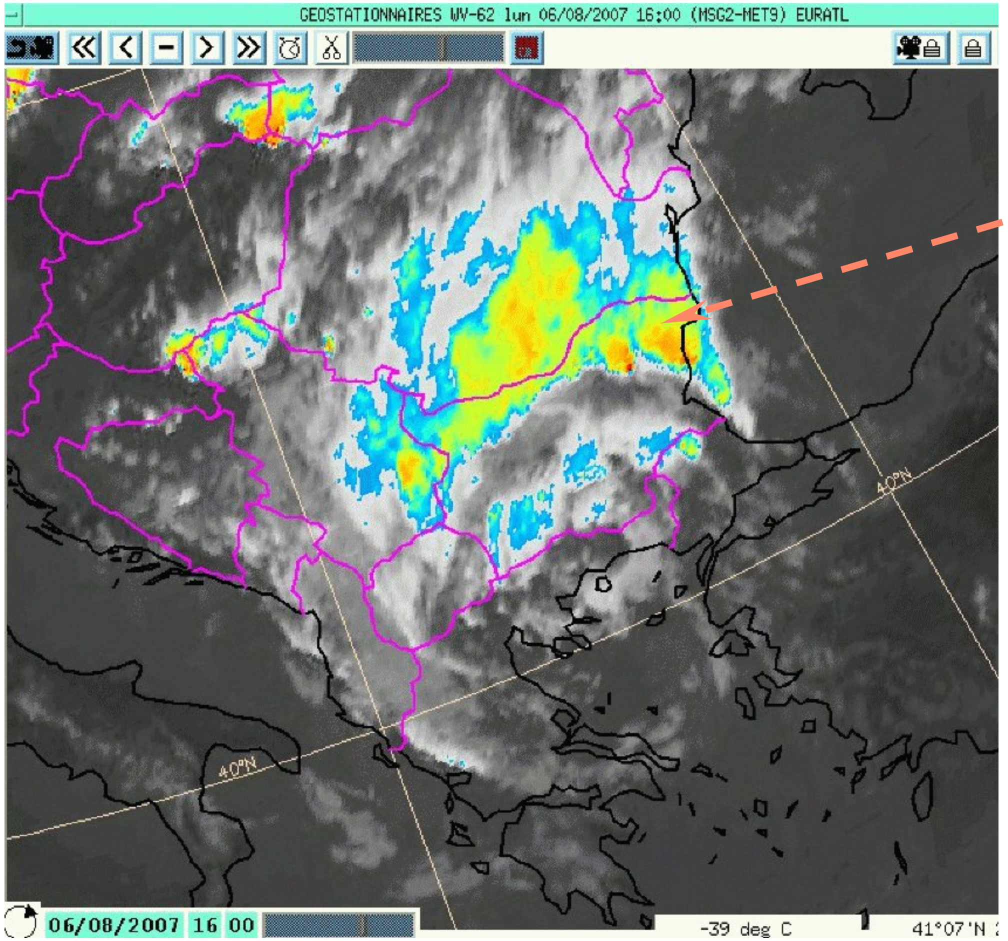

The process developed in a strong blocking regime that can generate conditions for severe weather over the same area for a long time.

UPPER-LEVEL ISOBARIC ANALYSIS

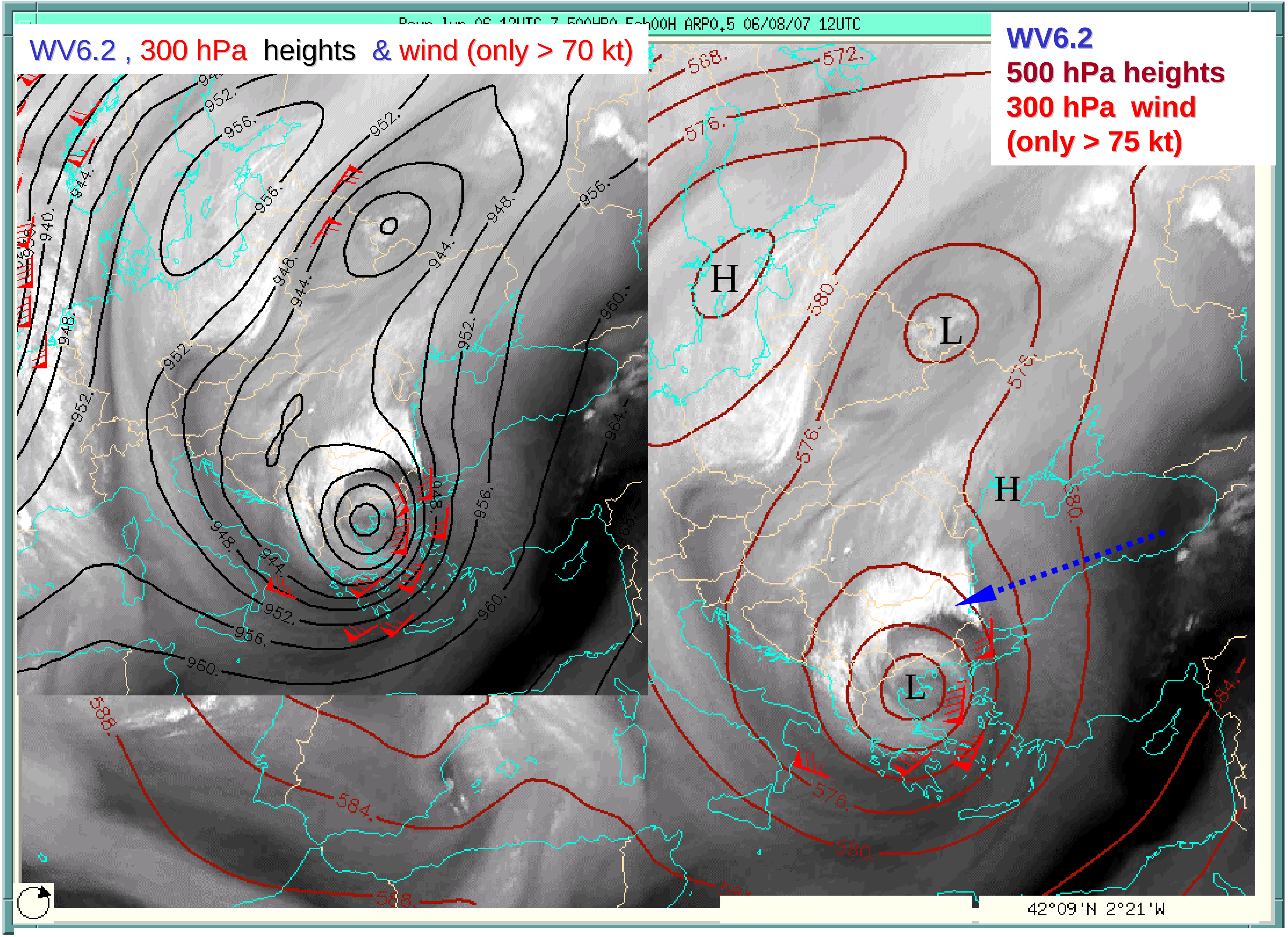

Diagnosis of upper-level forcing by satellite WV imagery:
Divergent flow at the <u>left exit of the upper-level jet in blocking circulation</u> (Carroll, 1997).

UPPER-LEVEL FLOW

***06 August 2007** Flash flood in Bulgaria*

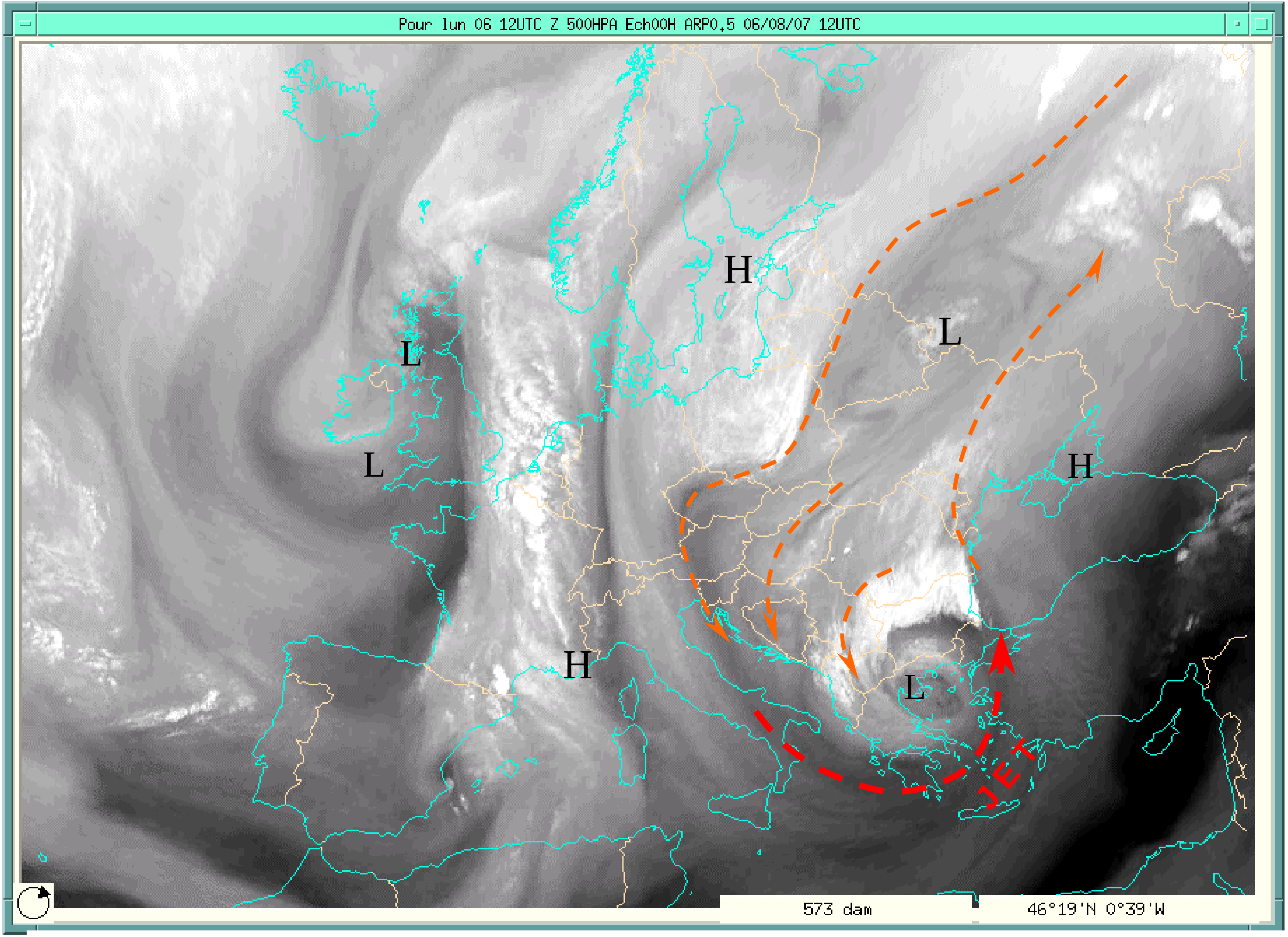

In a 6.2 μm image, the moisture boundaries are parallel to the flow between upper-level high and low systems. This helps in recognition of the circulation patterns.

FORCING OF CONVECTION IN BLOCKING REGIME

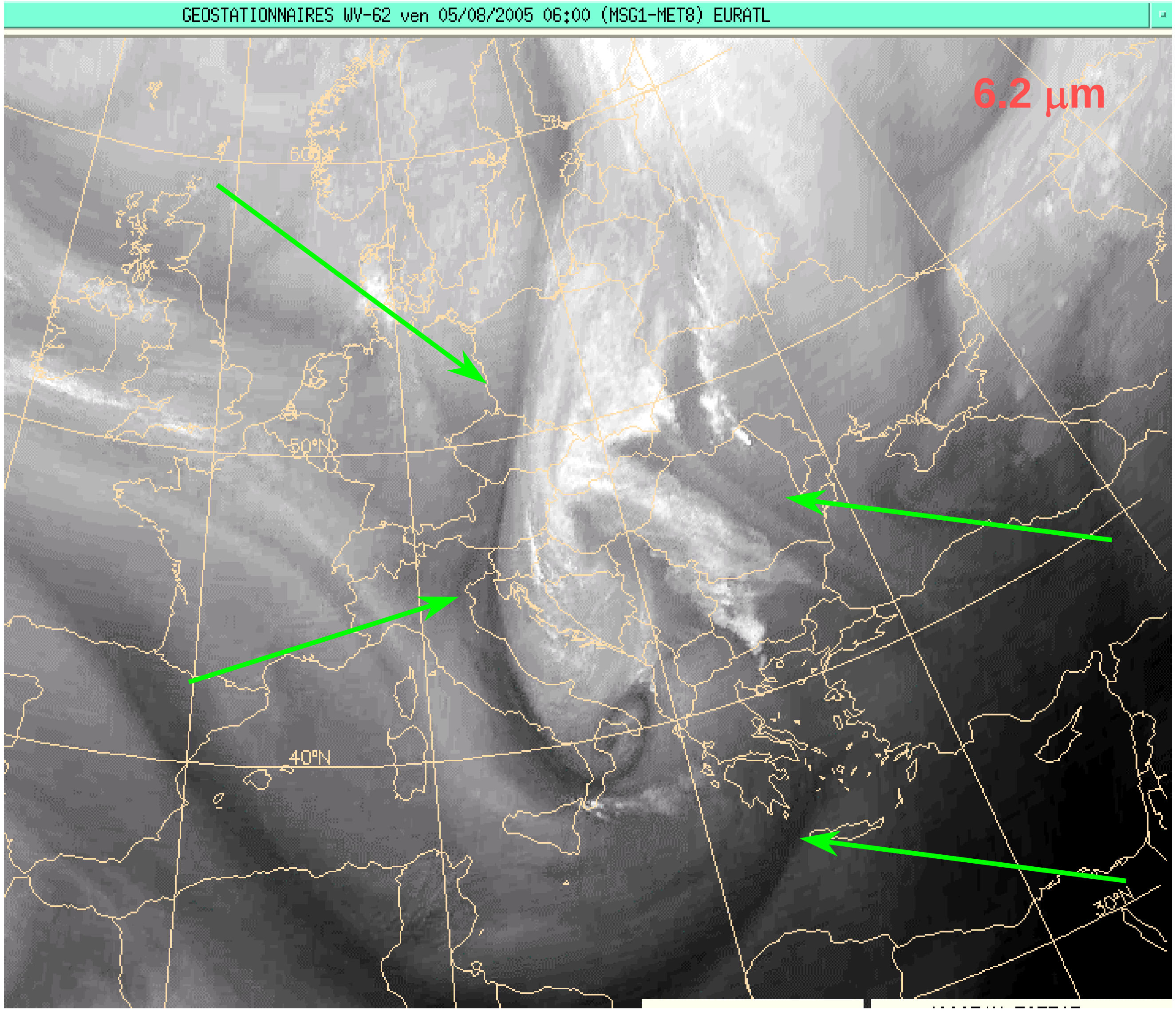

5 August 2005

Flash floods in Bulgaria

Blocking regime definition:

Synoptic-scale easterly winds

Looking at the moisture boundaries (at green arrows) in the WV image 6.2 μm, indicate the position of the blocking circulation (synoptic-scale easterly winds)

FORCING OF CONVECTION IN BLOCKING REGIME

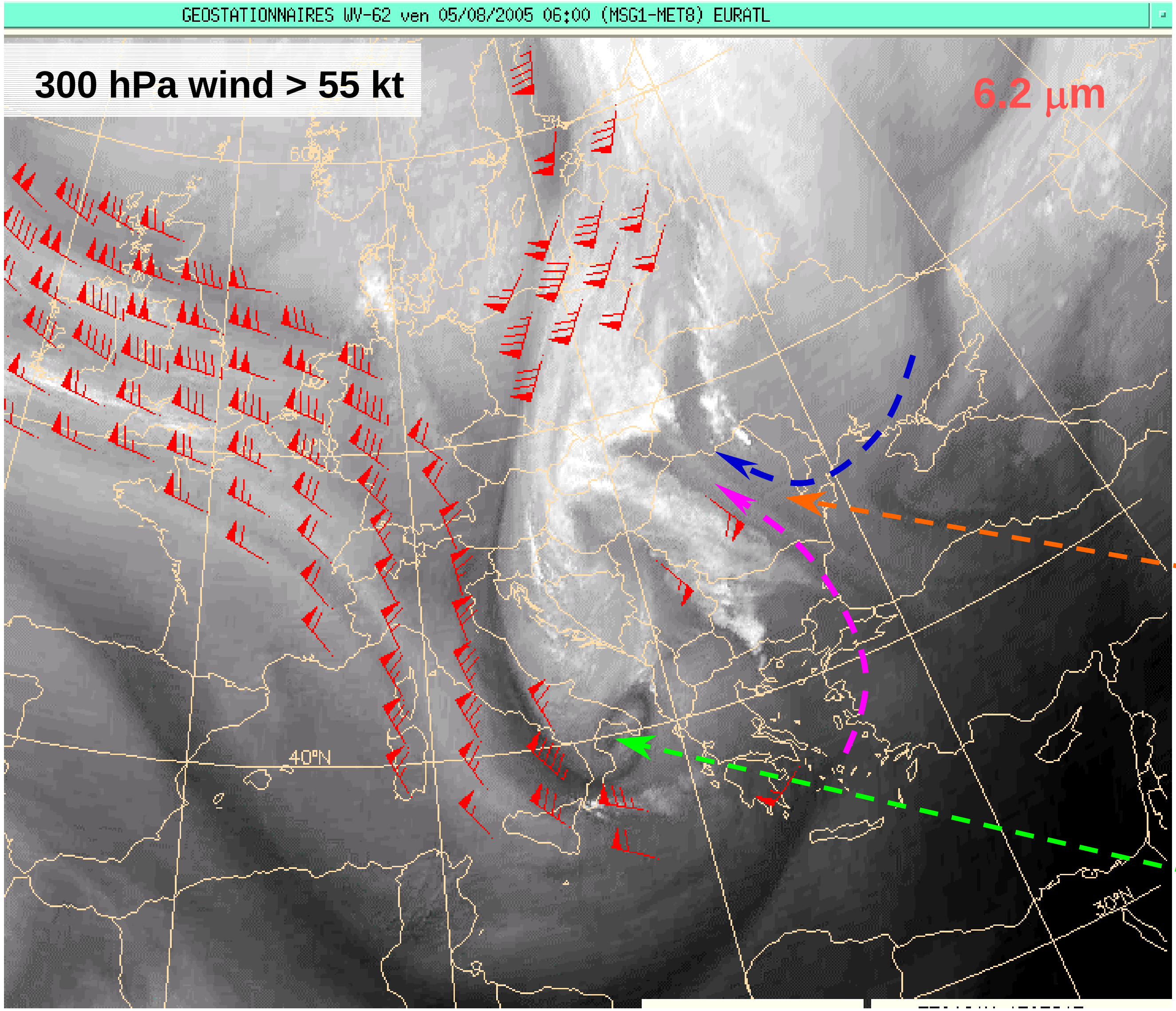

5 August 2005 06 UTC

Look at the moisture boundaries in WV imagery 6.2 µm for recognition of

Blocking regime:

Synoptic-scale easterly winds.

Upper-level VORTICITY structure advected with the jet into the blocking circulation.

ISOBARIC SURFACE ANALYSIS

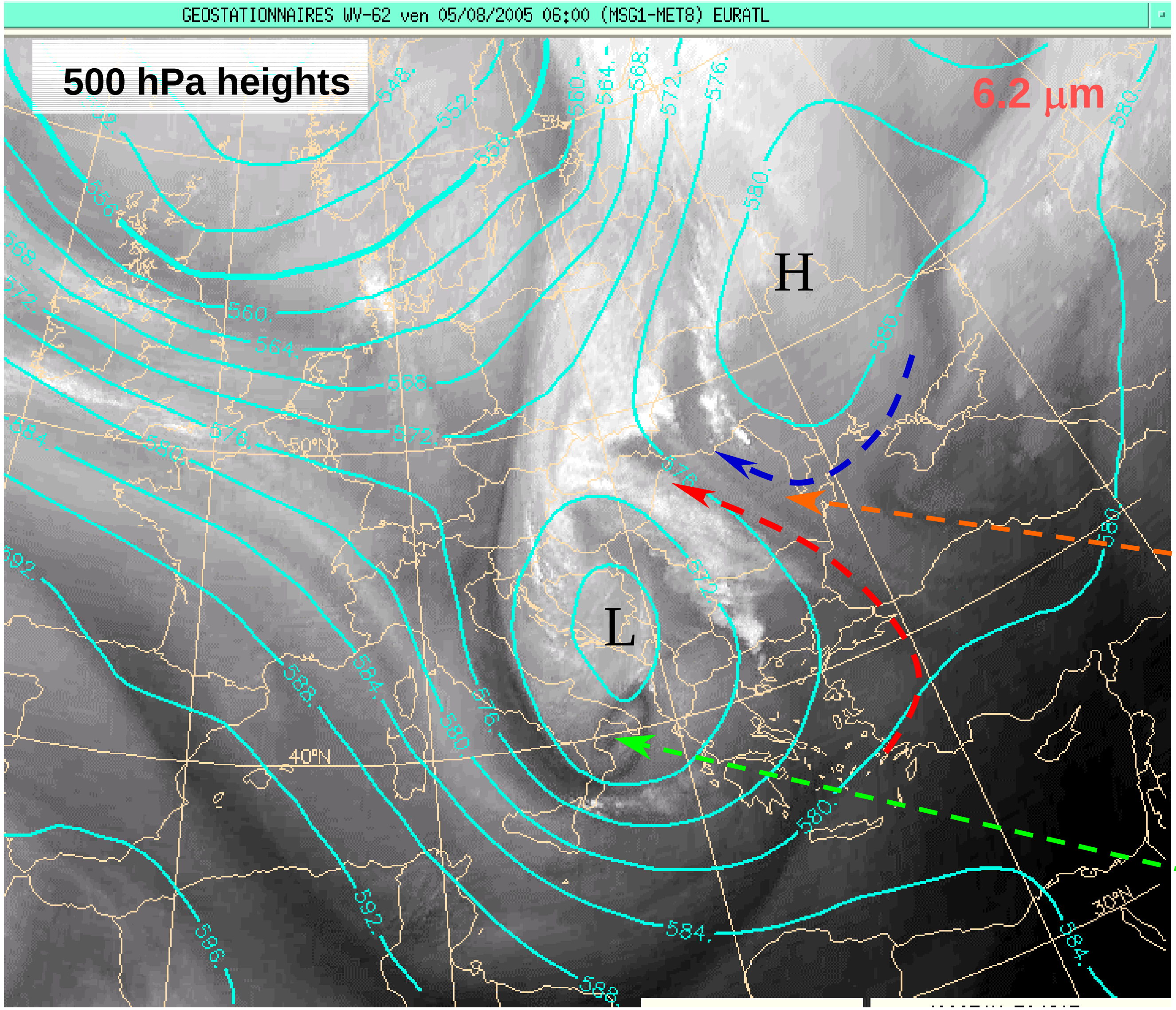

5 August 2005 06 UTC

Blocking regime:

Synoptic-scale easterly winds.

Upper-level VORTICITY structure not visible through Isobaric Surface Analysis.

It is obvious that the Diagnosis based on the 6.2 WV Imagery Analysis is much more efficient than using 500 hPa Isobaric Surface analysis, which does not provide a signal for an important vorticity feature of the upper-level dynamics.

ISOBARIC SURFACE ANALYSIS

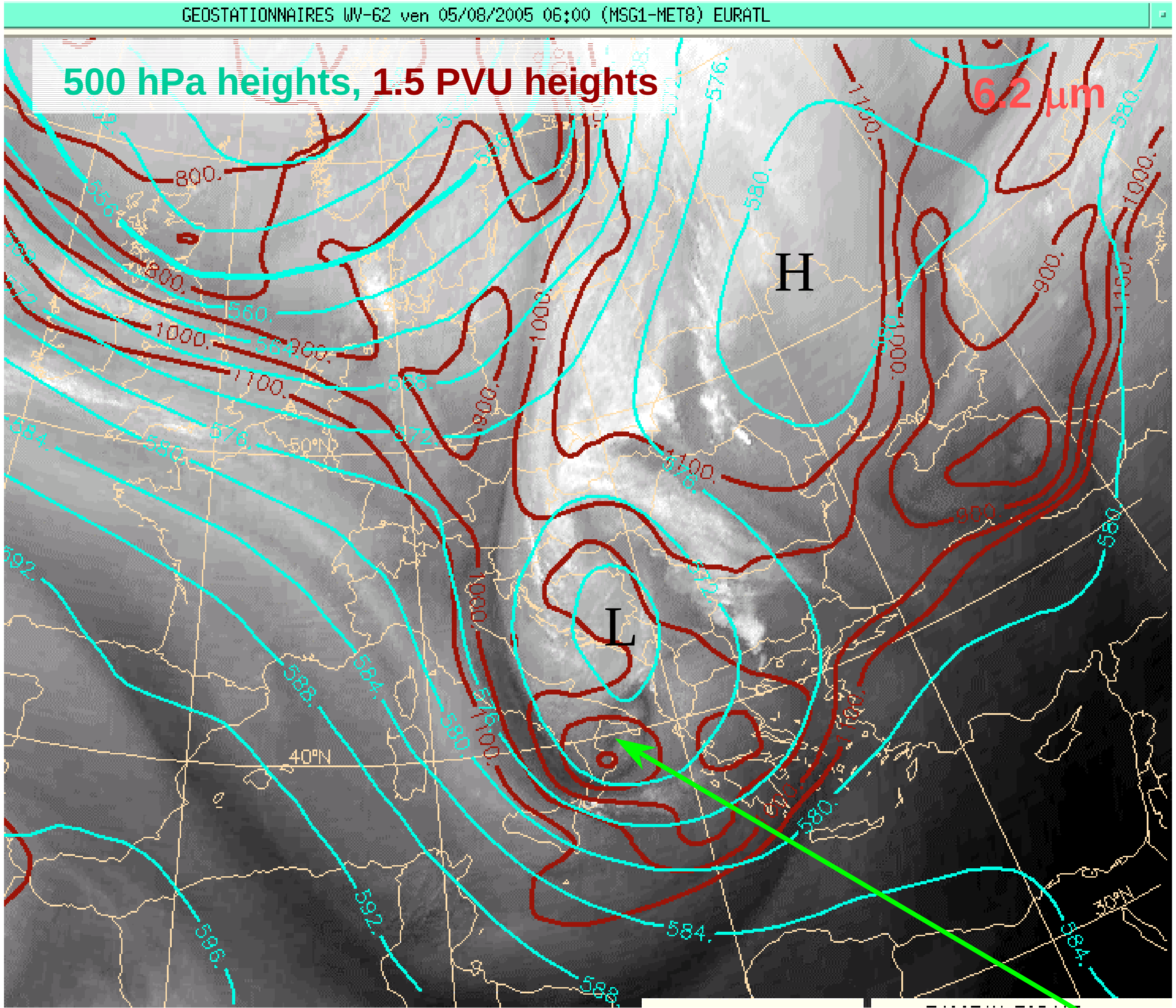

5 August 2005 06 UTC

The inspection of the blocking regime provides knowledge of the related pre-convective upper-level environment :

- ✓ **Left exit of a jet**
- ✓ **Dry intrusion and convective instability**
- ✓ **Vorticity advection over the same area for a long time**

Upper-level VORTICITY structure is well seen as a PV anomaly (minimum height of the dynamical tropopause and a dark dry/vorticity feature on the WV image).

PV anomaly advection

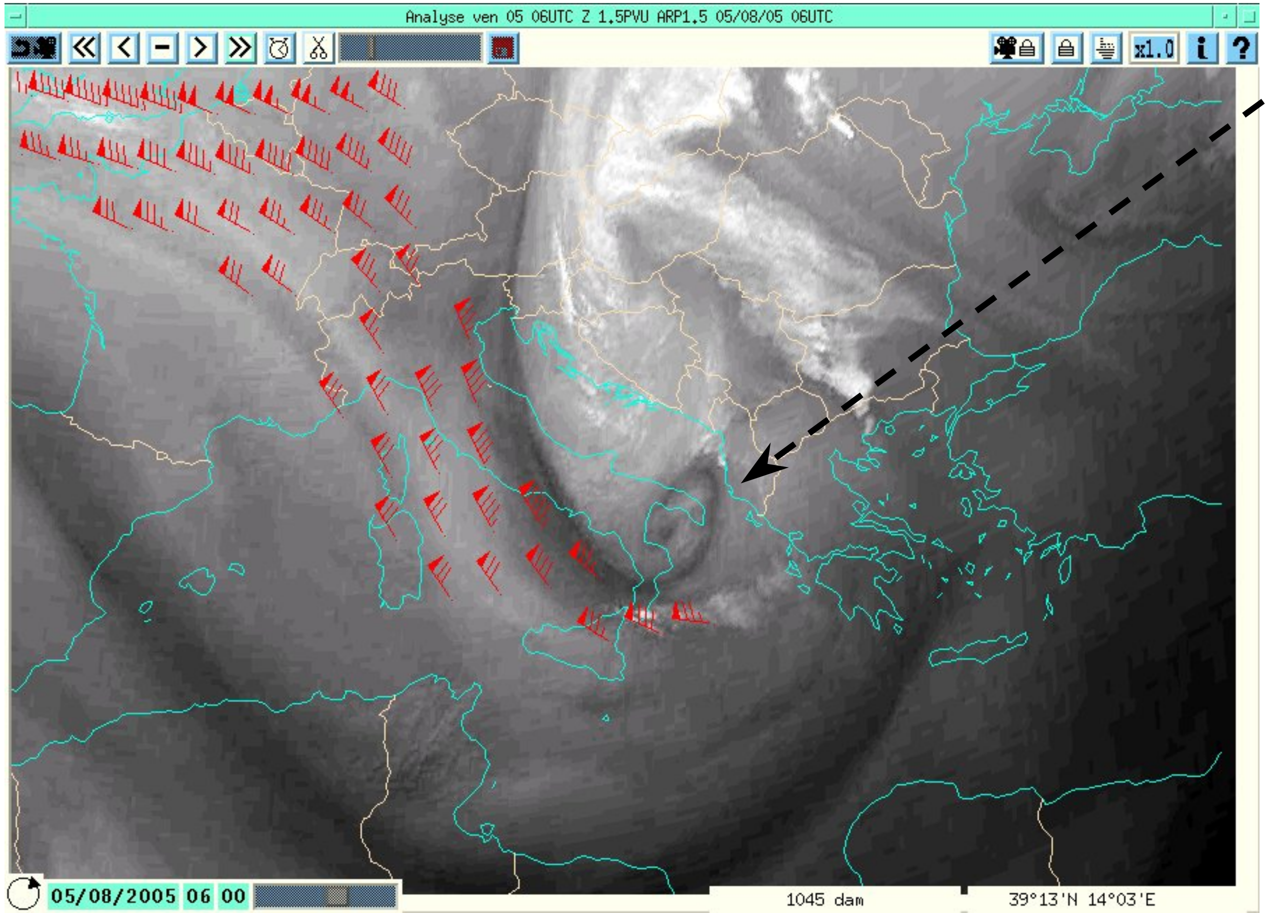

PV analysis

WV6.2

1.5 PVU wind (only > 65 kt)

A PV anomaly is always seen in the WV images, being a conservative Dynamic dry zone

(detected in the WV imagery more than 24 hours before the forcing of deep convective development).

Animated WV imagery show the evolution of the Dynamic dry zone and related patterns:

- PV anomaly advection, related to a jet (especially in blocking upper-level circulation),
- Probability for intensive convection in the leading diffluent-flow side of a PV anomaly .

Animation 2

Upper level forcing for vertical motion:

PV-anomaly advection and interaction with a low-level θ_w-anomaly

COUPLING of upper- and low-level forcing

5 August 2005 ***Flash floods in Bulgaria***

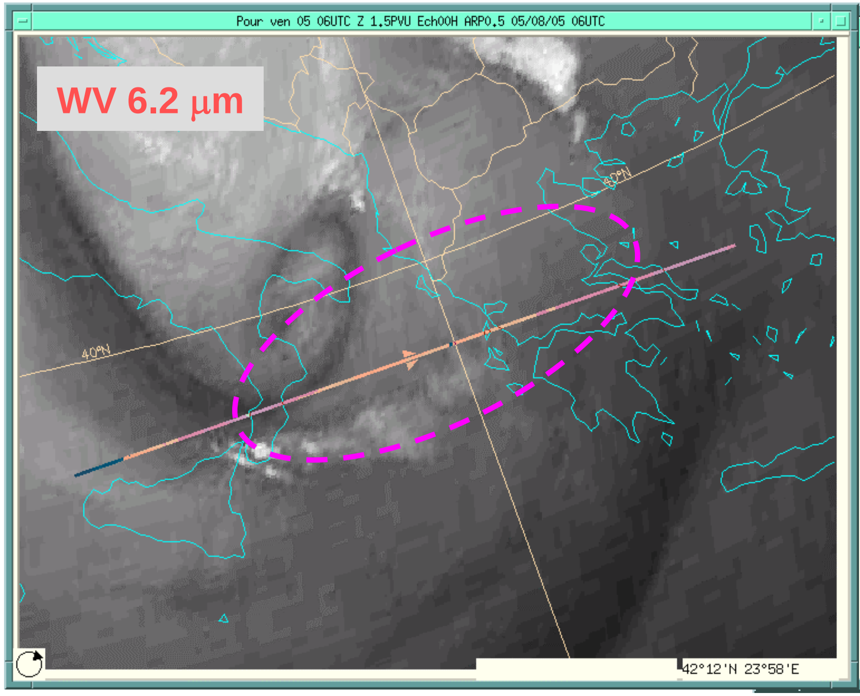

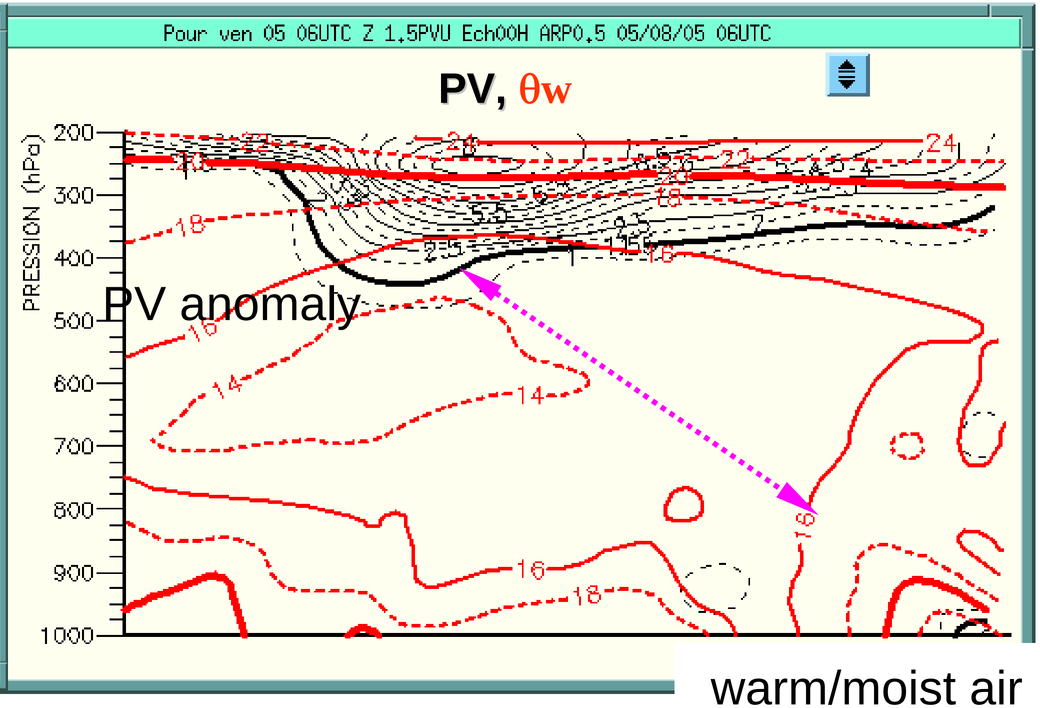

warm/moist air
(θw anomaly).

<u>The low-level conditions</u> (warm and moist air, convergence) and instability **are critical for the potential of the atmosphere to produce vertical motions.**

Rapid cyclogenesis and intensive deep moist convection develop as a result of PV anomaly advection and its interaction with a low-level θ_w anomaly (warm/moist air).

COUPLING of upper- and low-level forcing

***5 August 2005** Flash floods in Bulgaria*

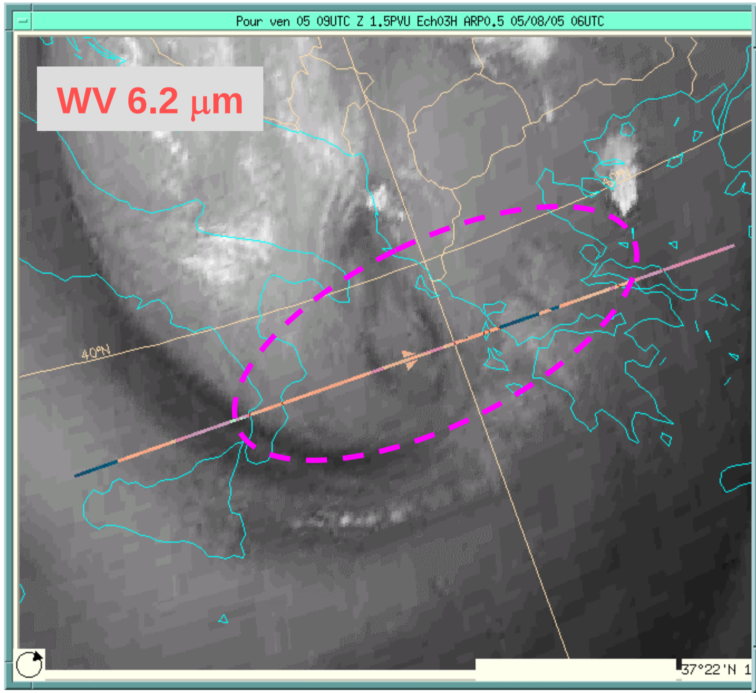

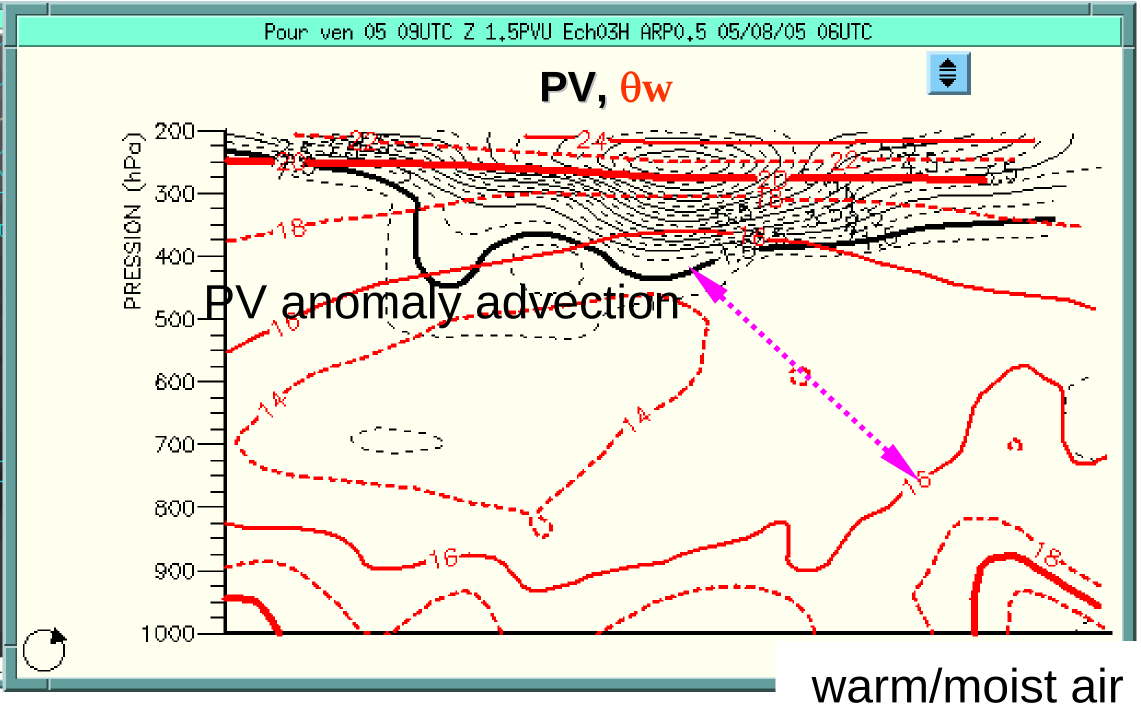

warm/moist air
(θw anomaly).

The upper-level PV anomaly and the low-level θ_w anomaly tend to be close each other and couple.

COUPLING of upper- and low-level forcing

5 August 2005 ***Flash floods in Bulgaria***

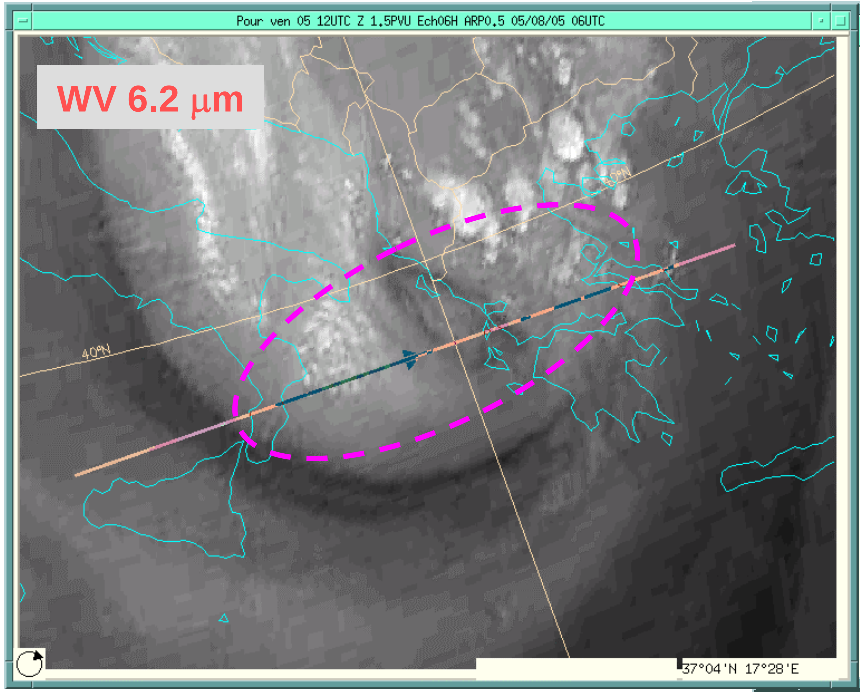

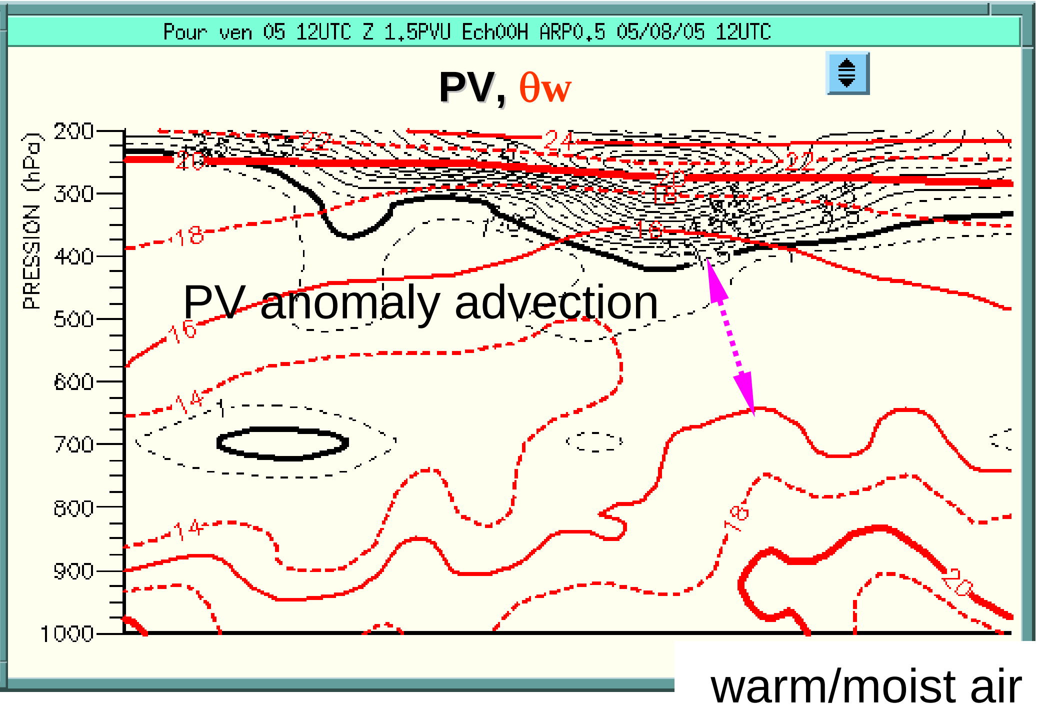

warm/moist air
(θw anomaly).

The upper-level PV anomaly and the low-level θ_w anomaly tend to be close each other and couple.

Leading edge of the dry vorticity WV imagery feature tends to curve cyclonically and remains closely in phase with the tropopause folding.

COUPLING of upper- and low-level forcing

***5 August 2005* Flash floods in Bulgaria**

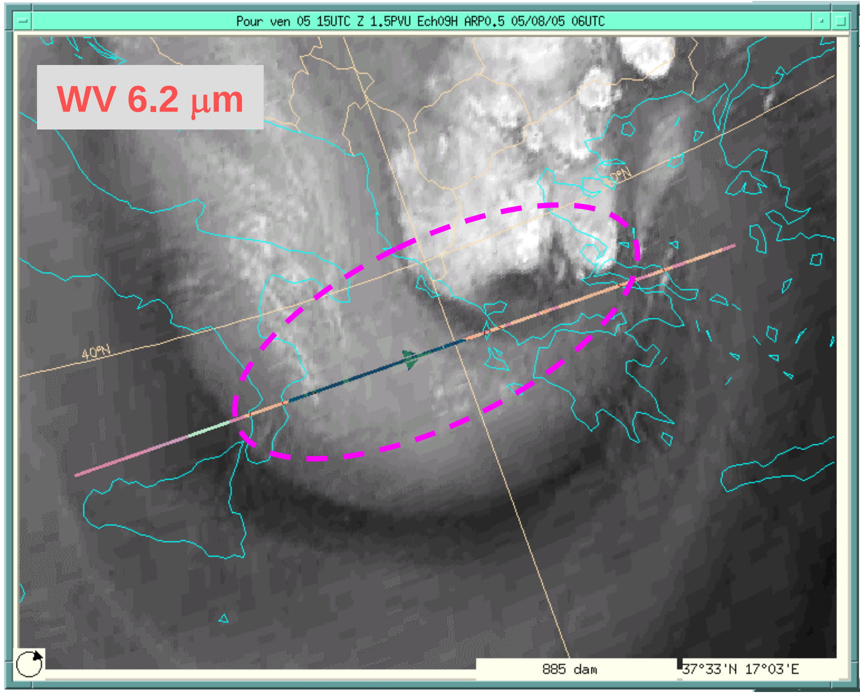

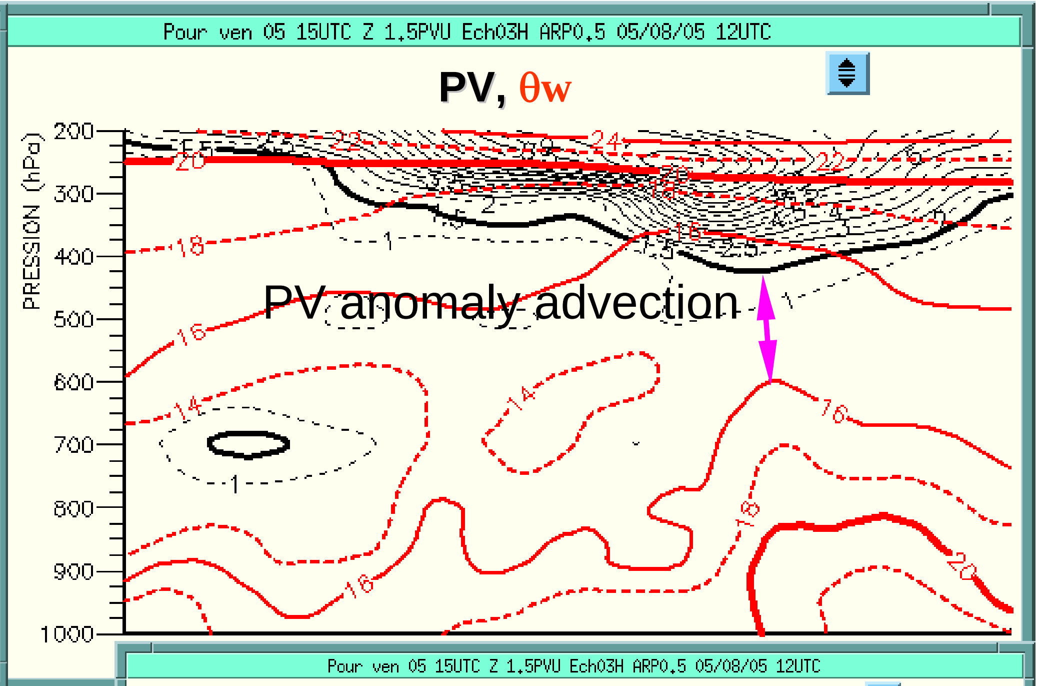

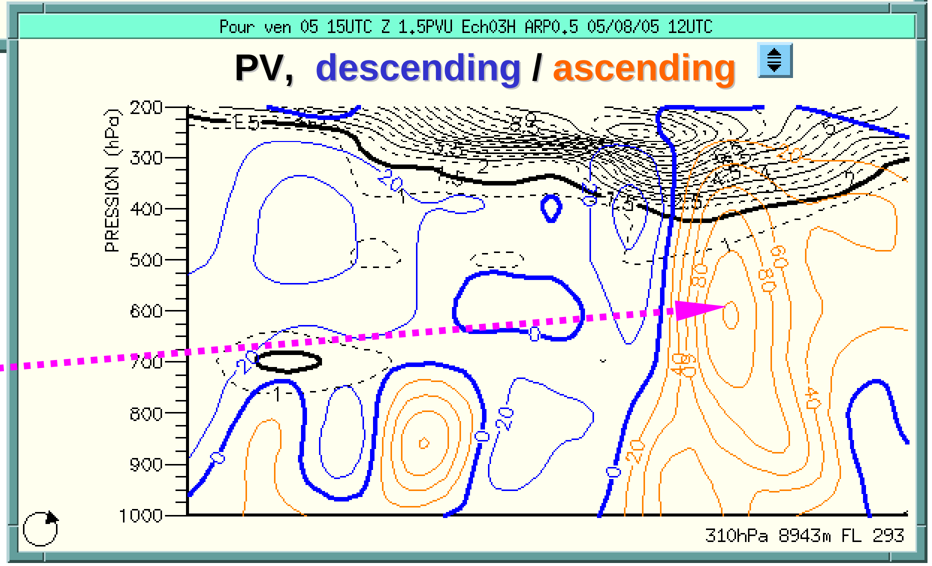

The tide coupling between the PV- and θ_w - anomalies is responsible for producing strong vertical motions in a deep tropospheric layer.

Interaction of a PV anomaly with the low-level thermodynamics

Detection of NWP errors in dynamical model performance

30 h accumulated rain forecast of ALADIN model

23 June 2006

Flash floods in Sofia, Bulgaria

(a) **06 – 12 UTC**

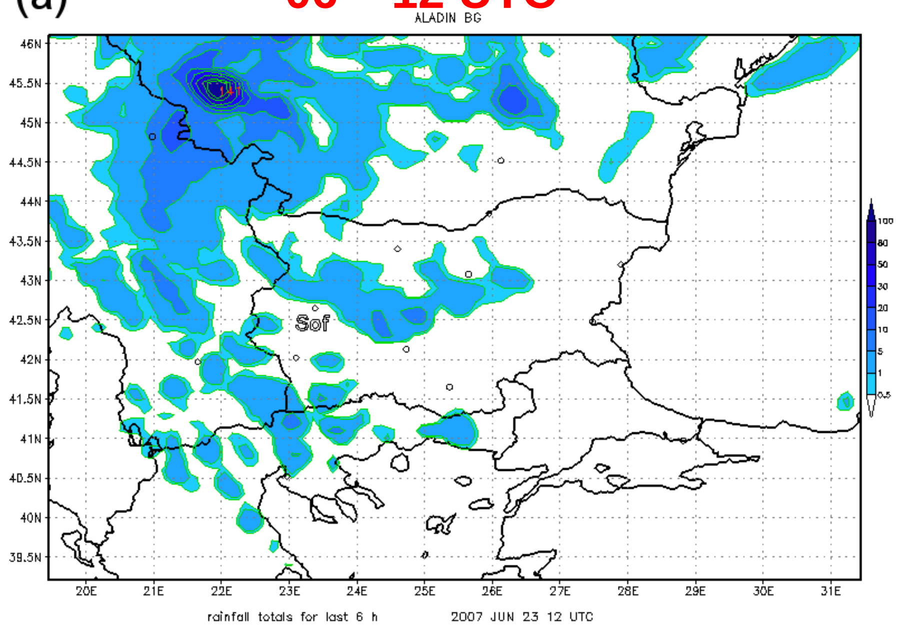

(b) **12 – 18 UTC**

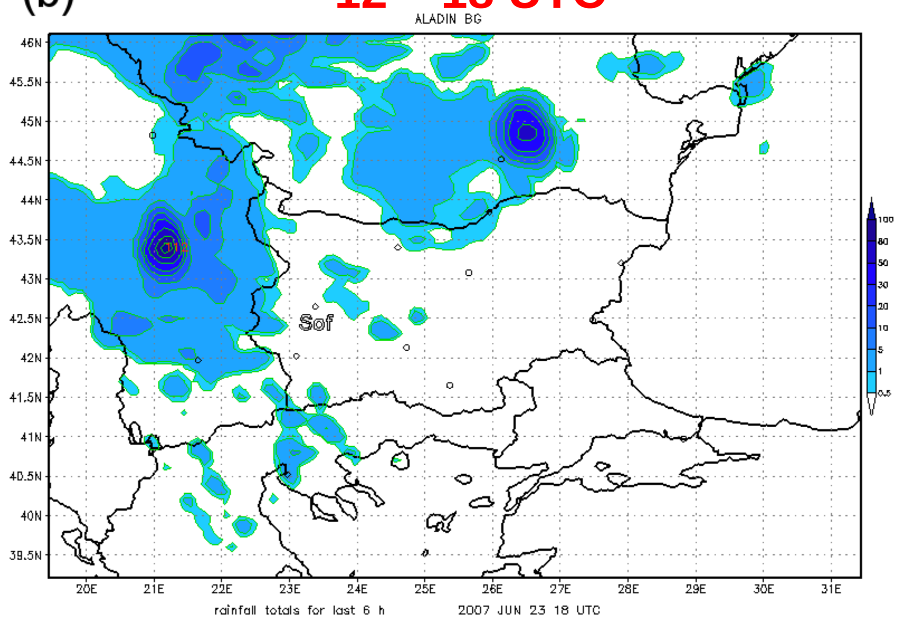

The 30 h NWP forecast of 6 h accumulated rainfall for 12 and 18 UTC on 23 June, shows only a small zone of less than 10 mm total rain for the western part of Bulgaria

23 June 2006

Flash floods in Sofia, Bulgaria

**Sofia,
a city boulevard**

The 30 h NWP forecast of 6 h accumulated rainfall for 12 and 18 UTC on 23 June, shows only a small zone of less than 10 mm total rain for the western part of Bulgaria, where the <u>heavy rainfall and flash flood was produced</u>.

6.2 µm WV 12 UTC

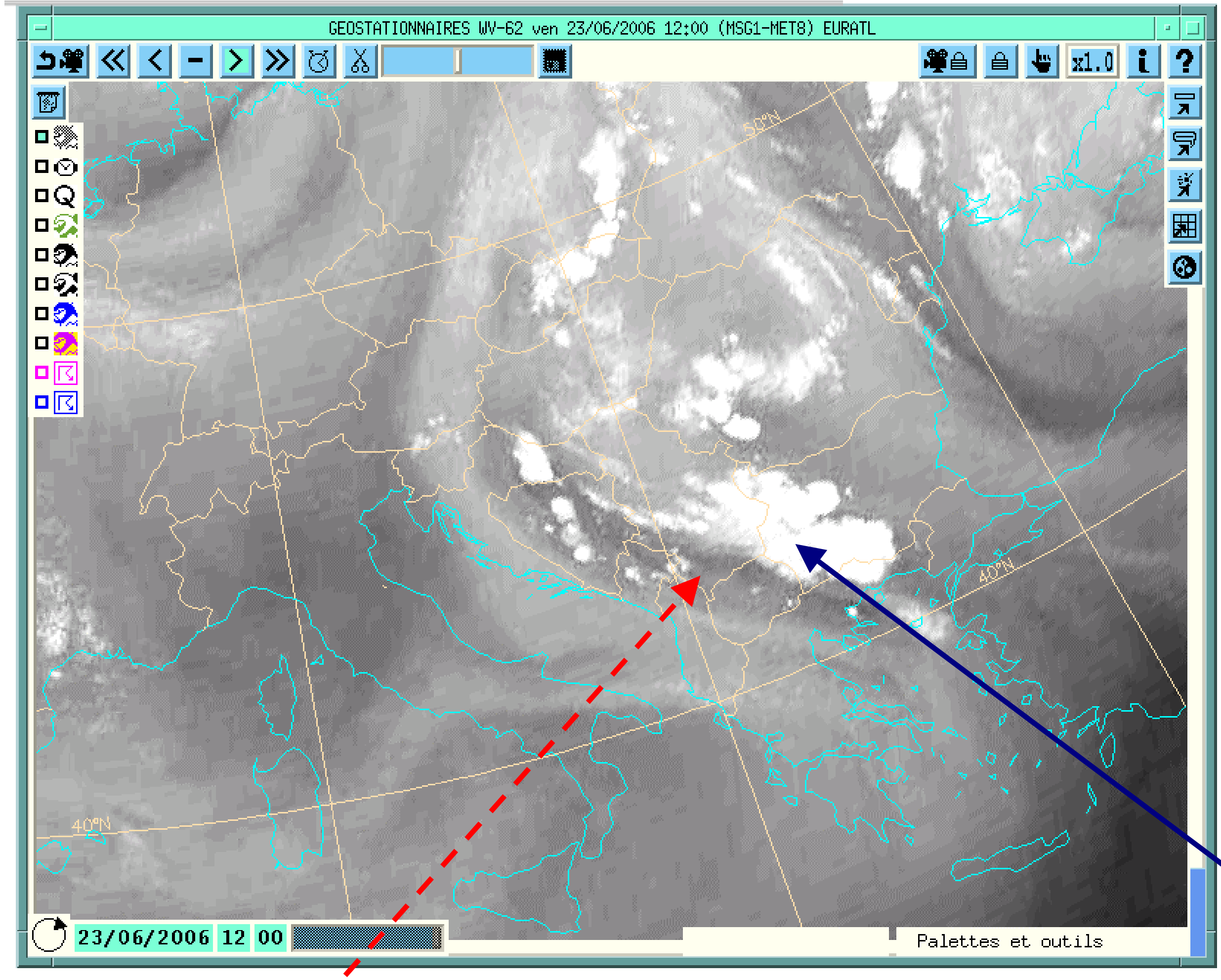

23 June 2006

Flash floods in Sofia, Bulgaria

upper-level forcing of convection as a result of vorticity advection

Sofia

Upper-level vorticity feature to the West of Sofia

6.2 µm WV 06 UTC

23 June 2006

Flash floods in Sofia, Bulgaria

WV imagery diagnosis of upper-level vorticity

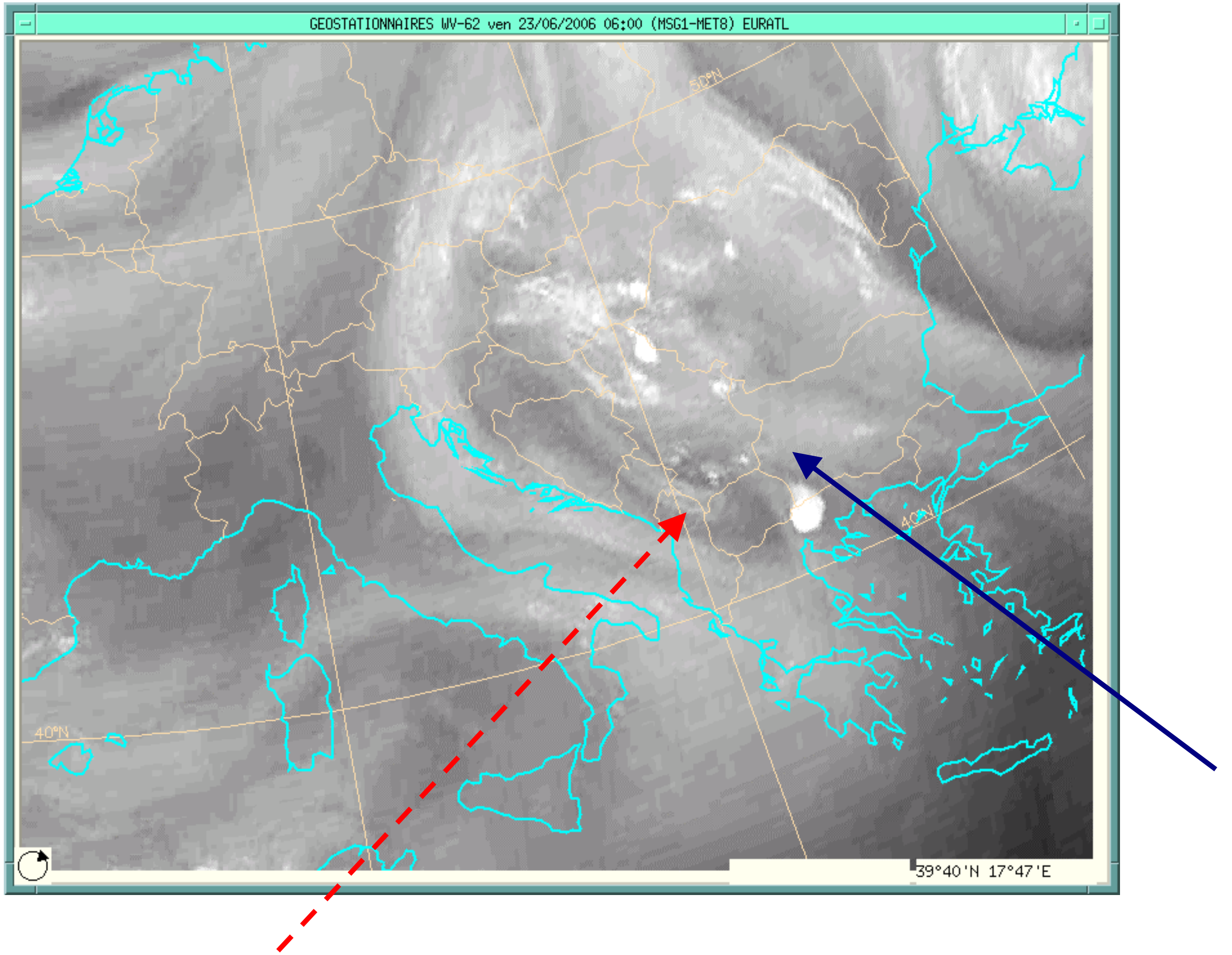

Upper-level vorticity feature approaching Western part of Bulgaria

6.2 μm WV 06 UTC 1.5 PVU heights

23 June 2006

Flash floods in Sofia, Bulgaria

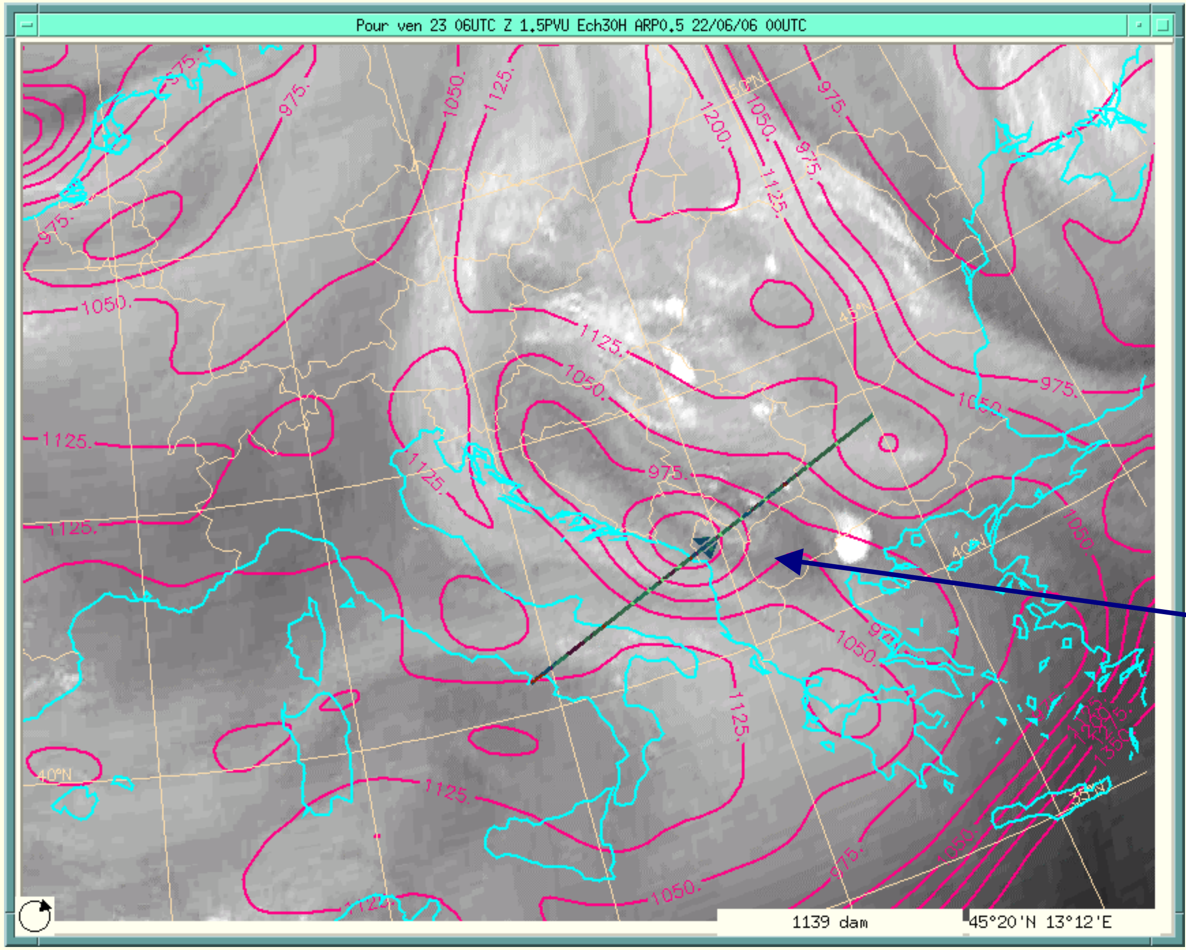

30 h forecast (red)

Check on the NWP PV forecast (ARPEGE)

Mismatch between the dynamical tropopause folding simulated by the NWP model and the vorticity pattern on the WV image

The area of the minimum height of 1.5 PVU surface (the dynamical tropopause) in the 30 h ARPEGE forecast (975 dam contour) does not mirror the specific dark vorticity feature on the WV image (Georgiev & Kozinarova, 2009).

Low-level perspective

06 UTC 23 June 2006

30 h forecast of θ_w | **Analysis of θ_w**

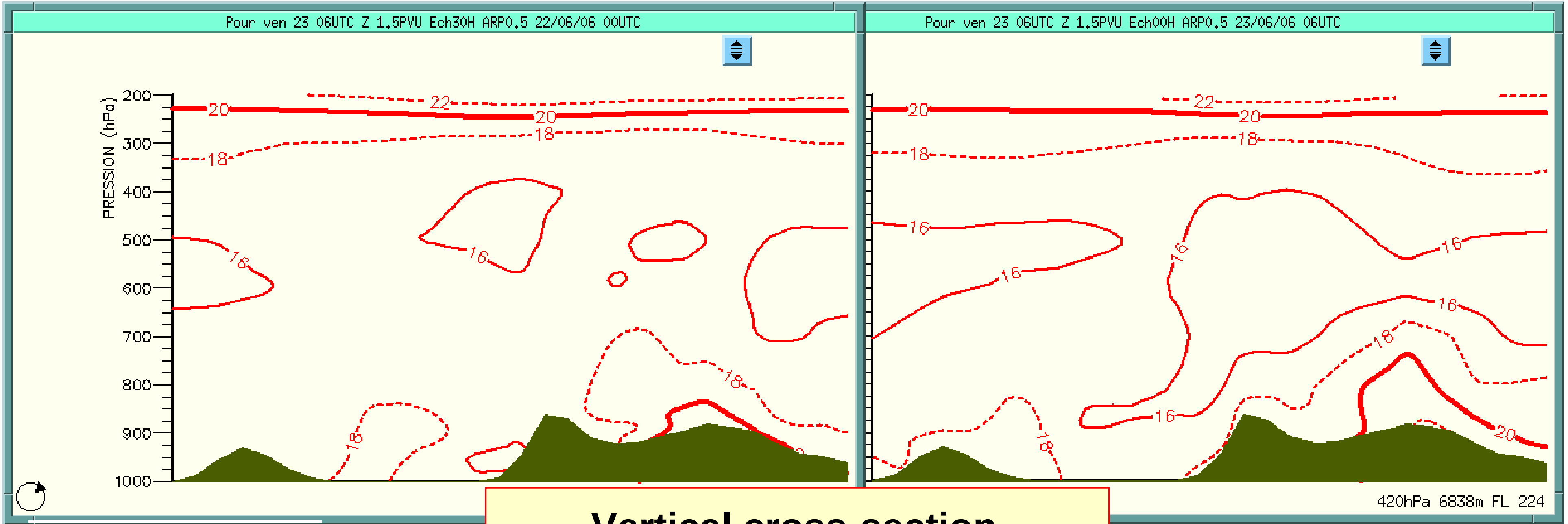

Vertical cross-section

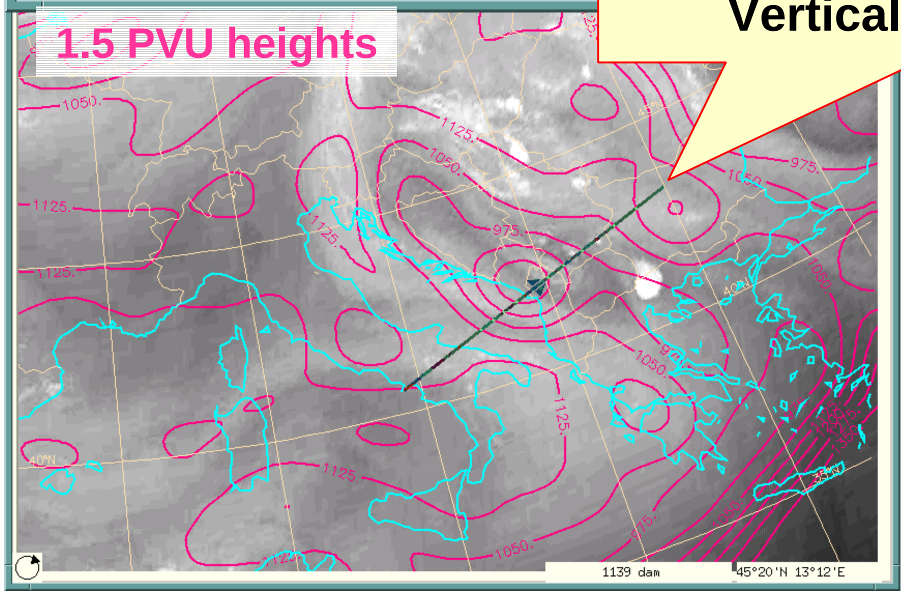

Thermodynamic analysis of the wrong NWP forecast.

06 UTC 23 June 2006

Upper and low-level perspective

30 h forecast of θ_w and PV | **Analysis of θ_w and PV**

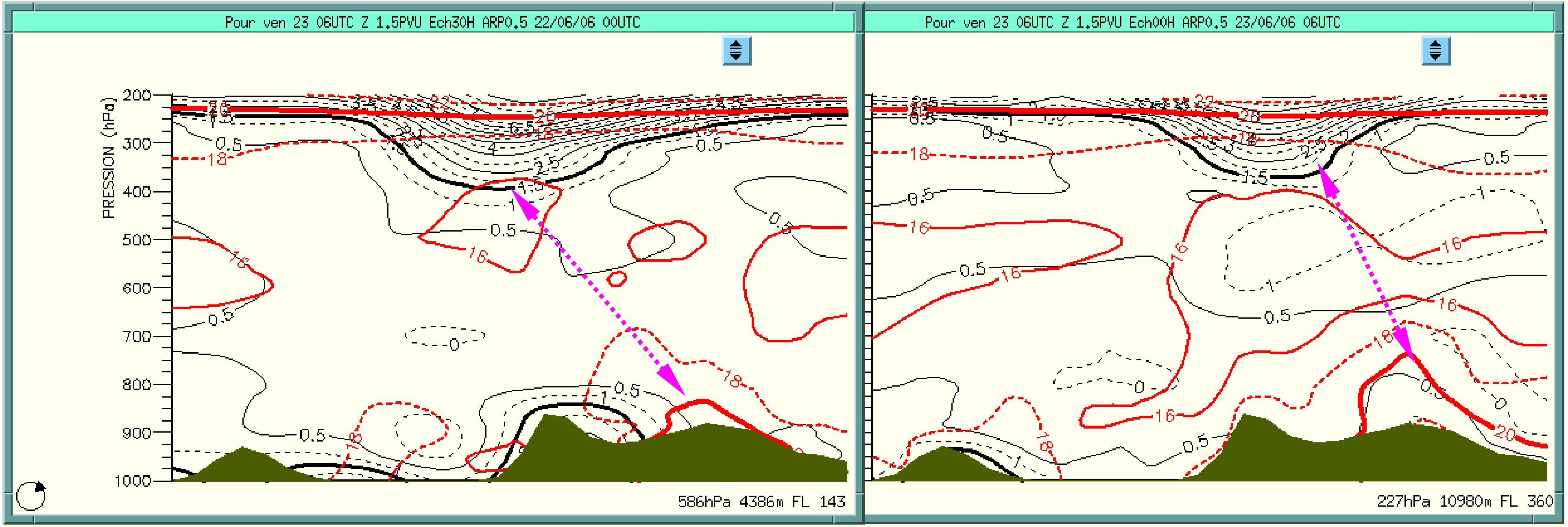

The NWP 30 h forecast underestimated the interaction between the PV anomaly and the low-level warm anomaly (θw maximum) showing the leading edge of the maximum folding (in 1.5 PVU thick contour) located about 200 km to the southwest of its actual position seen in the analysis and in the WV image.

The NWP model analysis shows that the low- and the upper-level thermodynamic features are in phase on 23 June that is an important condition favourable for convective development.

6.2 µm WV **06 UTC 1.5 PVU heights**

23 June 2006

Flash floods in Sofia, Bulgaria

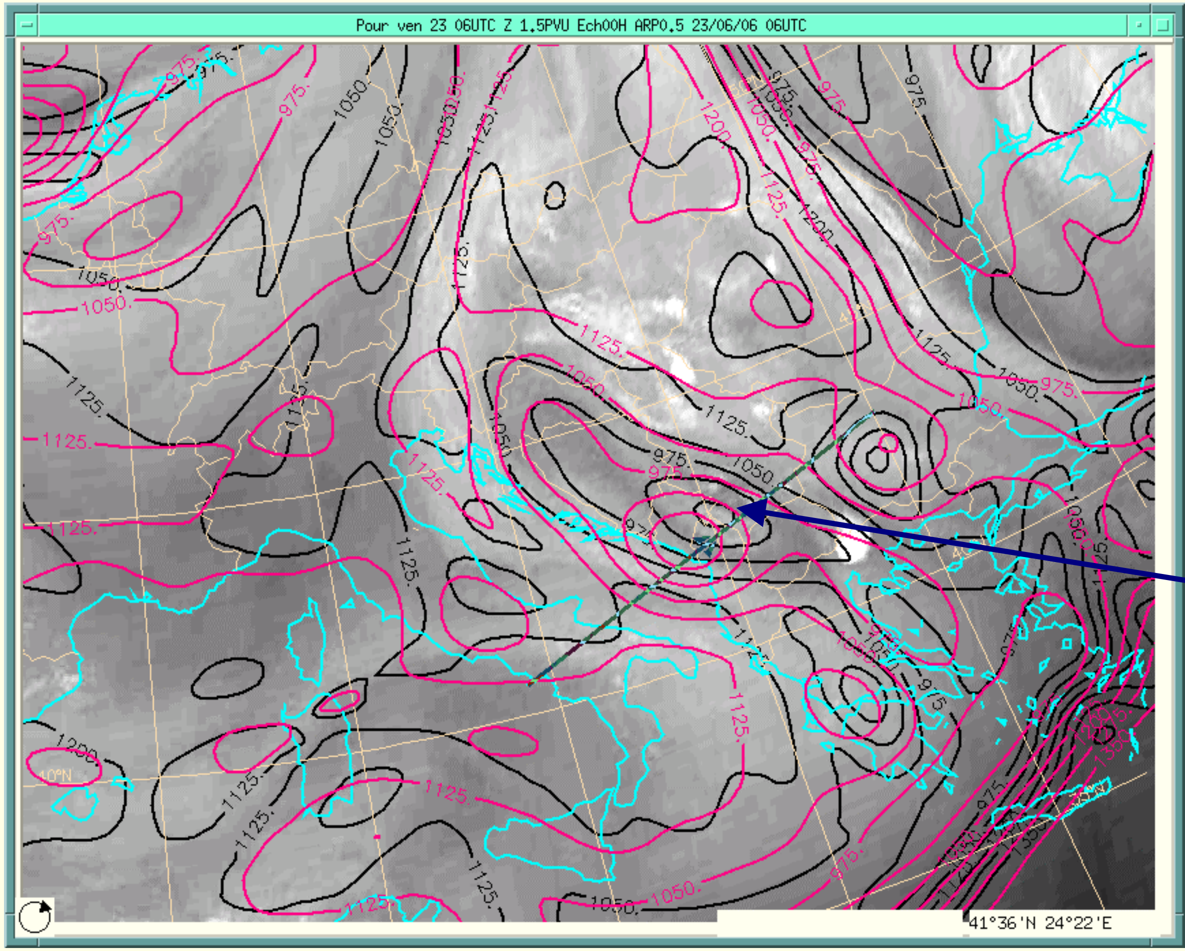

30 h forecast (red)
Analysis (black)

Wrong NWP PV forecast (ARPEGE)

Mismatch between the dynamical tropopause folding and the vorticity pattern on the WV image

In the 30 h ARPEGE forecast, the tropopause minimum is shifted about 200 km to the southwest from the real vorticity centre seen by the satellite image. The forecast underestimates the tropopause folding, simulating a weaker tropopause height gradient (a weaker upper-level jet) then in the analysis.

6.2 µm WV 06 UTC

23 June 2006

Flash floods in Sofia, Bulgaria

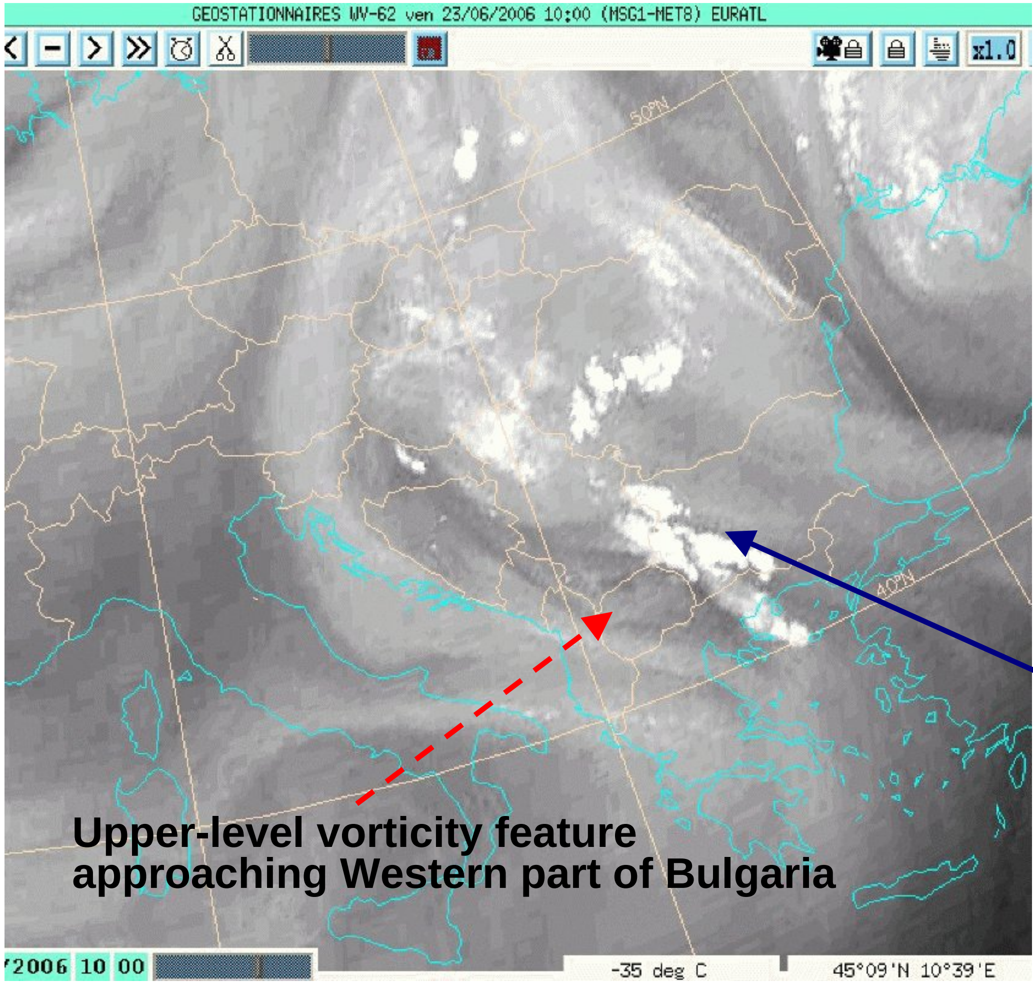

WV imagery diagnosis of upper-level vorticity advection and forcing of convection

Sofia

The leading edge of the dry vorticity WV imagery feature tends to curve cyclonically being in phase with the tropopause folding, which induces strong convective development in its leading diffluent part.

Animation 3

6.2 μm WV IMAGERY DIAGNOSIS

Convective development related to upper-level deformation zones

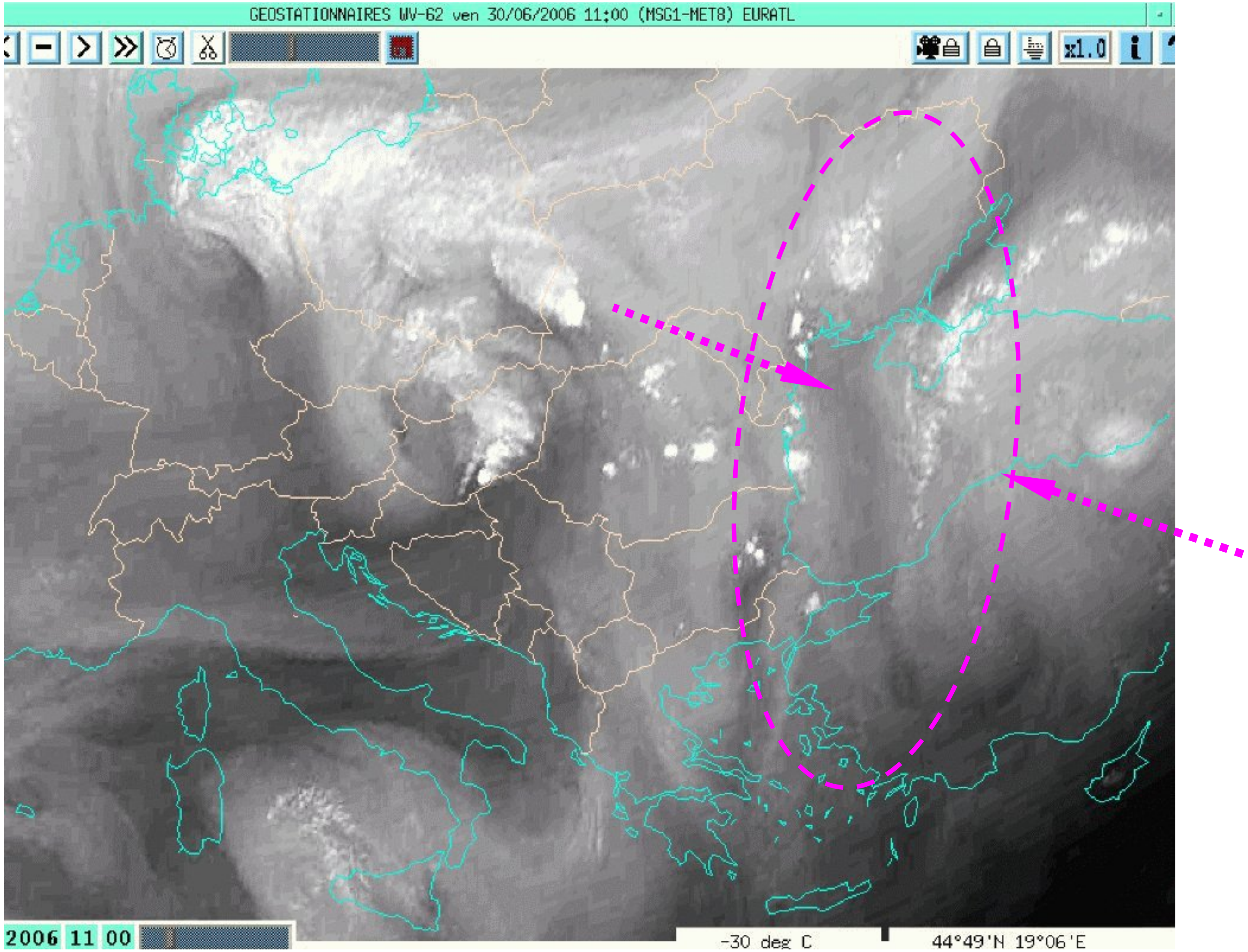

WV6.2

How to recognise deformation zones (which may be favourable for convection)?

Moisture boundaries, shrinking between dynamic (vorticity) features, tending to become close each other.

Animation 4

30 June 2006
06 – 12 UTC
WV 6.2

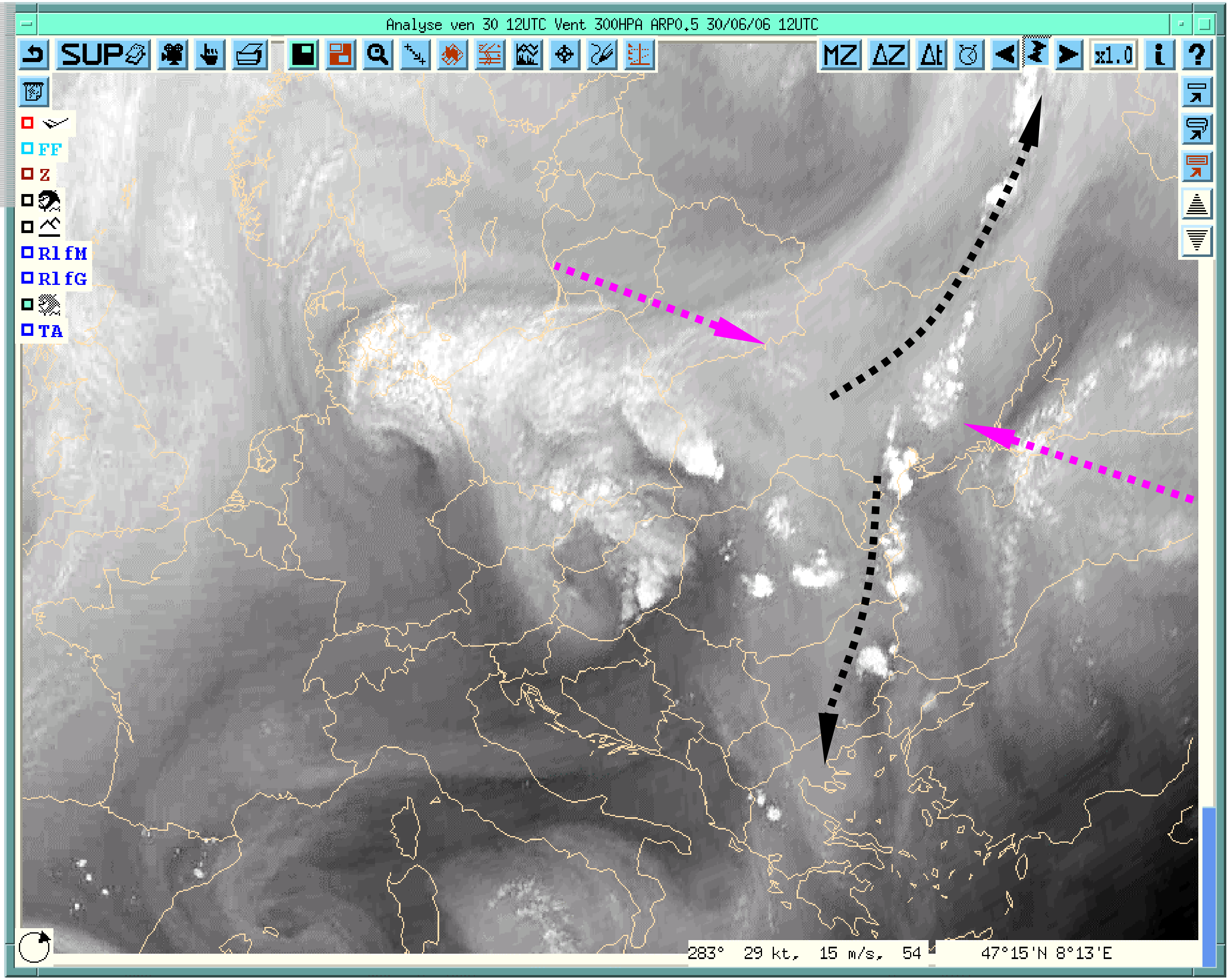

The deformation of the flow can modify and elongate the shape of the existing cloud, dry and moisture systems.

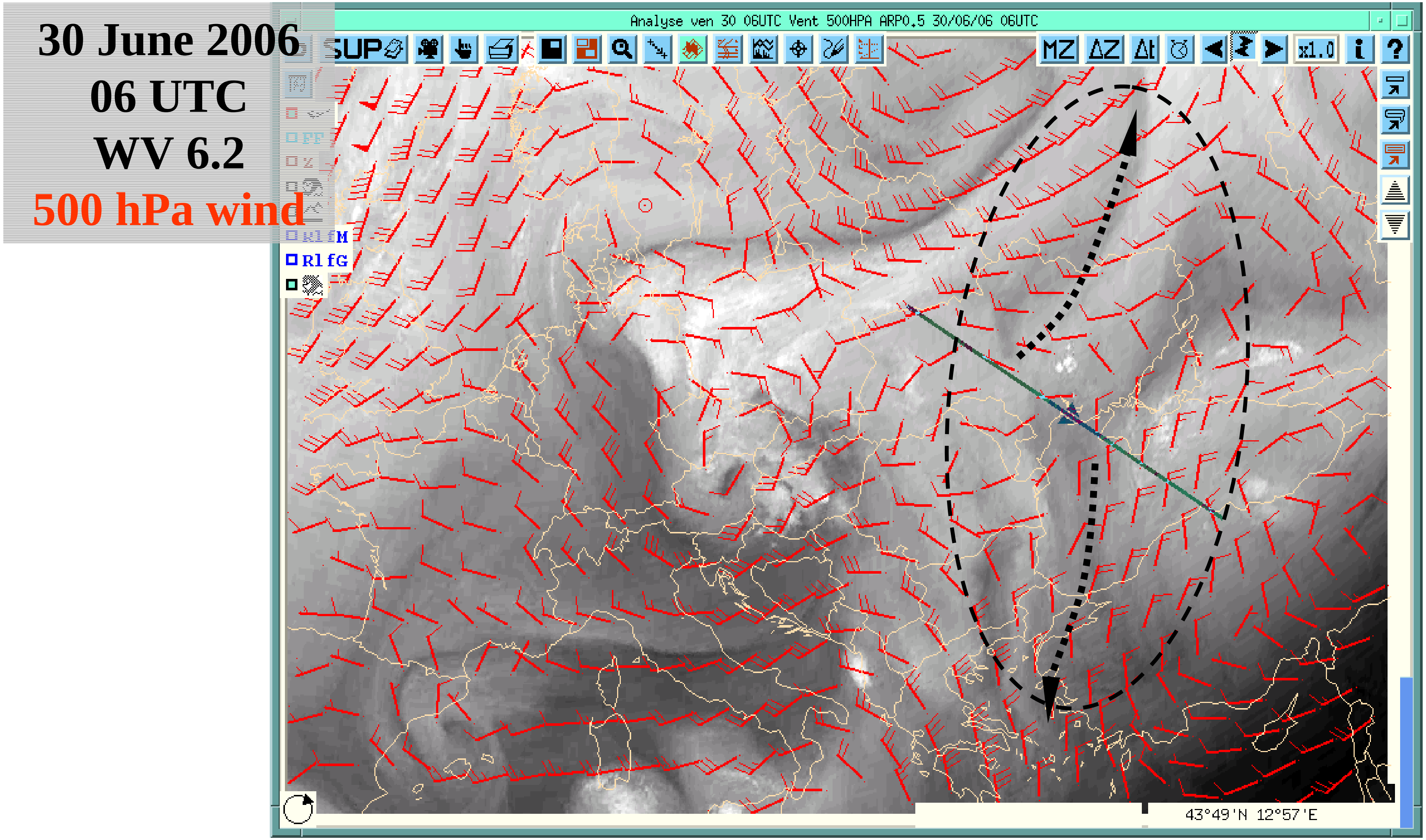

The horizontal deformation components of the wind tend to elongate the moist system along the deformation axis (along the corresponding moisture boundaries in the WV image).

30 June 2006
06 UTC
WV 6.2
Wet-bulb potential temperature at 300 hPa θw

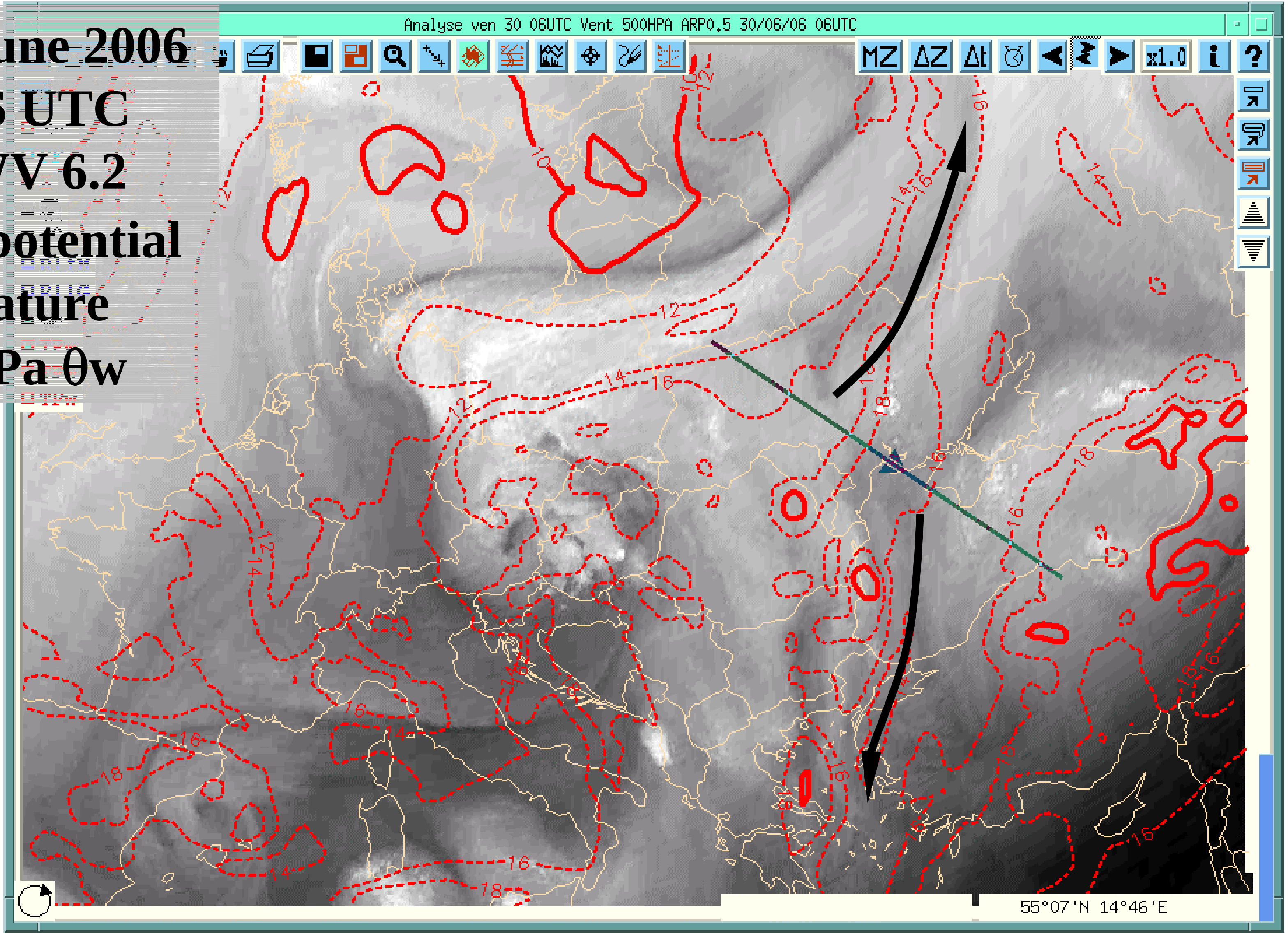

In certain conditions the horizontal deformation components of the flow may tend to increase and concentrate the temperature (or potential temperature) contrasts (see Martín et al., 1997).

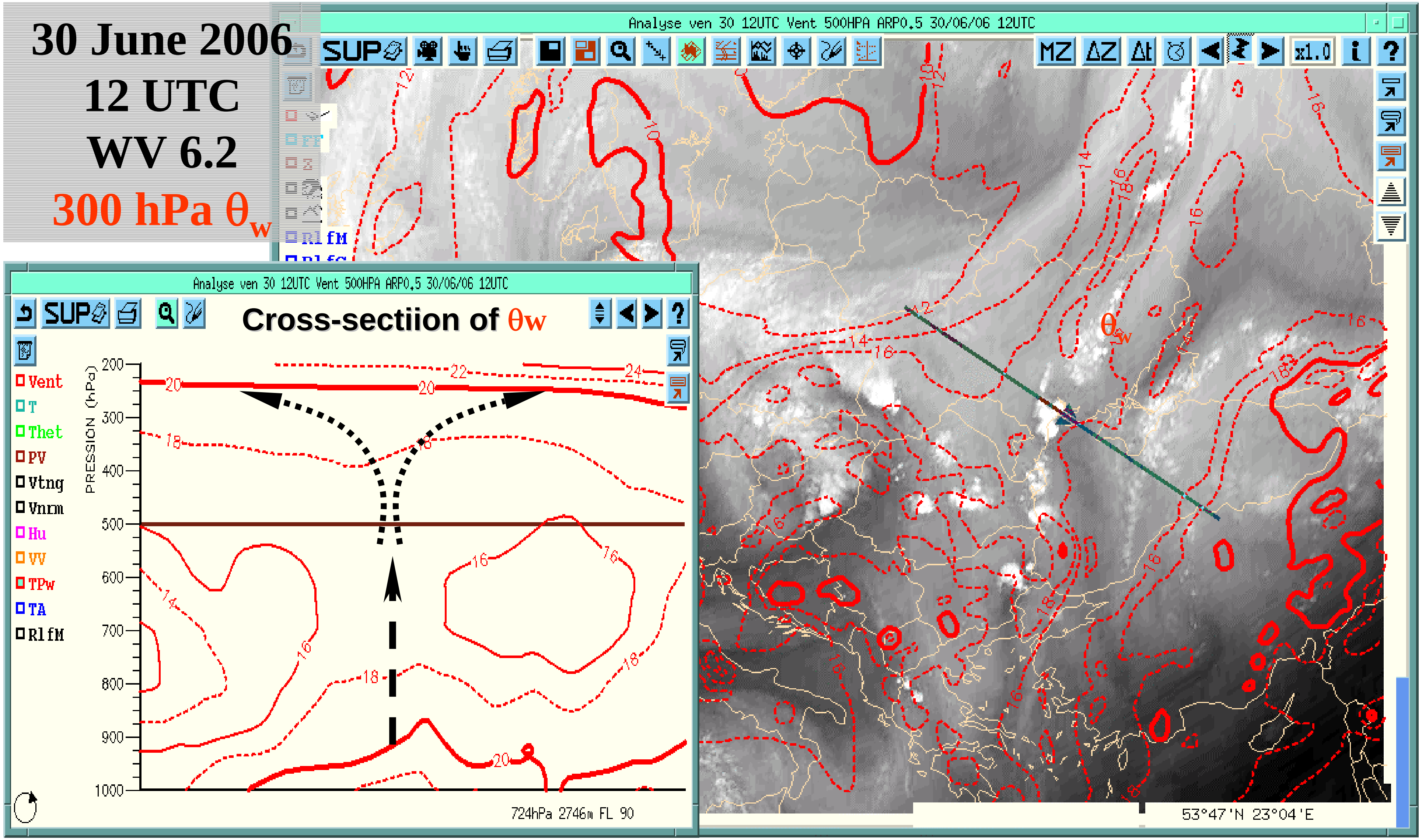

The middle troposphere at the centre of the deformation zone is unstable (weak vertical θ_w gradient), because of the diffluent upper-level flow there. Instability from low-level increases in the presence of a warm anomaly.

Animation 5

DEEP MOIST CONVECTION

Thermodynamic context as seen in MSG WV channels <u>6.2 and 7.3 µm</u>

<u>upper-level</u>

<u>mid-level</u>

<u>low-level</u>

CONVECTION at MOISTURE BOUNDARIES

30 March 2009 09 UTC

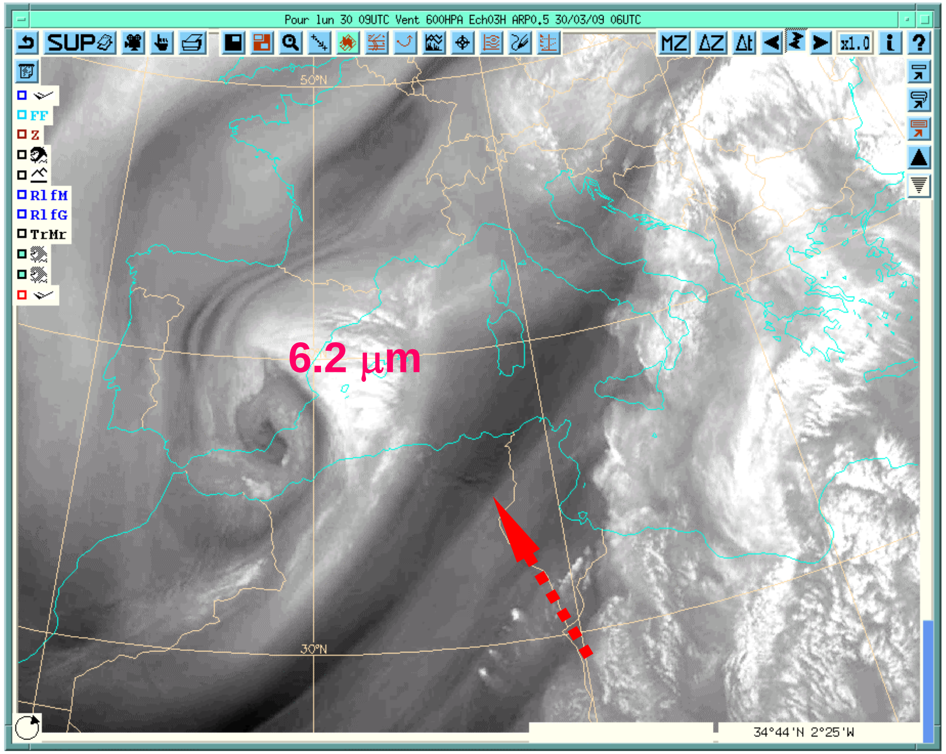

30 March 2009 09 UTC

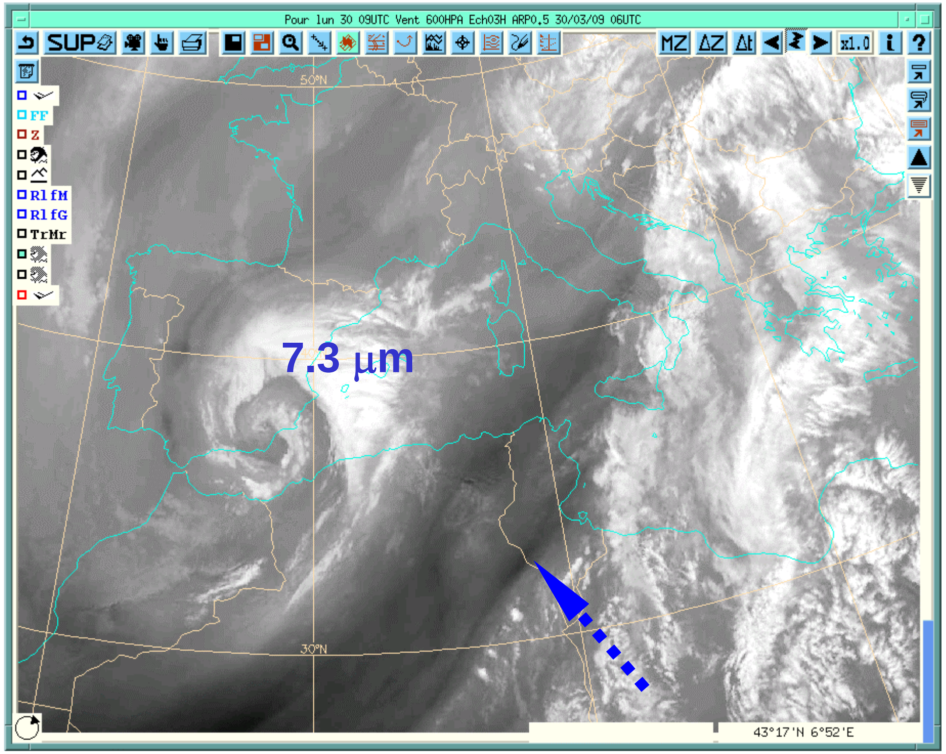

Convection often develops near moisture boundaries in WV images channel 6.3/6.2 µm (Roberts, 2000; Krennert, & Zwatz-Meise, 2003; Ghosh et al., 2008; Georgiev & Kozinarova, 2009)

Conditions conductive for convection are present at the <u>mid-level boundaries</u> seen in WV images channel 7.3 µm, being much more distinct than on the 6.2 µm WV images (Georgiev & Santurette, 2009).

CONVECTION INITIATION at JETS DETECTED BY WV IMAGERY

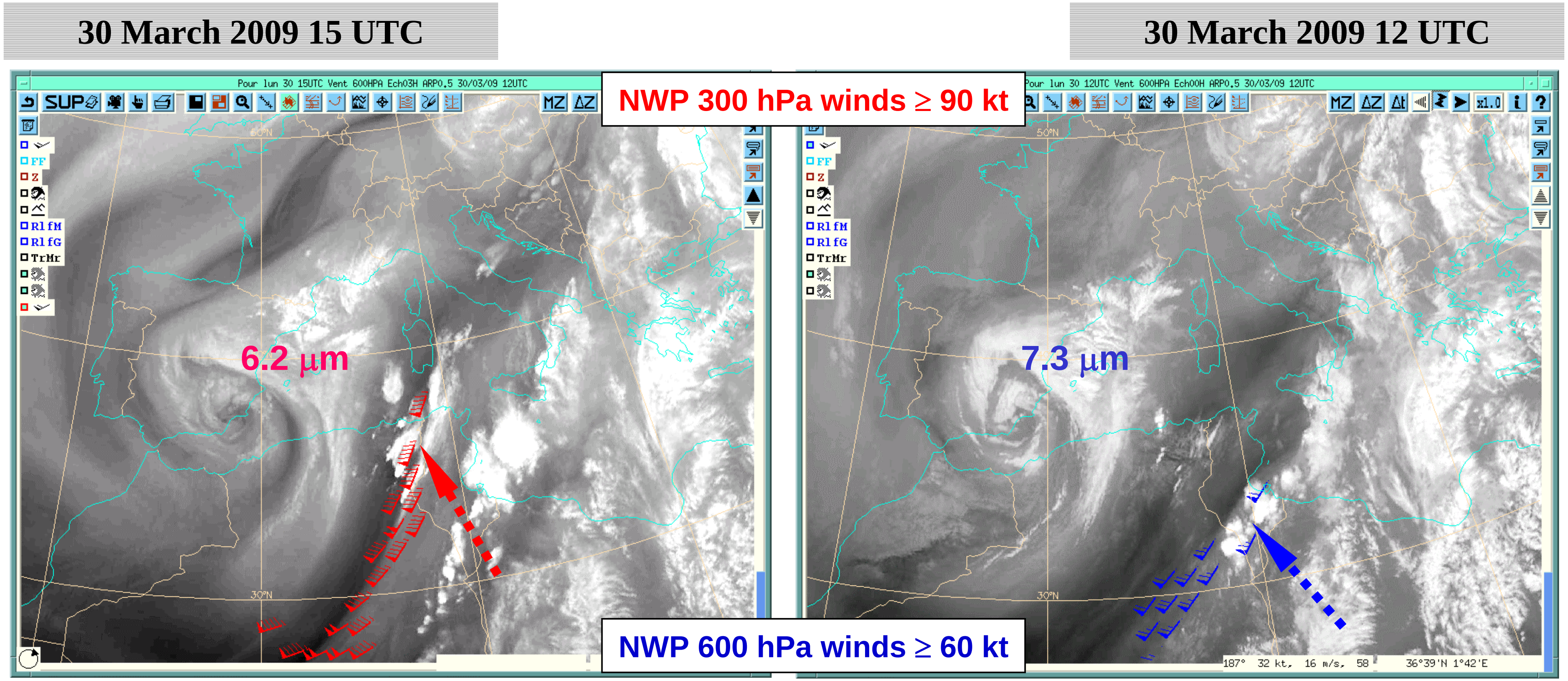

Convection initiates at boundaries of 6.2 µm images as a result of upper-level forcing for ascent at the left exit of a jet (see Carroll 1997).

Mid-level boundaries seen in 7.3 µm images are related to specific thermo-dynamic low-level convective environment (Georgiev & Santurette, 2009).

CROSS-SECTION

A **mid-level** moisture boundary in 7.3 µm images

30 March 2009 09 UTC

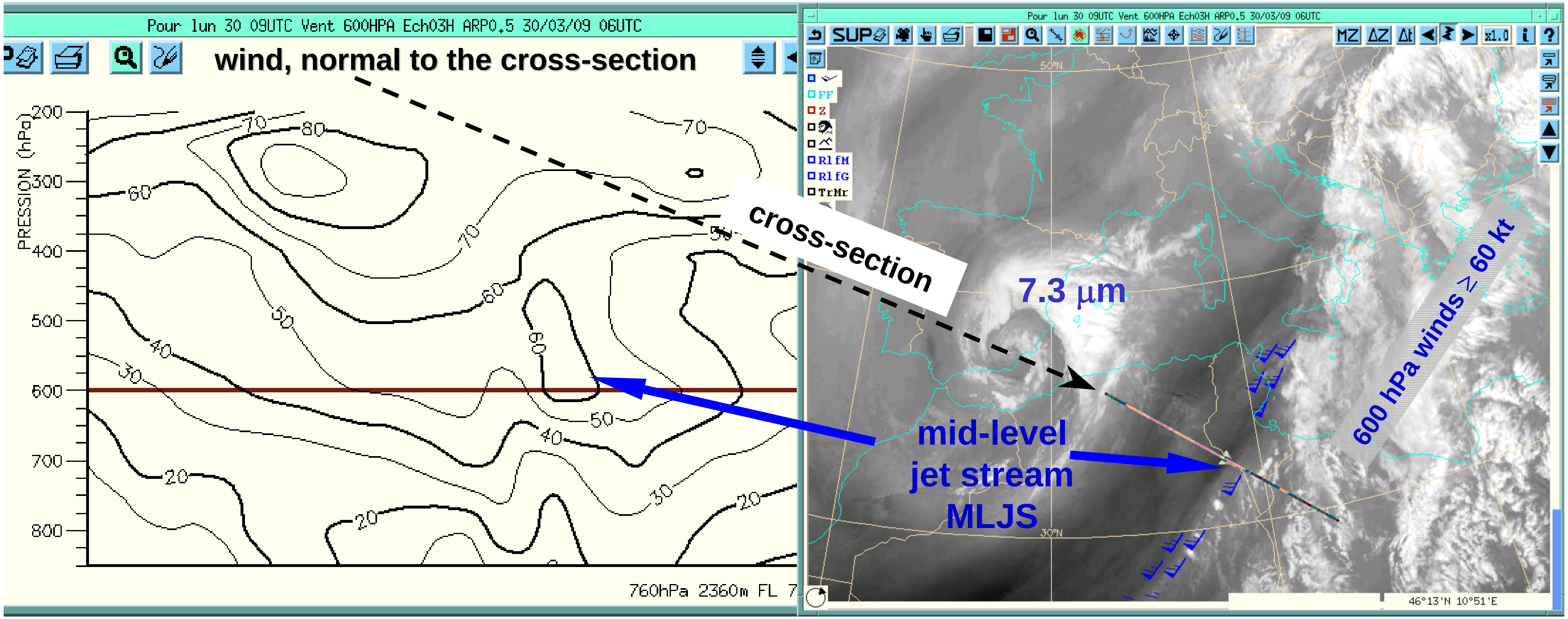

Such mid-level moisture boundaries are signatures of mid-level jet streams (MLJS), Georgiev & Santurette (2009).

A wind maximum usually appears at such moisture boundaries in 7.3 µm images at about 600 hPa level.

MIDDLE-LEVEL JET and BAROCLINC ZONE

30 March 2009 09 UTC

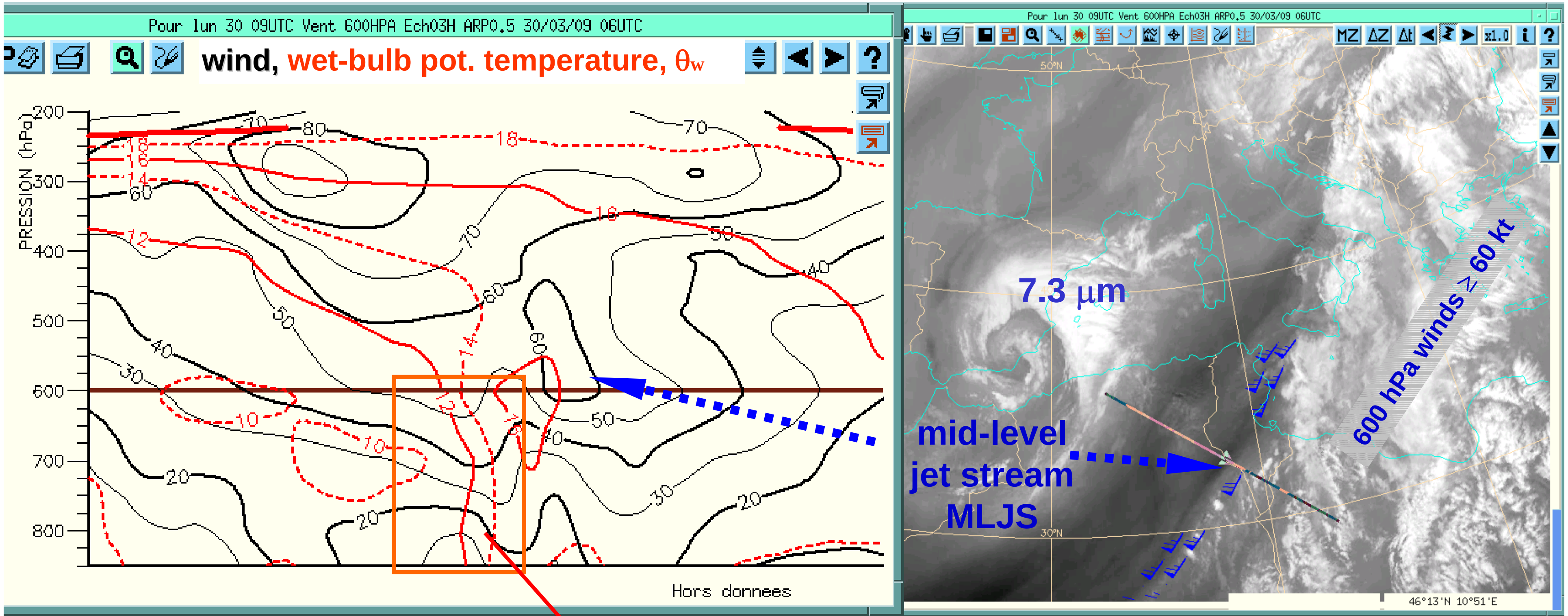

MLJS origin : low/mid-level baroclinic zone (strong θ_w gradient at 850 hPa)

Thermal wind relation :

$$\frac{g}{\theta_0}\frac{\partial \theta}{\partial x} = f\frac{\partial V_g}{\partial z}$$

θ is pot. temperature, reference value θ_o, g is the acceleration of gravity, f the Coriolis parameter, V_g is the y component of the geostrophic wind.

a strong horizontal θ_w gradient creates a strong vertical geostrophic wind gradient

The mid-level jets, detected by 7.3 µm images, originate from low-level baroclinic zones (Georgiev & Santurette, 2009) and are signatures for low-level conditions, favourable for convection.

WV IMAGERY DIAGNOSIS OF CONVECTIVE ENVIRONMENT

(JET STREAM ANALYSIS PERSPECTIVE)

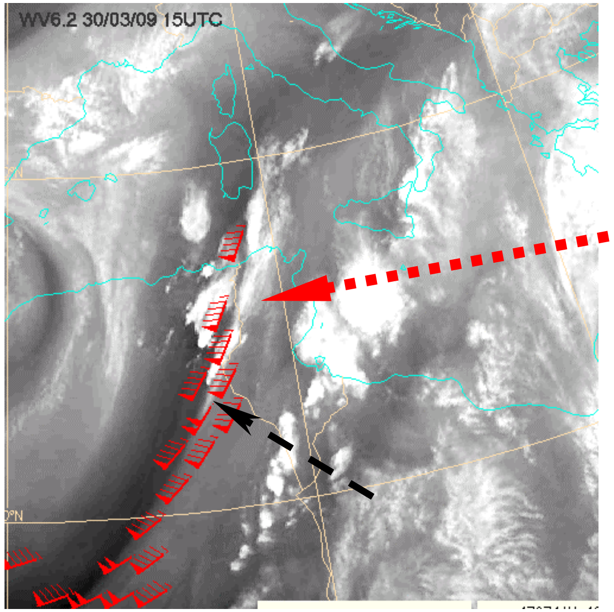

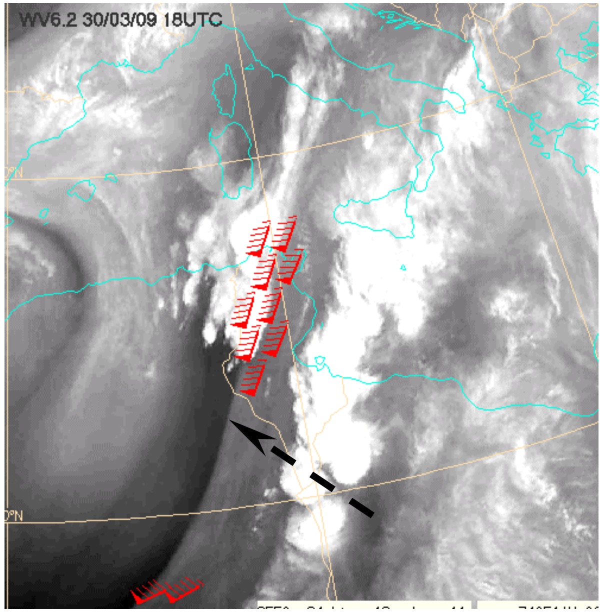

UPPR-LEVEL
FORCING
6.2 μm

Convection is most likely to develop *downstream left* of an upper-level moisture boundary

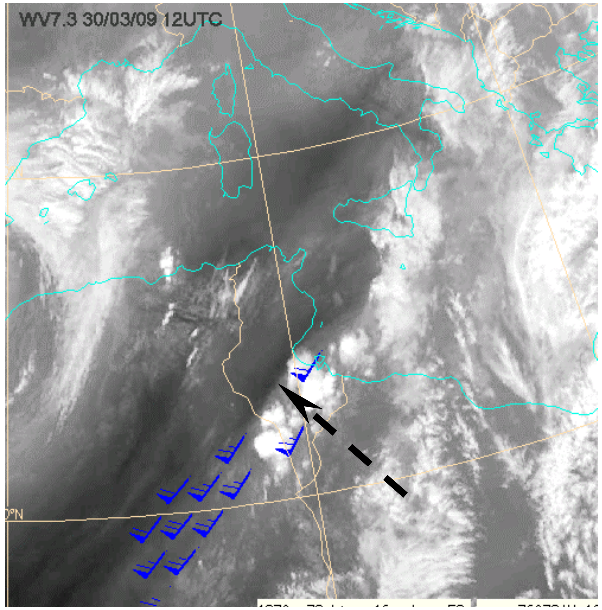

LOW-LEVEL
FORCING
7.3 μm

Convection is most likely to develop *downstream (right)* of a middle-level moisture boundary

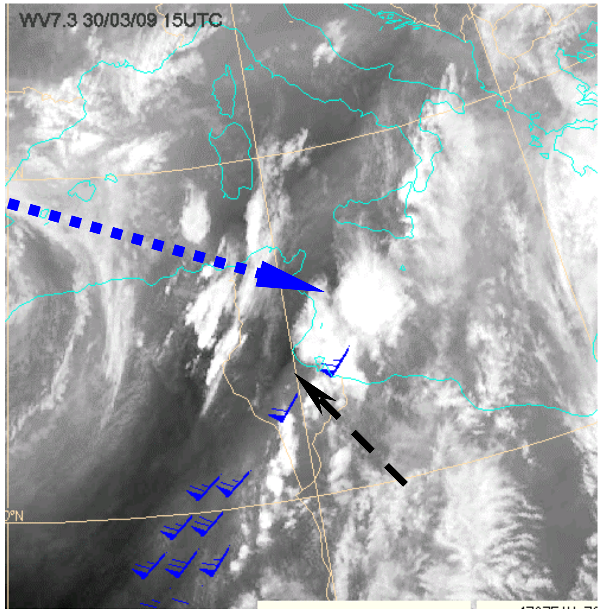

Conclusion remarks

Important principles for interpreting WV images in operational forecasting environment

- **To interpret WV images in the view of thermodynamic parameters and features, such as PV, mid/upper level wind components, wet-bulb potential temperature, etc., seen in NWP fields and vertical cross-sections.**
- **To estimate the potential for rapid cyclogenesis and deep moist convection through interaction of a PV anomaly (seen by WV channel 6.2 μm) and a low-level θw anomaly (warm/moist air).**
- **Looking at animated WV images 6.2 μm and 7.3 μm, to analyse the structure and behaviour of grey-shade features that may be extrapolated to predict time changes in the related thermodynamic and moisture conditions.**
- **To keep a critical mind when considering the NWP model output: Priority must always be given to the data from meteorological observations and satellite imagery.**

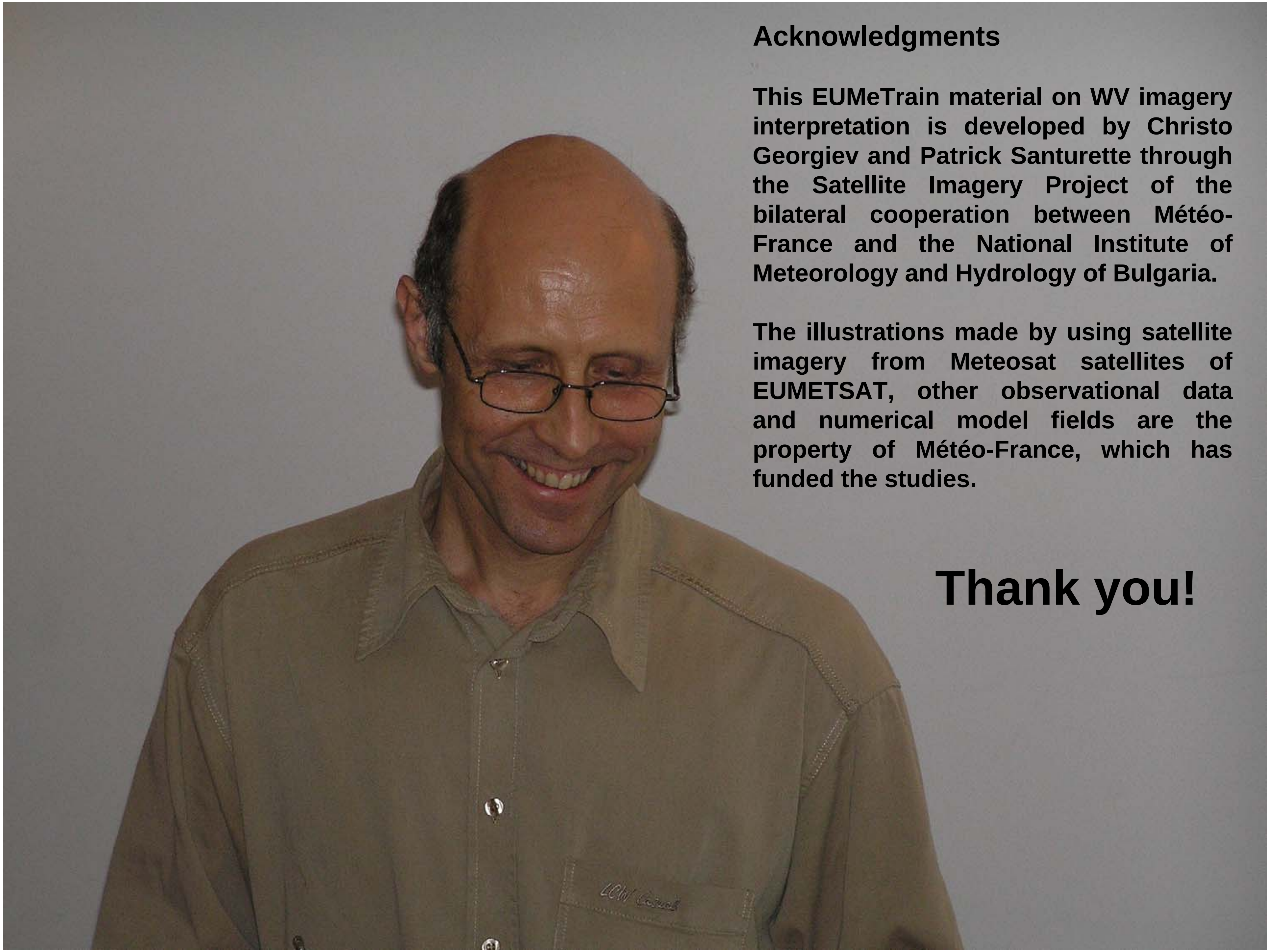

Acknowledgments

This EUMeTrain material on WV imagery interpretation is developed by Christo Georgiev and Patrick Santurette through the Satellite Imagery Project of the bilateral cooperation between Météo-France and the National Institute of Meteorology and Hydrology of Bulgaria.

The illustrations made by using satellite imagery from Meteosat satellites of EUMETSAT, other observational data and numerical model fields are the property of Météo-France, which has funded the studies.

Thank you!

References

Bader, M. J., Forbes, G. S., Grant, J. R., Lilley, R. B. E., Waters, A. J. (Editors). 1995. Images in weather forecasting. A practical guide for interpreting satellite and radar imagery. University Press, Cambridge, 499 pp.

Carroll, E. B. 1997. Use of dynamical concepts in weather forecasting. Meteorol. Appl. 4, 345–352. © UK Crown copyright, published by Met Office.

Doswell, C; A. III (1987) The distinction between large-scale and mesoscale contribution to severe convection: A case study example. *Wea. Forecasting*, v. 2, 3-16.

Georgiev, C. G. (2003). Use of data from Meteosat water vapour channel and surface observations for studying pre-convective environment of a tornado-producing storm. *Atmos. Res*., v. 67–68, 231–246.

Georgiev, C. G., Santurette, P., Dupont, F. and Brunel, P. (2007). Quantitative evaluation of 6.2μm, 7.3μm, 8.7μm Meteosat Channels Response to tropospheric moisture distribution. *In Proc*. *Joint 2007 EUMETSAT Meteorological Satellite Conference and the 15th AMS Satellite Meteorology & Oceanography Conference, Amsterdam, The Netherlands, 24-28 September 2007.*

Georgiev, C.G. and Santurette, P. (2009). Mid-level jet in intense convective environment as seen in the 7.3 µm satellite imagery. Atmos. Res., 93 (2009), pp. 277-285.

Georgiev, C.G. and Kozinarova, G. (2009). Usefulness of satellite water vapour imagery in forecasting strong convection: A flash-flood case study. Atmos. Res., 93 (2009), pp. 295-303.

Ghosh, A., Loharb, D., Dasc J. (2008) Initiation of Nor'wester in relation to mid-upper and low-level water vapor patterns on METEOSAT-5 images. *Atmospheric Research* 87 (2), pp. 116-135.

Hoskins, B., 1997. A potential vorticity view of synoptic development. *Meteorol. Appl*. 4, 325–334.

Krennert, T. & Zwatz-Meise, V. (2003). Initiation of convective cells in relation to water vapour boundaries in satellite images. Atmos. Res., v. 67–68, 353–366.

Martín, F., Riosalido, R., de Esteban, L., 1997. The Sigüenza tornado: a case study based on convective ingradients concept and conceptual models. Meteorol. Appl. 4, 191–206.

Roberts, N. M., 2000. The relationships between water vapour imagery and thunderstorms. JCMM Internal Rep. 110, 40 pp. © UK Crown copyright [Available from Joint Centre for Mesoscale Meteorology, Dept. of Meteorology, University of Reading, P.O. Box 243, Reading RG6 6BB, UK.]

Santurette, P., Georgiev C. G., 2005. Weather Analysis and Forecasting: Applying Satellite Water Vapor Imagery and Potential Vorticity Analysis. ISBN: 0-12-619262-6. Academic Press. Copyright ©, Elsevier Inc. 179 pp.

Saunders, R.W. and Brunel, P. (2005). RTTOV_8_7 Users Guide. NWPSAF-MO-UD-008.

Weldon, R. B., Holmes, S. J., 1991. Water vapor imagery: interpretation and applications to weather analysis and forecasting, *NOAA Technical. Report*. NESDIS 57, Washington D.C., 213 pp.